INSTITUTO SUPERIOR DE ENGENHARIA DO PORTO
MESTRADO EM ENGENHARIA QUÍMICA




High Pressure Technologies for Creating Added Value on Coffee Silverskin

EDUARDO PINHO NOGUEIRA BASTOS
outubro de 2019

POLITÉCNICO
DO PORTO

High Pressure Technologies for Creating Added Value on Coffee Silverskin

By

Eduardo Pinho Nogueira Bastos

INSTITUTO SUPERIOR DE ENGENHARIA DO PORTO

INSTITUTE OF THERMAL SEPARATION PROCESSES AT THE HAMBURG UNIVERSITY OF TECHNOLOGY

A dissertation submitted in partial fulfillment of the requirements for the degree of Master of Science
(Chemical Engineering: Energy and Biorefinery)

Oriented by:

Dr. Carsten Zetzl, Scientific Coordinator at the Hamburg University of Technology

Dr. Albina Ribeiro, Coordinator Professor at Instituto Superior de Engenharia do Porto

October 2019

Acknowledgments

I would like to express my gratitude towards Dr. Carsten Zetzl for accepting me in his research group as an intern, for his patience and, above all, for trusting me. I would also like to thank my colleagues at the TVT for all the help provided during my stay in Hamburg.

Also, I'm thankful for the thorough and precise review of this work rendered by Dr. Albina Ribeiro and for her guidance, even when half of Europe was tearing us apart.

Resumo

Este trabalho teve como objetivo o uso de técnicas de alta pressão, nomeadamente a extração supercrítica e extração com água líquida quente em condições alcalinas para valorização da *coffee silverskin*, um resíduo da torrefação e descafeinação do café. Este trabalho foi desenvolvido no âmbito de programa Erasmus+ na Hamburg University of Technology.

A recuperação de gorduras usando dióxido de carbono supercrítico foi realizada em nove combinações de diferentes pressões e temperaturas usando como biomassa pellets de coffee silverskin esmagadas com um almofariz e um pilão: 350, 400 e 450 bar e 40, 50 e 60 ºC. O rendimento mais alto foi de 3.34% a 450 bar e 60ºC, enquanto que o mais baixo foi de 2.33% a 350 bar e 40 ºC. O efeito da dimensão das partículas também foi estudado. Quatro tamanhos diferentes de partículas de *coffee silverskin* (22, 79, 379 e 1057 µm) sofreram extração a 450 bar e 60ºC e a sua extração foi modelada com o *software* "BatchSFE", desenvolvido pelo Institute of Thermal Separation Processes da Hamburg University of Technology. Para as três frações mais pequenas obtiveram-se rendimentos semelhantes (4.20% para 22 µm, 4.47% para 79 µm e 4.43% para 379 µm). Já a fração maior obteve um rendimento de 3.11%. A extração de proteínas através de água líquida quente foi estudada a 120 ºC e 20 bar, durante um período de 30 minutos usando concentrações de soluções de NaOH de 0, 0.01, 0.03 e 0.05 mol/L, e *pellets* de *coffee silverkin*. A adição de NaOH promoveu a extração dos aminoácidos. Sem adição de NaOH o rendimento foi de 2.0%, enquanto que a uma concentração de NaOH de 0.05 mol/L o rendimento foi de 5.6%. Para identificar o efeito de uma extração supercrítica antes de uma extração de água quente líquida, pellets previamente tratadas com dióxido de carbono supercrítico foram submetidas a um tratamento de água quente líquida a 120ºC durante 30 minutos com uma concentração de NaOH de 0.05 mol/L. Nestas condições o rendimento foi de 4.0%. O efeito da temperatura e o tempo de residência também foi estudado com *pellets* extraídas a 90, 105 e 120 ºC e 30 e 60 minutos. O rendimento mais elevado foi a 120 ºC durante 60 minutos (6.3%) e o mais baixo foi obtido a 90 ºC durante 60 minutos (1.4%). Os seguintes aminoácidos foram identificados: alanina, arginina, ácido aspártico, acido glutâmico, glicina, histidina, iso-leucina, leucina, lisina, metionina, fenilamina, serina treonina, tirosina e valina.

Palavras-chave: *coffee silverskin*, extração supercrítica, dióxido de carbono supercrítico, pré-tratamento com água quente líquida, hidrolise alcalina

Abstract

This work focused on the usage of high-pressure technologies, such as supercritical fluid extraction and liquid hot water treatment in alkaline conditions for the recovery of lipids and proteins in coffee silverskin, a by-product of coffee roasting and decaffeination. The work was developed within the scope of Erasmus+ program at the Hamburg University of Technology.

The extraction of lipids by means of supercritical carbon dioxide was studied using nine combinations of different pressures and temperatures and coffee silverskin pellets crushed with a mortar and a pestle as raw materials: 350, 400 and 450 bar, and 40, 50 and 60ºC. The highest yield was 3.34%, and it was obtained at 450 bar and 60ºC. The lowest yield was 2.33% and it was obtained at 350 bar and 40ºC. Furthermore, the impact of particle size was also studied. Four different particle sizes of coffee silverskin powder (22, 79, 379 and 1057 µm) were extracted at 450 bar and 60ºC, and modeled with the software "BatchSFE", developed by the Institute of Thermal Separation Processes of the Hamburg University of Technology. The three smaller particle ranges obtained similar yields (4.20% for 22 µm, 4.47% for 79 µm and 4.43% for 379 µm), whereas the biggest fraction obtained a yield of 3.11%.

The extraction of proteins by means of liquid hot water pretreatment was studied at 120 ºC and 20 bar with a residence time of 30 minutes using concentrations of NaOH of 0, 0.01, 0.03 and 0.05 mol/L and coffee silverskin pellets. The addition of NaOH improved the extraction of amino acids. At a concentration of NaOH of 0 mol/L the yield obtained was 2.0%, while at a concentration of 0.5 mol/L the yield was 5.6%. To observe the effect of supercritical fluid extraction on the protein recovery, pellets extracted beforehand were submitted at a liquid hot water at 120ºC for 30 minutes, at a concentration of NaOH of 0.05 mol/. The yield obtained was 4.0%. The effect of residence time and temperature was studied on the extracted pellets at 90, 105 and 120 ºC and 30 and 60 minutes, using a concentration of NaOH of 0.05 mol/L. The highest yield was 6.3%, obtained at 120 ºC and 60 minutes. The lowest yield was 1.4% at 90ºC and 60 minutes. The following amino acids were detected on coffee silverskin: alanine, arginine, aspartic acid, glutamic acid, glycine, histidine, iso-leucine, leucine, lysine, methionine, phenylamine, serine, threonine, tyrosine and valine.

Keywords: coffee silverskin, supercritical fluid extraction, supercritical carbon dioxide, liquid hot water pretreatment, alkaline hydrolysis.

Index

Figure Index

Table Index

Nomenclature

Abbreviation	Description
AA	Amino acid
AAR	Absolute relative deviation
as	As received
CO_2	Carbon Dioxide
CS or CSS	Coffee Silverskin
db	dry/basis
DG	Diglycerides
ES	Esterified Sterols
FAME	Fatty Acid Methyl Ester
FFA	Free Fatty Acids
GC-FID	Gas Chromatography-Flame Ionization Detector
GTR	Green Tea Residue
H^+ or H_3O^+	Hydronium
HCl	Hydrochloric Acid
HPLC-FLD	High Performance Liquid Chromatography with Fluorescence Detection
LHW	Liquid Hot Water
NA	Non-Analyzed
NaOH	Sodium Hydroxide
ND	Non-Detected
OH^-	Hydroxide
pI	Isoelectric Point
PID	Proportional–Integral-Derivative Controller
S	Sterols
sc-CO_2	Supercritical Carbon Dioxide
SCW	Subcritical Water
SFE	Supercritical Fluid Extraction
TG	Triglycerides
TUHH	Hamburg University of Technology
TVT	Institute of Thermal Separation Processes

Symbol	Description	Units
A	Area of mass transfer	m^{-2}
[NaOH]	Concentration of sodium hydroxide	mol/L
a_v	Specific surface area	m^{-1}
Bi	Biot number	
C_{fl}	Concentration of the solute in the bulk fluid	kg/m^3
C_i	Concentration of the solute in the fluid inside the particle	kg/m^3
C_{in}	Initial concentration of the solute in the bulk fluid	kg/m^3
C_{out}	Concentration of the solute in the fluid outside the extractor	kg/m^3
C_{sat}	Saturation concentration in the fluid	kg/m^3
C_{solid}	Concentration of the solute in the solid	kg/m^3
$C_{surface}$	Concentration of the solute in the fluid at the surface of the particle	kg/m^3
D_{ax}	Axial dispersion coefficient	m^2/s
d_{par} or d_p	Particle diameter	m
K	Partition Coefficient	
K1	First parameter of the Freundlich desorption isotherm	
L_{film}	Length of the film	m
$L_{reactor}$	Length of the extractor	m
m_{sub}	Mass transfer rate of the solute from the solid to the fluid	$kg\ m^{-3}\ s^{-1}$
$m_{sub,\ ext}$	Mass transfer rate of the solute from the particle surface to the bulk fluid	$kg\ m^{-3}\ s^{-1}$
$m_{sub,\ int}$	Mass transfer rate of the solute from the particle core to the surface	$kg\ m^{-3}\ s^{-1}$
$m_{sub,steady}$	Mass transfer rate on steady state	$kg\ m^{-3}\ s^{-1}$
P	Pressure	bar
Pe	Peclet number	
r	Particle radius	m
Re	Reynolds number	
Sc	Schmidt number	
Sh	Sherwood number	
T	Temperature	ºC or K
v	Average fluid velocity	m/s
$\dot{V}$	Solvent volumetric flow	m^3/s
v_0	Superficial fluid velocity	m/s
$V_{reactor}$	Volume of the extractor	m^3
z	Axial coordinate on the reactor	m

Greek Symbol	Description	Units
μ	Dynamic viscosity	$kg\ m^{-1}\ s^{-1}$
β	Global mass transfer coefficient	m/s
β_F	Mass transfer coefficient in the static fluid layer of the particle	m/s
β_S	Mass transfer coefficient in the solid	m/s
$\delta_{eff,solid}$	Effective diffusion coefficient of the solute in the solid	m^2/s
δ_{eff}:	Effective diffusion coefficient observed	m^2/s
δ_{solid}	Diffusivity coefficient of the solute in the solid	m^2/s
ε_{bed}	Porosity of the bed	
ρ_{app}	Apparent density	kg/m^3
ρ_{CO2}	Density of carbon dioxide	kg/m^3
ρ_{skel}	Skeletal density	kg/m^3

1. Introduction

1.1. Framework

This work was developed within the scope of the Erasmus+ Traineeship Program from February to June 2019 in the Institute of Thermal Separations Processes (TVT) of Hamburg University of Technology (TUHH).

On average, 30 hours per week were dedicated to the experimental procedures, bibliographic research, and discussion of the results with the project supervisor and colleagues.

1.2. Topics and Objectives

The two main topics of this work were supercritical carbon dioxide (sc-CO_2) extraction in a fixed fed extractor and subcritical water treatment in a batch reactor of coffee silverskin (CSS) for recovery of lipids and proteins, respectively.

Taking in to account the current necessities to reduce the ecological footprint, new techniques to create added value for industrial waste are paramount. Coffee silverskin is a byproduct of coffee roasting and decaffeination. Usually it is incinerated or disposed on a landfill, negatively impacting the environment and increasing the manufacturers expenditures. Thus, retrieving valuable compounds from it would bring ecological and economic benefits.

Supercritical fluid extraction (SFE) has become a subject of great interest in the last decades and became the extraction method of choice in several food processing industries *(*Jahurul *et al.* , 2012). Supercritical fluids solvents are used under a pressure and temperature above their critical points, presenting liquid-like density and gas-like viscosity (Kehili *et al.* , 2017). The usage of supercritical carbon dioxide (sc-CO_2) has been extensively studied, and it is proven to be a efficient and environmental friendly method for the extraction of several types of oil.

Liquid hot water (LHW) pretreatments have become one if the leading technologies that requires no chemicals other than liquid water at high temperatures. In LHW, water can act as a solvent and catalyst. LHW is proven to be an efficient method for the disruption of the cell's wall and minimal production of inhibitory products (Li *et al.* , 2017). Subcritical water (SCW) falls in the scope of LHW pretreatment. Water is maintained on the liquid state at elevated temperatures (100-374ºC) by pressurizing it. At these

conditions, water is comparable to other organic solvents such as methanol and acetone (Narita & Inouye, 2012).

The goal of this work is, from the two methods above, obtain compounds of high value that are present in the composition of coffee silverskin.

1.3. Description of the Workplace

The Institute of Thermal Separation Processes is one of the departments of Hamburg University of Technology. It is divided into three main areas of research: Nano-porous Materials, Molecular Methods for Separation Processes and Biorefinery. This work was developed within the scope of the latter. The Biorefinery Group focuses on high pressures technologies to create bio-based products, and since 2008 it has been developing the concept of "lignocellulose biorefinery".

The full experimental set-up was localized within the facilities of the TVT.

1.4. High-Pressure Biorefinery at the Hamburg University of Technology

The TVT has several years dedicated to the research and development of high-pressure biorefinery. In this section, an overview of the recent projects developed by the TVT is presented, as this work followed the same methodology and shared some of the equipment.

High-pressure technology can be used in the most diverse aspects of biomass processing: during the physical pretreatment with processes like pelletizing and extrusion, and during the physicochemical treatment by means of gas or liquid extraction and hydrolysis. Some of the benefits of these techniques include the increase of the rates of reaction and conversion. The variation of the process pressure, temperature and residence time allows control of the diffusion and adsorption conditions. (Smirnova *et al.* , 2011). Figure 1.1 illustrates some high-pressure processes and their respective extractible compounds.

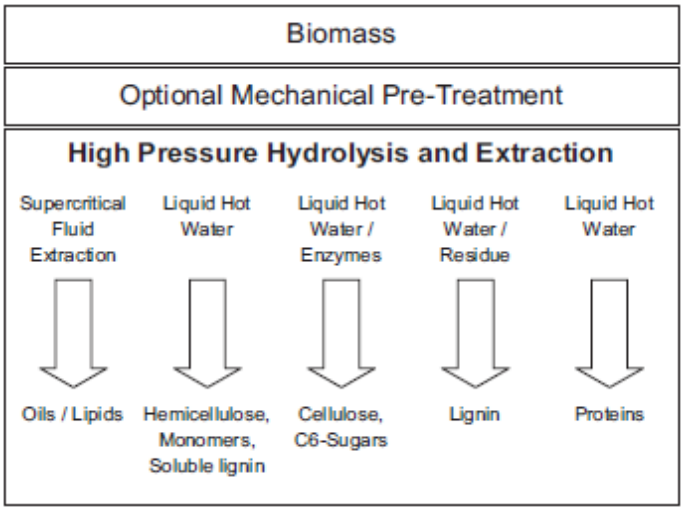

Figure 1.1: High pressure applications for added value from lignocellulosic (Smirnova *et al*., 2011)

In 2016, Reynolds *et al.* produce odor free lignin in a 40-L fixed bed unit. By means of liquid hot water treatment at 200ºC and 40 bar and using wheat straw pellets as the raw material, a hydrolysate rich in C-5 sugars was separated from a solid fraction rich in cellulose and lignin (33.2%). The solid fraction was then submitted to enzymatic hydrolysis until a maximum of 71.8% of lignin was obtained. Afterward, the lignin was submitted to a supercritical extraction process to remove free fatty acids and volatile organic compounds responsible for the usual bad odor of lignin (Reynolds *et al.* , 2016). The simplified flowsheet of the process is displayed in Figure 1.2.

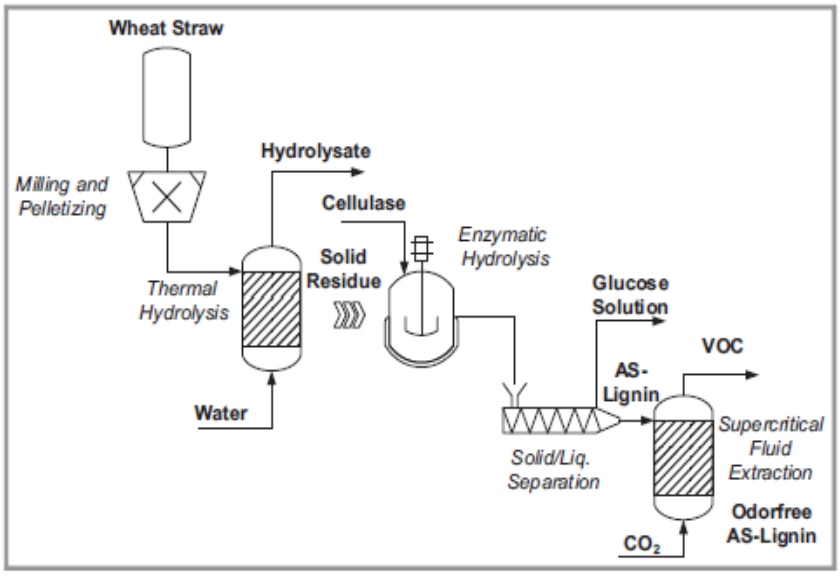

Figure 1.2: Process scheme of sequential hot water and enzymatic hydrolysis conducted (Reynolds et al, 2016)

Another article written by researchers from the Laboratory of Chemistry of Natural Substances (University of Sfax, Tunisia) and from the TVT focused on the valorization of Tunisian industrial tomato by-products. They were able to build a lab-scale high-pressure based biorefinery cascade. This work is even more interesting from the present study point of view as it used supercritical carbon dioxide as a solvent for the recovery of lipids and antioxidants, and liquid hot water treatment as a method for protein recovery.

At 400 bar, 40ºC and a flow rate of 4 gCO_2/min, they were able to retrieve 5.8 and 26.3% of the initial tomato peel and tomato seeds mass in form of oleoresin, respectively. This represented 95.1% and 98.6% of the oleoresins initially present in the peels and seeds of the tomatoes, respectively. These values were higher than the ones that were found in the literature at the time, that used a different method of extraction. These results supported the higher efficiency of supercritical fluid extraction. The oil extraction was following by a Liquid Hot water treatment at 90ºC and 1 bar in solution with a concentration of NaOH of 0.05 mol/L, for 30 minutes. Tomato peel and seeds that were submitted to sc-CO_2 extraction's results were compared with the ones from raw peel and seeds. This was it was possible to evaluate the effect of a previous supercritical extraction on the following steps of the cascade. Surprisingly, raw and pretreated samples did not have very different protein extraction yields from each other. However, both with pretreated peel and seeds the purity of the protein extract was higher. They assumed that the removal of lipids in the previous stage, lead to the removal of certain impurities (Kehili *et al.* , 2016).

In the following year, Kehili *et al.* performed more research on the supercritical fluid extraction of oleoresin, lycopene, and β-carotene from tomato peels. This time, parameters such as pressure, temperature, solvent flow rate, and particle size were altered. The highest temperature, pressure and flow rate lead to the highest extraction rates for oleoresin, lycopene, and β-carotene. Smaller particle sizes favored faster extractions. However, for better antioxidant activity of the extracts, mild conditions were preferred (Kehili *et al.* , 2017).

These works, with special emphasis to Kehili *et al.*, 2016, were a starting and reference point for the methodology and line of thought of this work.

1.5. Structure of the Report

This report is divided into five main chapters: Introduction, Literature Review, Methods and Materials, Results and Discussion, and finally Conclusion and Suggestions.

The Introduction gives a general presentation about the work and the work facilities, as well as the main goals of the work and a summarized experimental set-up.

The Literature Review focuses on the main subjects of the work. The composition of coffee silverskin was already investigated by some authors, which provides some background to this work. Theoretical concepts regarding mass transfer and diffusion through porous matrixes, which are related to supercritical fluid extraction, are presented. The effect of moisture, size particle, flow rate, pressure, and temperature are highlighted by several authors, which serve as a point of comparison for the results obtained in this work. As for the protein extraction, the literature provides data regarding the solubility of the amino acids in water and alkaline solutions, which makes it possible to compare with the obtained protein profile.

The Methods and Materials presents an overview of the experiments conducted throughout the work, of the equipment and raw material used. Possible experimental errors are presented.

The Results and Discussion shows the several results obtained, comparing them with values from the literature, and making room for discussion and possible explanations for subverted expectations.

The Conclusion and Suggestions synthesize the main results of the work. It states if the objectives of the work were attained, it mentions the drawbacks and offers suggestions for future works that, in the perspective of the author, would promote better and more precise results.

2. Literature Review

The quick augmentation of the world's energy consumption, altogether with the scarcity of non-renewable sources of energy and their hazards to the environment, created the need of producing alternative materials and energy that can efficiently substitute fossil fuels.

Lignocellulosic materials are one of the most promising materials to be used in biorefinery, and several methods have been developed to increase its potential. This thesis focused on the high-pressure methods for fractionation of coffee silverskin (CSS).

2.1. Lignocellulosic Biomass

Set aside the three basic chemical compounds, which are lignin, cellulose and hemicellulose, lignocellulosic biomass contains water and, proteins, minerals and lipids. To use biomass in an efficient way for biorefinery, there is the need to fractionate into its main constituents(Ortega, 2015). Figure 2.1 presents the range of weight percentages for the main constituents of lignocellulose.

Due to the crystalline characteristics of lignocellulose, it is resistant to degradation. The hydrophobicity of lignin "and encapsulation of cellulose by the lignin-hemicellulose matrix" also plays a role in its resistance. (Isikgor & Becer, 2015)

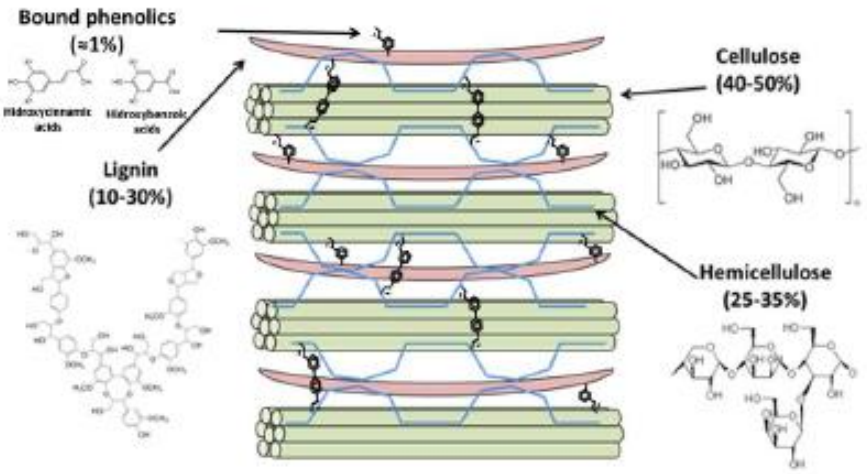

Figure 2. 1: Lignocellulosic biomass structure (Cocero *et al*., 2018)

All these different fractions represent potential sources for commodity chemicals, but as they have different chemical functionalities (link aromatic units form lignin, hemicellulose is made from C5 sugars and cellulose is made out C6 sugars), there is a need to recur to separation processes that are able to isolate the respective fraction and

break it into their individual building blocks (for instance, sugars for cellulose/hemicellulose and while lignin breaks in aromatic units) (Cocero *et al.* , 2018)

Cellulose, the most frequently found organic compound on the planet, is the main component of the cell walls in biomass. It is the main structural component of cells wall of biomass Its amount may vary. It is represented by the generic formula, $(C_6H_{10}O_5)_n$, by Figure 2.2. Cellulose, a long-chain polymer, has a high degree of polymerization (<10,000) and a great molecular weight (<500,000). Many glucose molecules make its thousands of units long crystalline structure, that makes it resistant (Basu, 2013). Cellulose is more resistant and consequently requires more demanding treatment. As it is formed by a long chain of one type of beads (a polymer of glucose), it forms crystals with the same chemical structure in every plant. It consists of a linear arrangement of glucose monomers, which are connected by β-(1-4)-glycosidic linkages. This leads to a crystalline and fibrous structure whereas hemicellulose has long branched sugar chains, amorphous structure (Ortega, 2015).

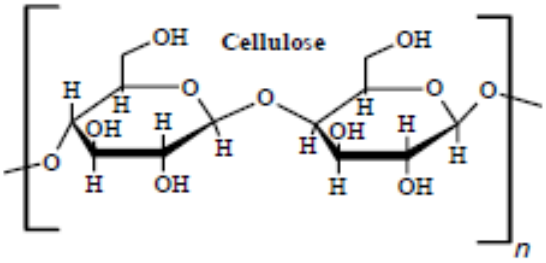

Figure 2. 2: Cellulose formula (Cocero *et al*., 2018)

Alongside with cellulose, hemicellulose is a constituent of a plant's cell wall. It is formed by groups of carbohydrates with a branched chain structure and a significantly lower degree of polymerization in comparison with cellulose. It is generally represented by the generic formula $(C_5H_8O_4)_n$. (Basu, 2013). Hemicellulose random and amorphous structure is formed by several heteropolymers that include xylan, galactomannan, glucuronoxylan, arabinoxylan, glucomannan, and xyloglucan. (Isikgor & Becer, 2015).

Lastly, lignin is a three-dimensional polymer of phenylpropanoid units. It has the function of cellular glue, that offers compressive strength to the plant's tissue and its individual fibers, stiffness to the cell wall and providing resistance against pathogens and insects (Isikgor, 2015). Lignin is an extremely complex branched polymer of phenylpropane. Its

three-dimensional units are primarily constituted of 4-propenyl phenol, 4-propenyl-2-methoxy phenol, and 4-propenyl-2.5-dimethoxyl phenol (Basu, 2013).

2.2. Coffee Silverskin: Properties and Composition

Coffee drinks and its derivates are amongst the most consumed beverages in the world. Table 2.1 displays the world production of coffee according to the exporting areas in 2016.

Table 2.1: Total world production of coffee in thousands of 60 kg bags in 2016 (Blinová et al., 2017)

Total	**151 623**
Arabicas	95 204
Colombian Milds	15 779
Other Milds	26 951
Brazilian Naturals	52 474
Robustas	56 419
Africa	16 353
Asia & Oceania	43 110
Mexico & Central America	17 740
South America	74 420

Coffee silverskin is an inner layer surrounding the coffee bean, and it is said to be the only by-product of coffee roasting. It represents 4.2 % w/w of all the coffee bean, meaning that every year several million thousands of coffee silverskin are either incinerated or disposed (Hijosa-Valsero *et al.* , 2018). Figure 2.3 schematizes a coffee bean, where silverskin serves as an inner layer.

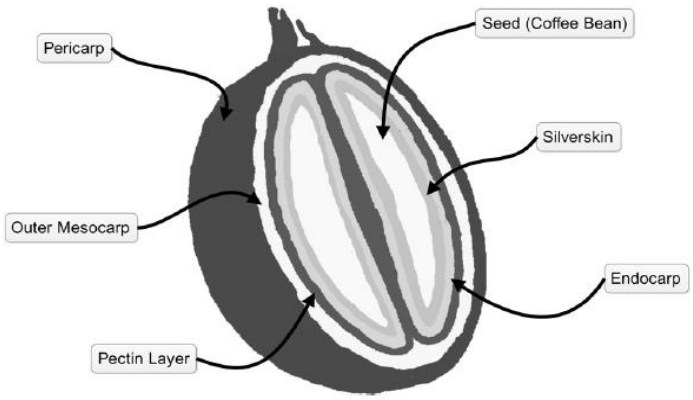

Figure 2. 3: Coffee bean structure (Bresciani, 2014)

There have been studies showing the composition of coffee silverskin, some of them are displayed in Table 2.2.

Table 2. 2: Constitution of coffee silverskin according to literature

Component	(Narita & Inouye, 2014) (%w/w, ar[1])	(Ballesteros *et al.* , 2014) (%w/w, db[2])	(Hijosa-Valsero *et al.* , 2018) (%w/w, db)
Proteins	18.6±0.6	18.69±0.10	14.43
Fat	2.2±0.1	3.78±0.4	4.97
Moisture	7.3±0.4	N.A.	4.81
Hemicellulose	N.A.	16.68±1.30	9.64
Cellulose	N.A.	23.77±0.09	10.33
Lignin	N.A.	28.58±0.46	29.1
Others	N.A.	N.A.	26.72

It is shown that CS is rich in proteins and presents a smaller fraction of lipids. As these are the components to be extracted in the experimental part of this work, more focus is given to them. The total amount of lipids is not as consensual as the percentage of proteins. Studies show that 2 up to 7% of coffee silverskin is constituted by fats, and that those results are dependent on the method of extraction (Toschi *et al.* , 2014).

Toschi *et al.*, studied extensively the total amount of fats present in CS using four different methods: Folch's method (it uses chloroform and methanol as solvents) (A), Soxhlet method with n-hexane (B) and petroleum ether (C) and direct solid-liquid extraction with n-hexane (D). The results are shown in Table 2.3

[1] %w/w, ar: weight percentage as received
[2] %w/w, db: weight percentage on a dry basis

Table 2. 3: Total lipid content (g/100 g CS) and lipid composition (% of total lipid matter) of CS as a function of the methods used (A, B, C, and D) (Toschi *et al.* , 2014):

	A	**B**	**C**	**D**
Total Lipids (%)	5.2±0.0	3.4±0.2	3.61±0.7	1.9±0.1
Lipid Profile				
FFA[3] (%)	58.4±2.3	20.7±3.8	24.1±3.4	30.9±7.0
S[4] (%)	16.7±0.3	12.9±0.4	13.7±0.9	32.9±5.6
DG[5] (%)	11.9±1.0	4.2±1.1	6.8±1.3	8.1±1.9
ES[6] (%)	3.7±0.5	14.6±2.7	6.4±1.4	9.1±1.8
TG[7] (%)	9.2±0.1	47.6±0.9	48.9±1.0	18.9±2.6

Not only it is observed that the amount of lipids retrieved is dependent on the method used, as the lipid profile is it as well. The polarity of the solvent seems to have importance: while method A used a slightly polar solvent and the lipid fraction was rich in FFAs and poor in triglycerides, the solvent used in B was unipolar and the lipid fraction was rich in triglycerides. The study showed, for the first time, the total fatty acid methyl esters composition and stated that its composition is similar to the one of coffee beans oil and roasted coffee beans oil. However, the discrepancies between the lipid profiles according to their extraction method makes these results somewhat inconclusive, therefore a precise lipidic composition of coffee silverskin is yet to be carried out.

[3] FFA: Free fatty acids
[4] S: Sterols
[5] DG: Diglycerides
[6] ES: Esterified sterols
[7] T: Triglycerides

The analyzed oil was obtained using method B since it is more sustainable than the others (Toschi *et al.* , 2014). Table 2.4 displays the most significant acids present in the coffee silverskin oil:

Table 2. 4: Total Fatty Acid Composition of CS, expressed in Lipid Basis (% of total fatty acids) (Toschi *et al.* , 2014)

	Total Fatty Acids (%)
Saturated Fatty Acids (CX:Y)[8]	
Palmitic acid (C16:0)	27.5±0.13
Behenic acid (C22:0)	11.5±1.86
Arachidic acid (C20:0)	10.8±1.54
Stearic acid (C18:0)	6.7±0.29
Unsaturated Fatty Acids	
Linoleic acid (C18:2)	29.2±2.14
Oleic acid (C18:1)	6.9±0.65

The study also found traces of myristic acid (C14:0), pentadecanoic acid (C15:0), heptadecanoic acid (C17:0), arachidonic acid (C20:4), and lignoceric acid (C24:0). The coffee silverskin oils according to Toschi *et al.* (2014) is richer in saturated fats than in unsaturated, their obtained percentage was of 60.63% and 39.37%, respectively.

Unfortunately, no protein profile was found in the literature. An overview of the amino acids retrieved through liquid hot water hydrolysis from coffee silverskin will be performed in this work.

[8] CX:Y; where X represents the total number of carbon atoms in the molecule, and Y is the number of insaturations

Besides the lipids and proteins, CS also contains phenolic compounds such as 3-, and 5-coumaroylquinic acid and antioxidant agents, which are linked to several health benefits. Nevertheless, this topic is still poorly investigated (Bresciani *et al.* , 2014).

2.3. Biomass Pretreatment

2.3.1 Milling

Milling is part of the physical pretreatment, alongside with grinding, and chipping. Its purpose is to reduce the particle size of lignocellulosic materials. Additionally, it causes a decrease in the degree of polymerization and decrystallization of biomass. The combination of physical pre-treatment alongside with other sorts of treatments is widely used. Usually, milling is the very first step of the pretreatment. The final size of the particle will depend on the type of physical pre-treatment done. "For example, after chipping and milling, the particle size reduces to 10–30 mm and 0.2–2 mm, respectively" (Mood *et al.* , 2013).

Particle size is very important regarding the rates of extraction of crude lipids, however, its reduction is limited due to the production of fines, which can lead to adverse effects on future steps of the process (Coats & Wingard, 1950). From a theoretical point of view, diminishing the particle size causes the diffusion pathway to be shorter, which leads to better extraction yields. The extraction, using supercritical carbon dioxide, of dog rose seed oil proved to be more efficient nine times when the average particle size changed from 1.4 mm to 0.27 mm (Jahongir *et al.* , 2019).

However, milling is an expensive process, not only it requires the initial investment to purchase the equipment, but it also has high energetical demands (Mood *et al.* , 2013). On an industrial scale, a cost evaluation should be performed to verify if the extraction rates increment due to smaller particle size is enough to compensate the milling's utility costs.

In this work, coffee silverskin pellets went through a milling and crushing process to evaluate the effect of particle size in the supercritical fluid extraction and liquid hot water hydrolysis.

2.3.1 Drying

The drying process of biomass consists of the removal of water by evaporation.

While in the biofuel industry, low moisture contents appear to be better, since high amounts of water in the biomass lead to low energy efficiency, low combustion temperatures, and the emission of hydrocarbons and particles (Ståhl *et al.* , 2004) in the field of supercritical extraction processes, Mouahid *et al.* , 2016, stated that optimal results were obtained when the samples presented a moisture content from 3 to 12%. Water could act as a barrier to the diffusion of CO_2 and the solutes. However, in other studies, water may act as a co-solvent, and therefore improve the extraction of polar compounds. Another example of the role of water in CO_2 extraction is the decaffeination of coffee. The presence of water in the coffee bean is essential to release the caffeine from its bound with the coffee matrix. Although caffeine is soluble in critical CO_2 without the presence of water its removal is not possible. Nevertheless, large amounts of water in the biomass may cause the blockage of the tubes during the CO_2 decompression, as the dragged water freezes. Therefore, a balanced moisture content is desired (Ponte, 2017).

The drying method appears to be important as well. Airflow drying followed by microwave radiation seems to improve the kinetics of the extraction using supercritical carbon dioxide of carotenoids from *Dunaliella salina* microalgae, when compared to only air flow drying and freeze-drying (Mouahid *et al.* , 2016).

The process of drying occurs through several stages that are displayed in Figure 2.4:

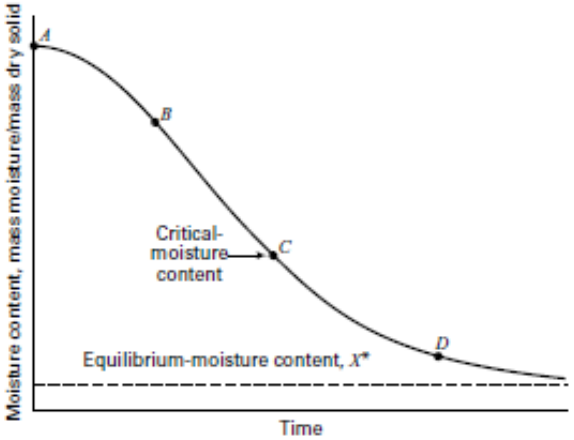

Figure 2. 4: Evolution of the moisture content as a function of time, and the different stages of the drying process (Seader *et al.*, 2011)

.

From stage A to B, the wet solid is being preheated to an exposed-surface temperature equal to the wet-bulb gas temperature. During this period, the moisture is evaporated at an increasing rate. From B to C the drying rate is constant. C represents the critical moisture content, and at this point, the drying rate starts to decrease. The moisture almost does not cover the surface of the solid. In the final period from D to E, evaporation occurs from water contained in the pores. The rate falls exponentially with decreasing moisture content. The equilibrium moisture content is then reached, meaning that there is no more loss of water and the drying can be terminated (Seader *et al.* , 2011)

2.4. Supercritical Fluid Extraction

It has been reported that supercritical fluid extraction (SFE) can be the most effective and efficient process to extract botanical valuable compounds. SFE uses supercritical fluids as solvents. Supercritical fluids are gases in high compression conditions, combining properties of gases and liquids altogether. Supercritical fluids have liquid-like density and gas-like viscosity (Kehili *et al.* , 2016). This leads to extractions which are very difficult, or even impossible, to perform with normal solvents. This process can be done extremely fast, within 10 to 60 minutes. Another important advantage is that a slight modification on temperature or pressure (once the conditions are made subcritical) will result in the precipitation of the solute. Supercritical fluids are able to produce a product free from solvent residues (Sapkale *et al.* , 2010). Furthermore, it has been described as an environmentally friendly and safe process (Kehili *et al.* , 2017).

Although carbon dioxide is the preferred supercritical solvent, many compounds can also be used, such as “ethylene, methane, nitrogen, xenon, and fluorocarbons”. However, carbon dioxide has been preferred in supercritical fluid extraction because it presents a lower critical temperature and pressure (Mouna, 2017).

In a nutshell, advantages of this technique include high selectivity, short time periods of extraction, non-toxic solvents are used and the production of solvent-free extracts. This combination of characteristics allows supercritical fluid extraction to be used in various industries such as cosmetic, pharmaceutical, and food.

2.4.1 Supercritical Carbon Dioxide: Properties & Set-Up

Carbon dioxide (CO_2) has been the main solvent used in SFE. Its supercritical temperature and pressure are 31ºC and 74 bar, respectively.

The application of this process using supercritical carbon dioxide (sc-CO_2) has been of main interest in the last decades, due to its critical temperature being close to room temperature, making it possible for biological materials to be processed at temperatures around 35ºC. At 200 bar the density of CO_2 is similar to the one of hexane, and its solvation characteristics are non-polar. Around its supercritical region, carbon dioxide dissolves triglycerides at concentrations up to 1% w/w.

Figure 2.5 displays a CO_2 pressure-temperature phase diagram. From the critical point (CP), the distinction between liquid and gas vanishes (Cristina, 2014).

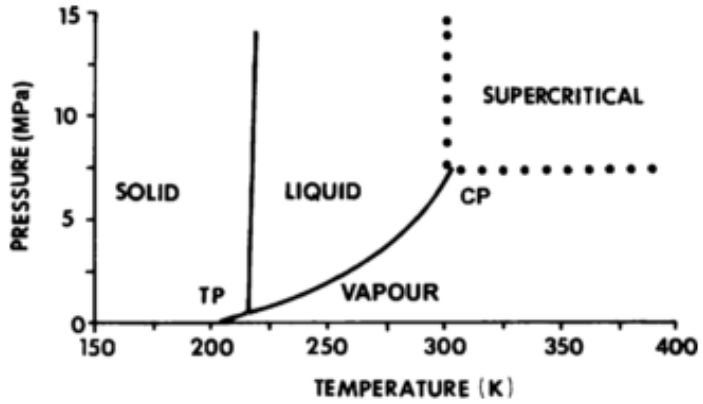

Figure 2. 5: CO2 pressure-temperature phase diagram (Cristina, 2014)

Figure 2.6 displays a sketch of a typical supercritical extraction unit for sc-CO_2.

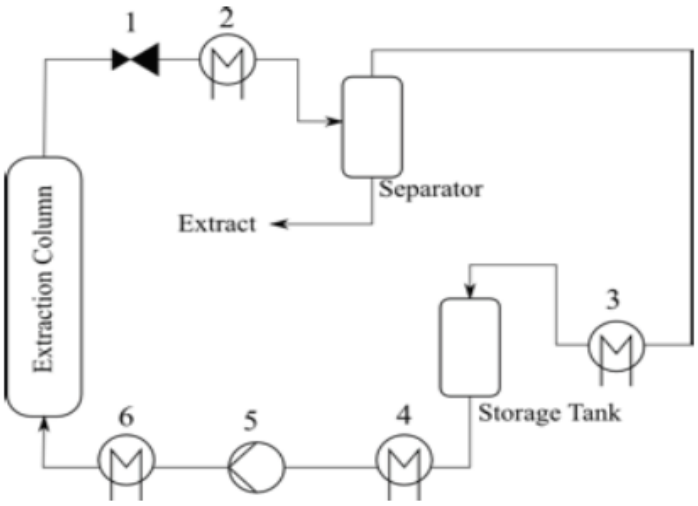

Figure 2. 6: Supercritical fluid extraction unit. 1-Decompression valve, 2-Heating for separation, 3- Cooling for storage, 4- Condensing for pump, 5-Pump, 6- Heating to extraction conditions (Baudron, 2014)

The fluid exits the storage tank and it is condensed (4) before reaching the pump (5) that increases the fluid pressure the operation pressure. Afterward, the fluid is heated (6) to the operating temperature. It then enters the extraction column from the bottom where the extraction between the supercritical fluid and the biomass occurs. After leaving the extractor, the fluid is decompressed (1), losing much of its solvent power. A heater is placed after the decompression (2) to avoid the formation of solids. In the case of carbon dioxide, those solids are known as “dry ice”. The mixture flows to the separator, where the extract precipitates due to the loss of the solvent power. Optionally, the fluid may be reused and flows back to the storage tank after being cooled down even further (3).

2.4.2 Solubility of Oils in Supercritical Carbon Dioxide

By nature, supercritical CO_2 is a non-polar, so the extractability of the compounds will depend on their functional groups, their molecular weight and polarity. Compounds with low polarity can be extracted at lower pressures (75-100 bar). Some examples are esters, ethers, ketones, and aldehydes. Other compounds with a moderate polarity usually are not soluble, such as proteins, polysaccharides, sugars, glycosides and inorganic salts (Kumar, 2015). This means that there is a high selectivity for lipids. With sc-CO_2 it possible to remove the lipids contained in coffee silverskin, while maintaining in the pellets the proteins, and sugars to be extracted in the following processes of the cascade.

The solubility of compounds in carbon dioxide is governed by its density and temperature. An increase of pressure will increase the carbon dioxide density which leads to higher solubility values. But temperature also affects density: the higher the temperature the lower the density. This would mean that the higher the temperature, the lower would be the solubility. Nevertheless, an increase in temperature will increase the vapor pressure which dictates a higher solubility. This density-vapor pressure relationship with temperature causes inflection points that can be seen in Figure 2.7**,** showing the solubility of peanut oil in carbon dioxide as a function of pressure and temperature. Before this point, density has the leading role, and a decrease in temperature causes solubility to go up. Afterward, the effect of vapor pressure becomes stronger, and higher temperatures promote higher solubilities (Baudron, 2014).

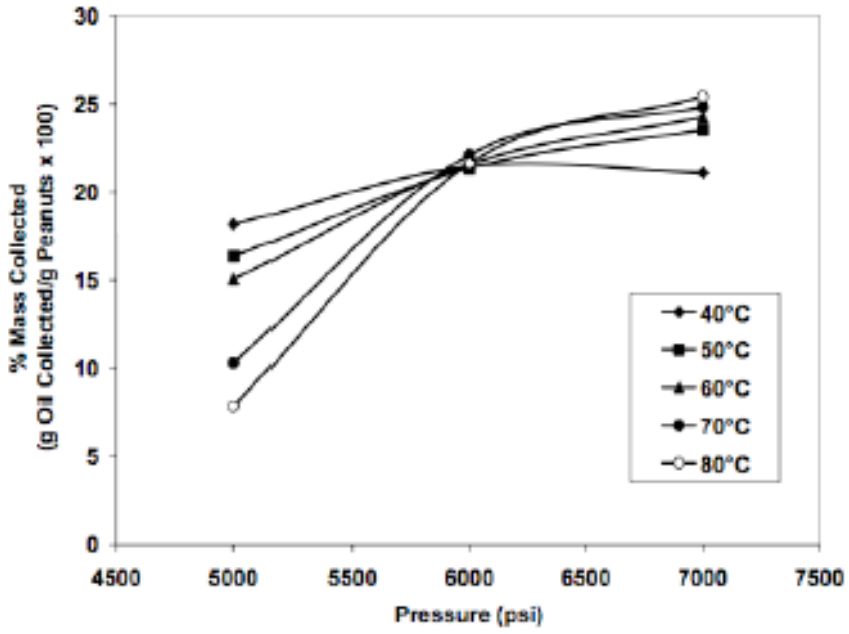

Figure 2. 7: Peanut oil extraction yield as a function of pressure and temperature, illustrating the inflection point (Baudron, 2014)

The solubility of coffee oils in supercritical CO_2 has been studied by De Azevedo *et al.* (2008a) The solubility was modeled by the equation proposed by Chrastil. Chrastil's equation can correlate the solubility of solids and liquids in supercritical fluids as a function of temperature and density. It has become very common to use this equation to extrapolate experimental data regarding the solubility of sundry compounds in supercritical fluids. It is able to reproduce experimental data in a fairly simple way (Bitencourt *et al.* , 2018). This model assumes that an equilibrium between the solute and

the fluid exits, forming a solvate complex that is constituted by molecules of the solute surrounded by molecules of the solvent. The relationship between the solubility of the solute in the supercritical solvent (C_{sat}), density of the solvent (ρ_{CO2}), and the temperature (T) is established using the adjustable parameters: k, A, and B. These parameters are obtained by minimizing the deviations between experimental and calculated data. Equation 2.1 displays Chrastil equation:

$$C_{sat} = {\rho_{co2}}^{k} \times e^{(\frac{A}{T} + B)} \tag{2.1}$$

Where C_{sat} is expressed in g_{oil}/L_{CO2}, ρ_{co2} is in g/L and T in K.

Figure 2.8 shows the experimental results, and the lines represent the data predicted by Chrastil equation (de Azevedo *et al.* , 2008a).

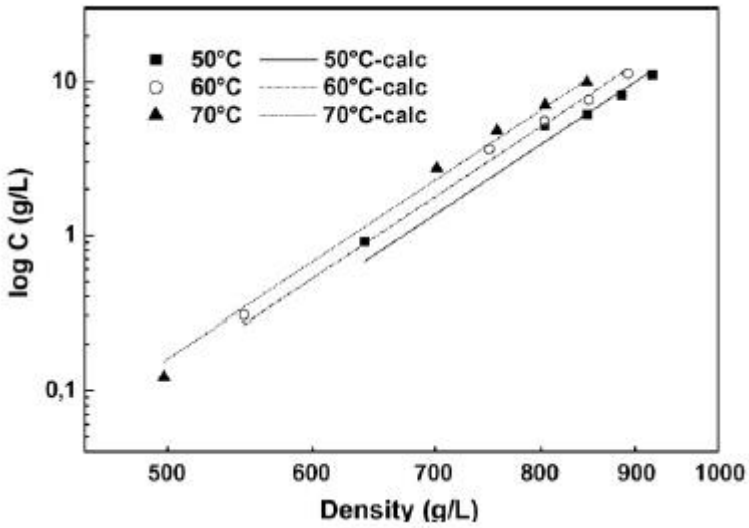

Figure 2. 8: Experimental data of the logarithm of green coffee oil solubility as a function of CO2 density) and results from the model of Chrastil (de Azevedo, 2008a)

The data by de Azevedo (2008a) follows the equation 2.2:

$$C_{sat} = {\rho_{CO2}}^{7.90} \times exp(-\frac{2869.20}{T} - 42.63) \tag{2.2}$$

Based on this equation. it is possible to estimate the solubility of the lipids contained inside coffee silverskin pellets at a given temperature and pressure, assuming that the composition from coffee bean oil is similar to the one from coffee silverskin.

2.4.3 Effect of the Particle size, the Shape of the Extractor and Solvent Flow Rate:

The influence of the particle size is unquestionable: mass transfer in gas extraction from solids heavily depends on the transport rate of the solid phase, and the size of the particle affects the transportation path. Smaller particle sizes cause the surface area exposed to the solvent to be higher (Baudron, 2014).

Smaller mean particle size favors the decaffeination of coffee beans, as it can be seen in Figure 2.9. Nevertheless, the extraction of theobromine from cocoa seed shells is hindered by particle size reduction as it is displayed in Figure 2.10. This is a matter of geometry. The original particles maintain an ellipsoid shape (like a bean) which provides space for the solvent to flow between the several layers of the particle (Brunner, 1994).

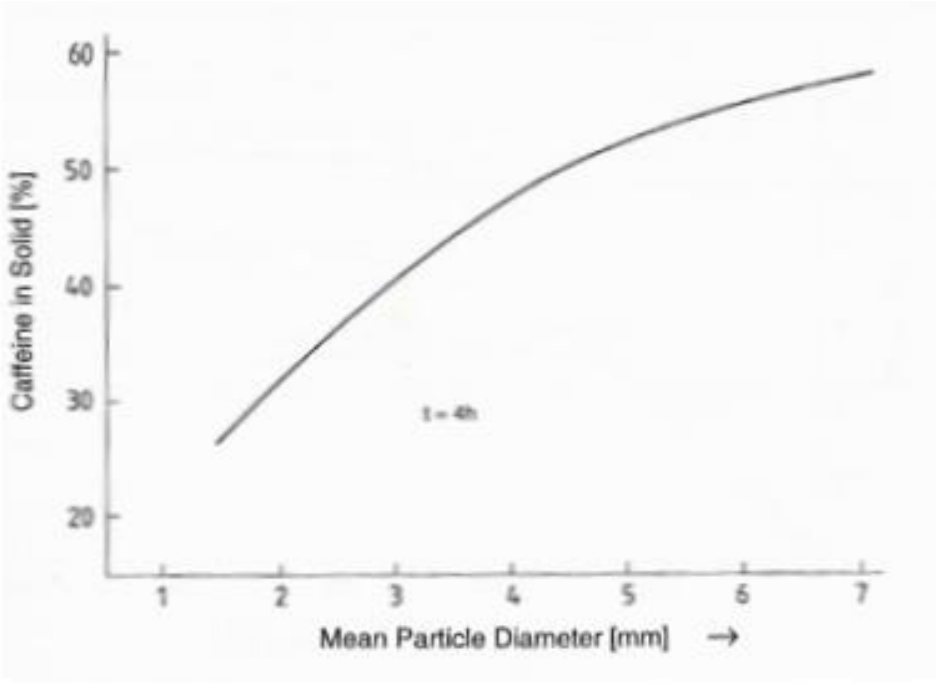

Figure 2. 9: Dependence of the extraction rate of caffeine as the function of the particle size of the coffee beans (Brunner, 1994)

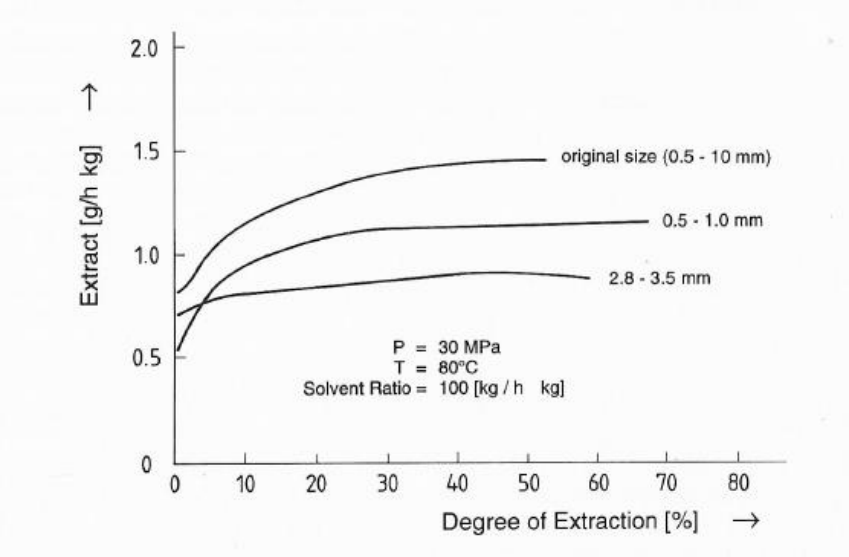

Figure 2. 10: Extraction of theobromine as the function of cocoa seed shell size (Brunner, 1994)

Furthermore, particles too small may lead to the formation of an air cake at the exit filter of the extractor, which clogs the column. This also causes "channeling", which is the formation of shortcuts that do not allow good contact between the solvent and the substrate, thus undermining the efficiency of the extraction (Baudron, 2014).

In SFE, axial dispersion of the fluid is observed. The hydrodynamic flow across the bed is not uniform, which causes axial dispersion. Radial distribution of the porosity is one of the causes. The porosity of the fixed bed increases in the neighboring of the wall (up to ε=1). This influence can be neglected when the ratio between the extractor diameter and particle diameter is higher than 10 (Brunner, 1994). Figure 2.11 displays the effect of the distance from the extractor's wall on the extractor's porosity.

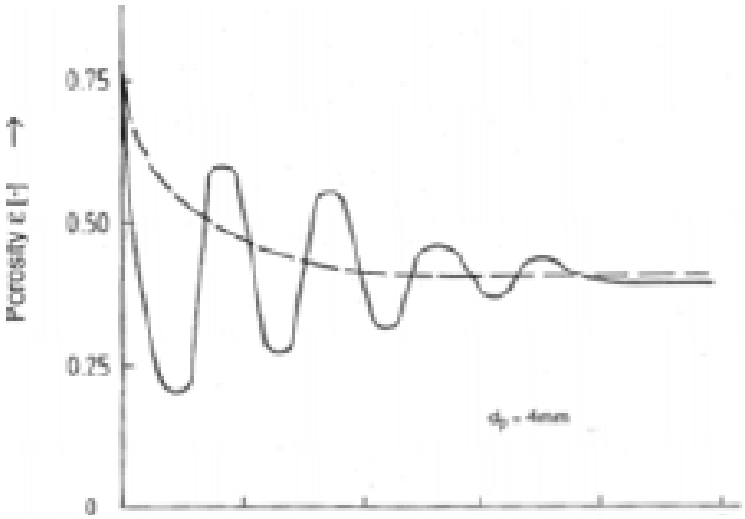

Figure 2. 11: Radial distribution of porosity in a fixed bed of particles (Brunner, 1994)

When external mass transfer resistance exists, the flow rate of the solvent is a relevant parameter. An increment of the flow rate causes an increase in the fluid velocity. Since the fluid flows around the solid, higher velocities decrease the thickness of the boundary layer, where the solute is diffused, which enhances the transfer rate. It also dilutes the extract, and since the mass transfer is driven by concentration difference, mass transfer is further improved (Baudron, 2014).

The flow rate has an influence on the solvent ratio, which the amount of solvent per amount of biomass input load. The higher the flow rate the higher the solvent ratio will be, given that the substrate amount is constant. The solvent ratio is the most important parameter once the pressure and temperature conditions are selected. Increasing solvent ratio leads to an enhanced extraction, this is shown in Figure 2.12, regarding the extraction of caffeine using supercritical CO_2 as a solvent.

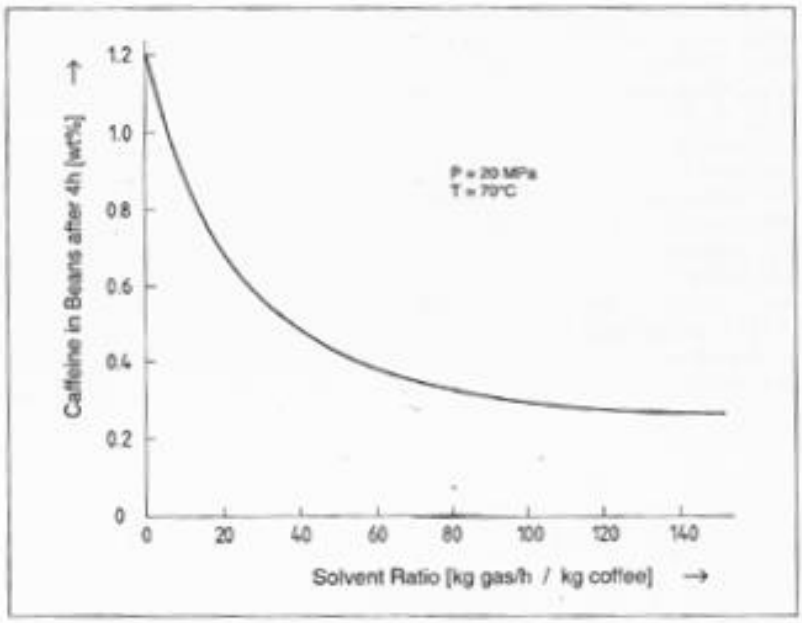

Figure 2. 12: Amount of caffeine in the coffee beans after 4 hours as the function of solvent ratio (Brunner, 1994).

Nevertheless, higher solvent ratios cause an increment in operational costs: larger equipment are required for higher solvent ratios, but as it also leads to greater extraction yields. Operation costs must be calculated according to each specific process (Brunner, 1994).

2.4.5 Extraction Process

Supercritical carbon dioxide flows around the particles to extract the solute which is present on their surface and inside them. The compounds found on the surface are easily accessible and are required only to be diffused through the film (or boundary layer) to be extracted. On the other hand, the solute inside the particle must be first through the pores of the particle, before reaching the bulk of the fluid. Figure 2.13 shows a visual display of the diffusion process during the supercritical fluid extraction.

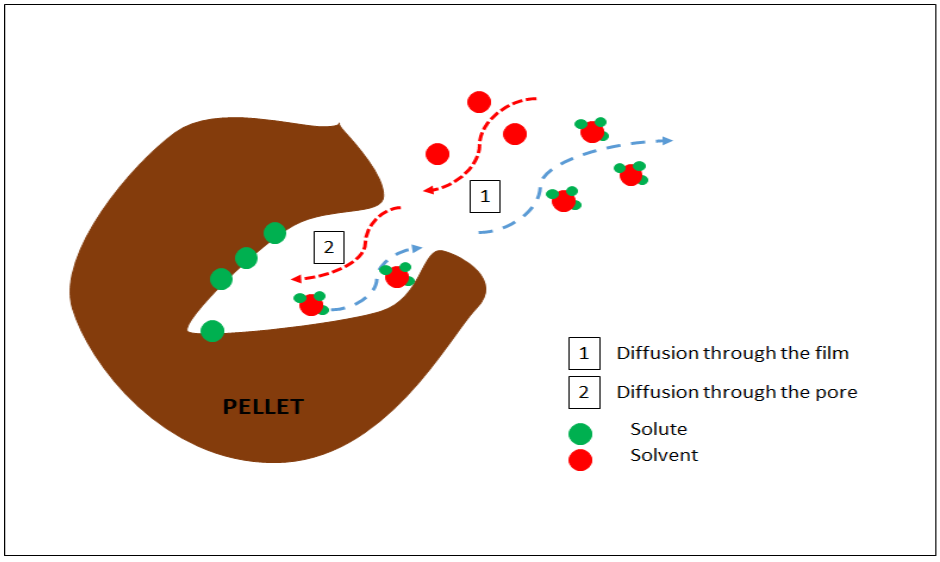

Figure 2. 13: Visual display of the diffusion process during the supercritical fluid extraction.

The extraction process in a fixed bed is characterized by three phases: I- constant extraction rate (CER), II- falling extraction rate (FER), and III- diffusion controlled (DC). These phases are shown in Figure 2.14. During the first stage, the extraction is quick, as the solute has only to be diffused through the film. As the amount of solute decreases, the second phase is reached. Now the solute is deeper inside the particle, which means that diffusion through the solid exists, which slows down the extraction. Lastly, at the end of the extraction, the solute is bound to the solid matrix, thus desorption is required so that it can be dissolved in the fluid. This limits the extraction even more (Baudron, 2014).

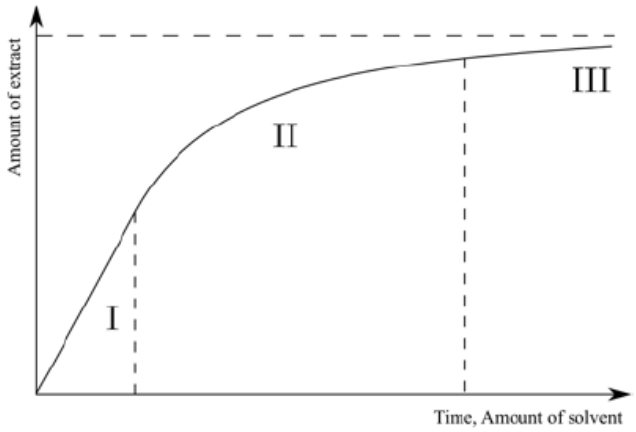

Figure 2. 14: Typical extraction curve of solids in a fixed bed (Baudron, 2014).

Figure 2.15 illustrates the behavior of the solute-solid interactions on the three stages of the extraction. In red, the solute with no interaction with the solid is displayed. Stage I is loaded with this kind of solute, both on the surface and within the particle, while in stage II it can only be found in a smaller amount inside the pores. In purple, the solute that is bound with the solid is shown (Baudron, 2014).

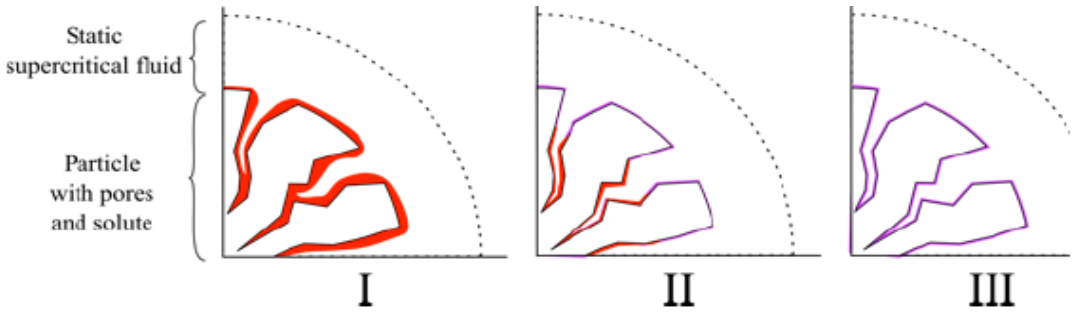

Figure 2. 15: Evolution of the solute profile throughout the extraction (Baudron, 2014).

2.4.6 Modeling

Supercritical fluid extraction is based on mass transfer concepts, such as particle and extractor dimensions, time of extraction, solvent flow, among others. For this reason, several mass balances, particle size estimation, solvent flow measurement must be performed in order to obtain the mass transfer parameters of the extraction, such as mass transfer coefficient, effective diffusion coefficient, dimensionless numbers, etc.

The values were obtained using the software "*BatchSFE*" developed by the Institute of Thermal Separation Processes of the Hamburg University of Technology. Three models were applied, and each one of them was based in one of the 3 stages of the extraction process (CER, FER and DC).

Constant Extraction Rate: Steady-state Extraction

Based on the mass balance of the first section of the extraction curve, and with the knowledge of the solubility of coffee oil silverskin oil in carbon dioxide (C_{sat}) at a given pressure and temperature, the solvent volume flow ($\dot{V}$) and the transfer surface area (A), which is equivalent to the sum of the surface area of all particles, it is possible to estimate the global mass transfer coefficient, β, and the number of transfer units (NTU). Figure 2.16 displays a very simple representation of the extraction in a fixed bed extractor.

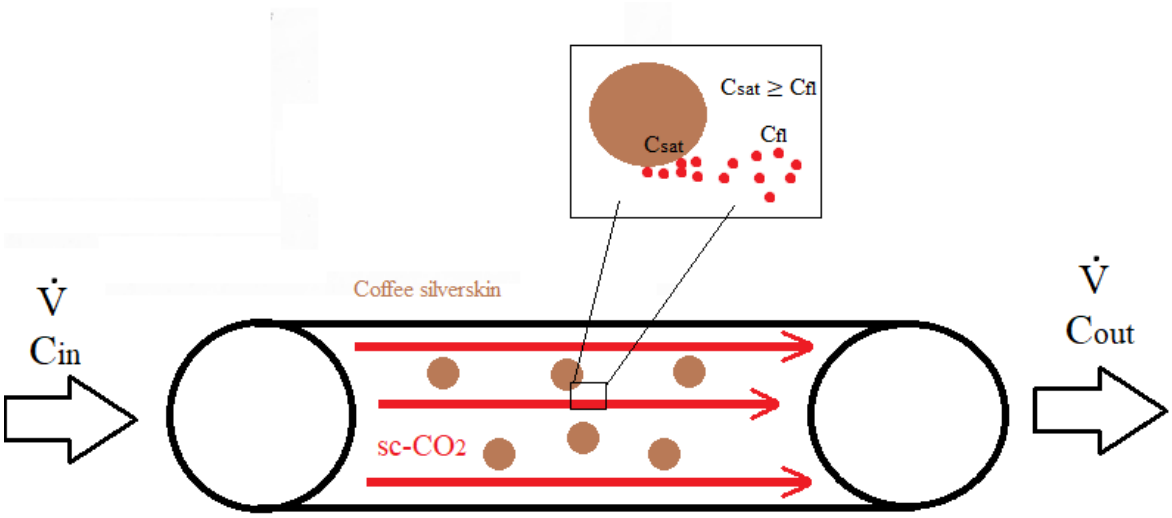

Figure 2. 16: Visual representation of the extraction process in a fixed bed extractor.

At the entrance of the extractor, the concentration of the solute in the fluid (C_{fl}) is represented by $C_{in,}$ whereas at the exit of the extractor it is represented by C_{out}. According to the schematic display presented in Figure 2.16, the balance for the whole extractor is given by Equation 2.3 (Schlunder & Tsotsas, 1988):

$$\dot{V}dC = \beta\,(C_{sat} - C_{fl})\,dA \Leftrightarrow$$

$$\Leftrightarrow \int_0^C \frac{dC}{C_{sat} - C_{fl}} = \frac{\beta\,dA}{\dot{V}} \Leftrightarrow$$

$$\Leftrightarrow \frac{C_{sat} - C_{out}}{C_{sat} - C_{in}} = e^{-\frac{\beta\,dA}{\dot{V}}} = e^{-NTU} \Leftrightarrow$$

$$NTU = \frac{\beta\,A}{\dot{V}} \tag{2.3}$$

And with the dimensionless numbers, Reynolds (Re), Schmidt (Sc), and Sherwood (Sh), are given by Equations 2.4, 2.5, and 2.6:

$$Re = \frac{\rho_{fluid}\,v\,d_p}{\mu_{fluid}} \tag{2.4}$$

$$Sc = \frac{\mu_{fluid}}{\rho_{fluid}\,\delta_{eff}} \tag{2.5}$$

$$Sh = \frac{\beta_F\,d_p}{\delta_{eff}} \tag{2.6}$$

Where ρ_{fluid} is the density of the solvent, μ_{fluid} is the viscosity of the solvent, d_p is the diameter of the particle, is the effective diffusion coefficient and β_F is the external mass transfer coefficient.

And the average flow velocity, v, is given Equation 2.7:

$$v = \frac{v_0}{\varepsilon_{bed}} \tag{2.7}$$

With v_0 being the superficial flow velocity and ε_{bed} being the porosity of the bed.

Equation 2.8 represents the macroscale phenomenon in a non-steady-state and considering that axial dispersion occurs (Baudron, 2014):

$$v\frac{\partial C}{\partial z}+\frac{dC}{dt}-\frac{D_{ax}\cdot\partial^2 C_{i(z,t)}}{\partial z^2}=m_{sub} \quad (2.8)$$

Where D_{ax} represents the axial diffusion coefficient, z represents the axial coordinate on the extractor and $m_{sub,steady}$ is mass transfer rate from the solid to the fluid

The axial diffusivity coefficient for spherical particles, D_{ax}, can be calculated with the Equation 2.9 (Lin *et al.* , 2013):

$$D_{ax}=\frac{v\,d_p}{Pe} \quad (2.9)$$

And the Peclet-Reynolds number relation is given by Equation 2.10 (Lin *et al.* , 2013):

$$Pe=\frac{0.2}{\varepsilon_{bed}}+\frac{0.011}{\varepsilon_{bed}}(\varepsilon_{bed}\,Re)^{0.48} \quad (2.10)$$

But assuming a steady state extraction (stage I), so that there is no change in the concentration of the solute in the bulk of the fluid with time, and that axial dispersion is neglectable, Equation 2.11 is obtained from Equation 2.8:

$$v\frac{\partial C}{dz}=m_{sub,steady} \quad (2.11)$$

Where $m_{sub,steady}$ is mass transfer rate from the solid to the fluid assuming steady-state extraction.

Some authors described that effect of axial dispersion in SFE can be neglected because the particle size is too small in comparison with the bed diameter (ratio smaller than 0.1) (Huang, 2015).

There are two points of view regarding the driving force: macro-scale and micro-scale. In the former, the driving force is the difference of concentration of solute in the solid and the bulk fluid phase and is represented by the overall mass transfer coefficient, β. On a micro-scale, first the solute must be diffused through the pores of the solid particle to

reach the surface, and afterward, it is diffused across the static layer (film) in the direction of the bulk fluid.

For the macro-scale the balance is as follows in Equation 2.12:

$$m_{sub} = \beta\ a_v(C_i - C_{fl}) \tag{2.12}$$

Where C_i is the concentration of the solute in the fluid in contact of the particle and C_{fl} is the concentration of the solute in the bulk fluid.

As for the micro-scale diffusion through the pores occurs, $\beta_{S\ is}$ the mass transfer coefficient in the solid. Afterward, there is diffusion through the film, with β_F being the mass transfer coefficient in the film:

$$m_{sub,int} = \beta_s\ a_v\ \left(C_i - C_{surface}\right) \tag{2.13}$$

$$and\ \beta_s = \frac{\delta_{solid}}{r_{particle}} \tag{2.14}$$

$$m_{sub,ext} = \beta_F\ a_v\ \left(C_{surface} - C_{fl}\right) \tag{2.15}$$

$$and\ \beta_F = \frac{\delta_{eff}}{L_{film}} \tag{2.16}$$

Where $C_{surface}$ is the concentration of the solute in the fluid at the surface of the particle, δ_{eff} is the effective diffusion coeffient, L_{film} is the length of the film. And in steady state extraction rate, both Ci and Csurface will be equal to Csat.

From the values of β_S and β_F, the Biot number (Bi) is calculated according to equation 2.17. The Biot number relates the external and internal mass transfer.

$$Bi = \frac{\beta_F}{\beta_S} = \frac{\beta_F\ r_{particle}}{\delta_{eff,solid}} \tag{2.17}$$

The higher the Biot number the lower is the external mass transfer resistance.

The overall mass transfer coefficient is given by both external and internal coefficients by equation 2.18:

$$\frac{1}{\beta} = \frac{1}{\beta_S} + \frac{1}{\beta_F} \tag{2.18}$$

And since the diffusion in the pores is slower than in the film:

$$\frac{1}{\beta_F} \ll \frac{1}{\beta_S} \rightarrow \beta \sim \beta_S \, , and \; \beta_S = \frac{\delta_{eff,solid}}{r_{particle}} \tag{2.19}$$

In the steady-state stage, the solvent is saturated, so Ci is equal to Csat. Substituting the terms from equation 2.19 in equation 2.11 and 2.12, equation 2.20 is obtained:

$$m_{sub,steady} = \frac{\delta_{eff,solid}}{r_{particle}} a_v \left(C_{sat} - C_{fl}\right) \Leftrightarrow$$

$$\Leftrightarrow v \frac{\partial C}{\partial z} = \frac{\delta_{eff,solid}}{r_{particle}} a_v \left(C_{sat} - C_{fl}\right) \Leftrightarrow$$

$$\Leftrightarrow \frac{C_{sat} - C_{out}}{C_{sat} - C_{in}} = e^{-\left(\frac{\delta_{eff,solid} \cdot a_v}{v \times r_{particle}} \times L_{reactor}\right)} \tag{2.20}$$

In which, a_v is the specific surface area of a sphere:

$$a_v = \frac{6}{d_p} \tag{2.21}$$

The experimental data was inserted in the software, and the effective diffusion coefficient of the solute in the solid, $\delta_{eff,\,solid}$, can be determined.

To visually understand the diffusion of the solute in the particle and in the fluid, Figure 2.17 is displayed (Baudron, 2014):

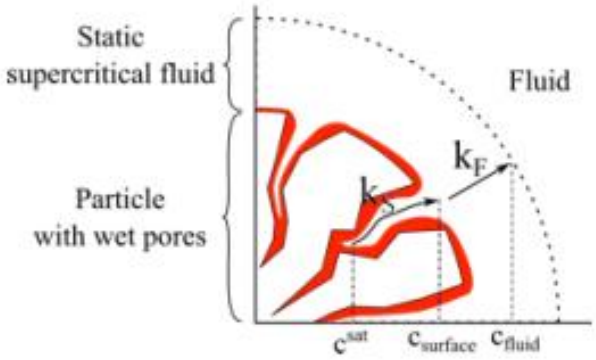

Figure 2. 17: Steady state model and diffusion of the solute, in red,) within the particle pores and through the film (Baudron, 2014).

Falling Extraction Rate: Shrinking Core

As the extraction goes, the amount of solute starts to deplete. This means that the solvent has to go deeper in the particle to extract the solute, making the internal diffusion path longer. The extraction is no longer occurs in a steady state. Desorption is not considered as there is no solid-fluid interaction at this point. From equation 2.8 we discard the effect of axial dispersion and equation 2.22 is obtained:

$$v\frac{\partial C}{\partial z}+\frac{dC}{dt}=\ m_{sub} \tag{2.22}$$

From the previous modeling, the internal diffusion coefficient is known. For spherical particles, the relationship is according to equation 2.23 (Baudron, 2014).

$$m_{sub}=\ \frac{1-\varepsilon_{particle}}{\varepsilon_{particle}}\frac{3\beta_F}{r}\left(C_{i,r}-C_{fl}\right) \tag{2.23}$$

All the parameters are rewritten, and the Biot number is used as the fitting parameter in this new model:

$$Bi=\frac{\beta_F\ r}{\delta_{eff,solid}} \tag{2.24}$$

The $\delta_{eff,solid}$ is known from the last modeling in steady state. Changing the Biot number in the software, so that it may fit the experimental data, gives access to the β_F. Using β_F and the Sherwood correlation with the Reynolds and Schmidt numbers, the effective diffusion coefficient, δ_{eff}, is calculated using Equation 2.25:

$$Sh = \frac{\beta_F \, d_p}{\delta_{eff}} = Sh_0 \; + a \, Re^b Sc^c \tag{2.25}$$

Where Sh_0, a, b and c are parameters dependent on the geometry of the reactor and particle and flow conditions. The values of these parameters change according to the authors, Table 2.5 displays some examples of the different parameters of Sherwood-Reynolds-Schmidt correlations.

Table 2.5:Sherwood correlation parameters values

Correlation	Sh_0	a	b	c	Validity	Source
Steinberger & Treybal (1960)	2	0.35	0.62	0.33	Single sphere 1<Re<3x10^4 0.6<Sc<3200	(NPTEL, 2019)
Tan et. al (1988)	N.D.	0.38	0.83	0.33	2<Re<40 2<Sc<20	(Lin *et al.*, 2013)
Catchpole (1993)	N.D.	0.82	0.66	0.33	1<Re<70, 3<Sc<11	(Lin *et al.*, 2013)
J.W. King (1997)	N.D.	0.26	0.5	0.33	Re < 1 70<Sc<100	(Baudron, 2014)

Diffusion Controlled: Diffusion, Desorption and Dispersion Model

Lastly, the remaining solute is bound with the solid, so there is a partition between the solid and the fluid phase. A desorption model is considered. Now, no shrinking core is taken into consideration. The diffusion path of the solute inside the particle is defined as an average length. The hypothesis is that the average path is determined by assuming that the surface of the area that is still rich in solute is six times smaller than the surface area of the full particle (Baudron, 2014). This model is named VT-II and it was developed by staff members of the TVT. Figure 2.18 displays a diagram of the solute rich core assumed by this model.

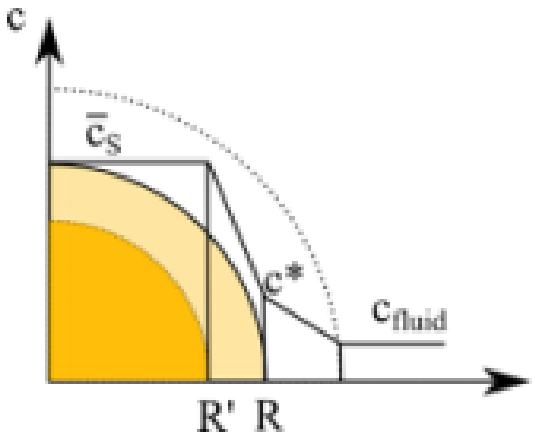

Figure 2. 18: Solute rich core, in yellow, in the VT-II model (Braudon, 2014)

In which:

$$\left(\frac{R'}{R}\right)^2 = \frac{1}{6} \tag{2.26}$$

With the known β_S and β_F from the previous models, the overall mass transfer coefficient, β, is calculated. The driving force is the difference of concentrations between the fluid in the pores and the bulk fluid as in Equation 2.12.

But now, the concentration inside the pore is defined by an equilibrium between the solid and the fluid phase. The relationship is expressed by the partition coefficient, K, according to equation 2.27.

$$C_i = K\, C_{solid} \tag{2.27}$$

Equation 2.27 displays the relation between the Biot number and the external and overall mass transfer coefficient as an arrangement of equation 2.17:

$$\frac{\beta_F}{\beta} = 1 + Bi \tag{2.28}$$

And with the introduction of the partition coefficient, the definitions of equation 2.28 changes:

$$\frac{\beta_F}{\beta} = 1 + Bi \cdot \frac{K}{6} \tag{2.29}$$

By manipulating K, so it may fit this model, a new Bi is obtained. In turn new values for β_F, β_S, and β, δ_{eff}, and Sh are obtained as well.

The dimensionless numbers calculated by the software can be inserted in a chart to be compared with some existing empirical correlations. Figure 2.19 displays a graphic containing some Sherwood correlation according to different authors (Zetzl, 2019)

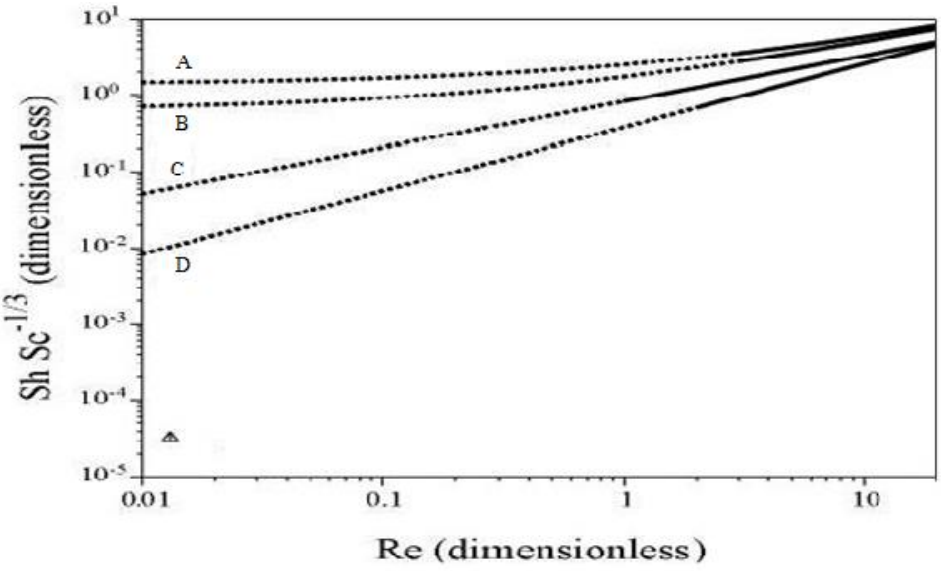

Figure 2. 19: Sherwood-Schmidt number as function of Reynolds number. A, B: Wakao & Kugei, (1982) for Sc = 3 and Sc = 32, respectively. C: Tan et al. (1988). D: King & Catchpole (1993) (Zetzl, 2019).

2.5. Liquid Hot Water Treatments for Protein Extraction

Liquid hot water (LHW) pretreatment combines the usage of high-temperature water at high pressures, which are employed to assure that the water is kept in a liquid state known as subcritical water (SCW). It has been demonstrated that LHW is an efficient method to treat lignocellulosic biomass (Mood *et al.* , 2013). In alkaline hydrolysis, biomass is treated with a basic solution of high pH. An overview of the current state of the art for the extraction of proteins from biomass using LHW and alkaline hydrolysis is given below.

2.5.1 Proteins

Proteins are polymers composed of carbon, hydrogen, oxygen, nitrogen, and sulfur, whose basic structural units are amino acids (AA). There are 21 different types of AAs, which can be obtained by hydrolysis processes. Their classification is dependent on their carbon chain's characteristics. They contain acid and basic functional groups. In amino acids, the carboxyl group binds with the amine group of another AA by a peptide bond, as displayed in Figure 2.20 (Gunawardena, 2019).

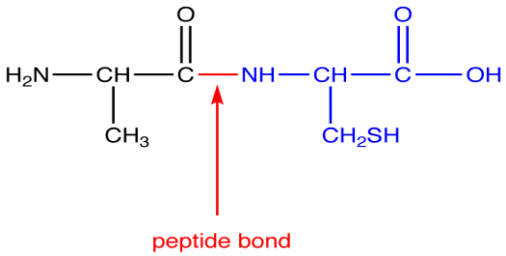

Figure 2. 20: Visual display of a peptide bond in a protein (Gunawardena, 2019).

Amino Acid Solubility: Effect of pH and Temperature

The solubility if a given amino acid is dependent on the value of its isoelectric point (pI). The pI represents the pH value for which the molecule has no charge. Near it, the solubility of a given AA is at a minimum. Amino acids can be divided as hydrophilic (polar) and hydrophobic (non-polar). Hydrophilic amino acids can be divided into three other categories: neutral, acid (negatively charged) and basic (positively charged). The acidic amino acids, aspartic and glutamic acids, possess a carboxylic acid as part of their side chain, which makes them donor of protons. The basic AA, such as lysine, histidine, and arginine, are proton acceptors (Kovach, 2013). There are also some special cases of amino acids, which do not fit the former categories, and these include glycine, cysteine,

selenocysteine, and proline. Table 2.6 displays the classification and the isoelectric point of some of the existing amino acids (Ball (2019) Sigma Aldrich (2019)).

Table 2. 6: Examples of some of the amino acids and respective classification and pI (Ball (2019) Sigma Aldrich (2019)).

	Classification	**pI**
Alanine	nonpolar	6.0
Valine	nonpolar	6.0
Serine	polar, uncharged	5.7
Threonine	polar, uncharged	6.5
Arginine	basic	10.8
Histidine	basic	7.6
Lysine	basic	9.8
Aspartic acid	acidic	3.0
Glutamic acid	acidic	3.2
Glycine	special	6.0

The minimum of solubility of an amino acid is found in the vicinity of the isoelectric point and the solubility increase is directly proportional to the quantity of acid or base added (Needham, 1970). These conclusions lead to believe that in general, at a very high or a very low pH, the overall solubility of a random mix of proteins would be higher than at a neutral pH (distilled water at 25ºC). Figure 2.21 demonstrates that idea. DL, L-, or D-, are referred to the optic properties of the amino acid (Fuchs *et al.* , 2006):

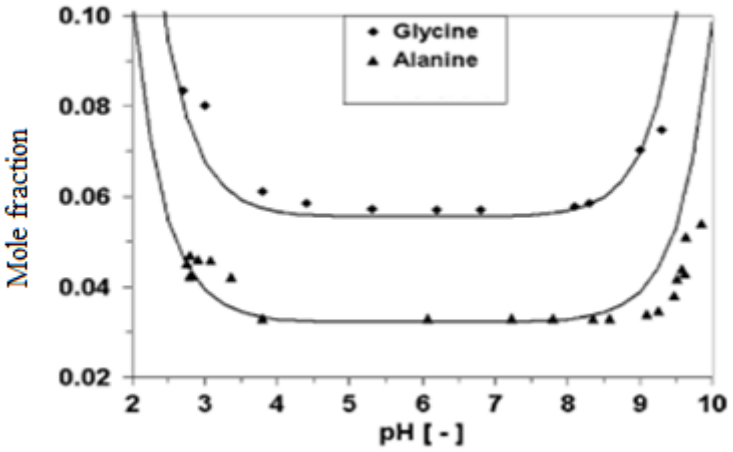

Figure 2. 21: Solubility of glycine and DL-alanine (mole fraction) in aqueous electrolytes as function of pH at 298K (Fuchs *et al*., 2006)

For instance, the solubility of alanine, which pI is 6, is at a minimum at the boundaries of its isoelectric point. At very low and very high pH, the solubility increases. The same can be observed with glycine, which isoelectric point is also 6.

Temperature also plays a critical role in the solubility of amino acids. Higher temperatures increase the ionic power of water, which drives the formation of hydronium (H_3O^+) and hydroxide ions (OH-). Thus, water starts to act as an acid or basic catalyst (Powell *et al.* , 2016). Figure 2.22 displays the solubility (in molar fraction) of some amino acids as a function of the water temperature.

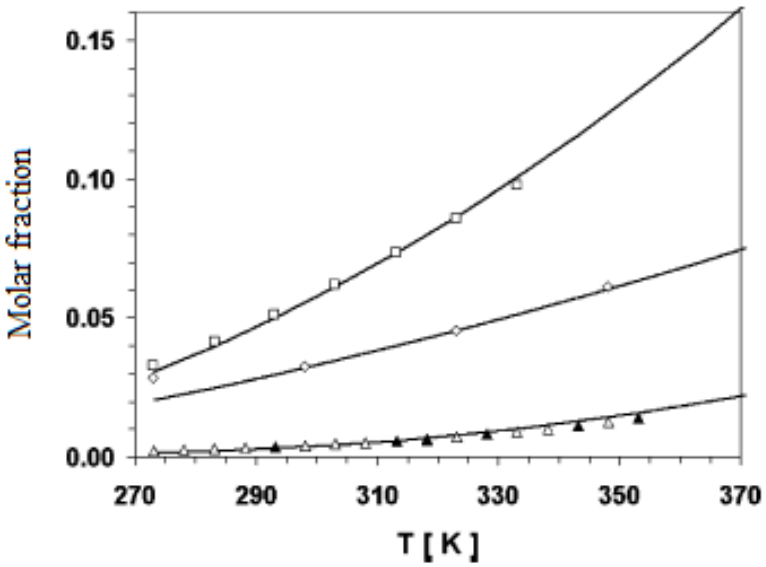

Figure 2. 22: Solubility of glycine (squares), DL-alanine (diamonds), and DL-methionine (triangle) in water (molar fractions) as a function of temperature (Fuchs et al., 2006)

In conclusion, the solubility of amino acids varies widely. They can either be (almost) completely insoluble or dissolve in their hundreds of milligrams per milliliter of solvent (Nahar *et al.* , 2017).

2.5.2 Liquid Hot Water for the Extraction of Amino Acids

In its subcritical state, water acquires new proprieties. The ionic product, kW, increases, making it greater in three orders of magnitude when compared to water at ambient conditions. The increase in kW drives the formation of hydroxide (OH^-) and hydronium (H_3O^+) ions, which makes subcritical water act either as an acid or as a basic catalyst (Powell *et al.* , 2016). The maximum value of the ionic product of water is found at a temperature of 300°C (Kw = 10^{-11} and pK_w =11). A medium rich in OH^- and H_3O^+ is created, favoring reactions such as hydrolysis. In a hydrolysis reaction, a molecule is split into two by the addition of a water molecule (Alonso, 2018). Due to these properties, LHW can be used as a solvent and reactant simultaneously. Subcritical water (SCW) displays properties of a nonpolar solvent, making it suitable for C–C bond formations. Table 2.7 shows the pKw of water at different conditions of temperature and pressure (Wu *et al.* , 2008).

Table 2. 7: pKw of water at different temperatures and pressures (Wu *et al.*, 2008)

	Ordinary water	**Subcritical water**	**Supercritical water**	
Temperature (ºC)	25	250	400	400
Pressure (MPa)	0.1	5	25	50
pKw	14	11.2	19.4	11.6

LHW is regarded as a clean process as it produces no toxic substances and it is more environmentally friendly than using organic solvents (Contreras *et al.* , 2019), which has been attracting interest for biomass conversion including hydrolysis of lignocellulose, proteins, carbohydrates, lipids, and extraction of bioactive compounds (Powell *et al.* , 2016).

Rogalinski *et al.* , (2008) concluded that LHW is suitable for high yields of sugar recovery from rye straw and rye silage, although undesired degradation products are formed at more severe conditions. In this case, the particle size did not interfere with the yield of extraction and, in fact, the results were slightly higher for untreated biomass. From an industrial point of view, this means that the comminution would not be necessary, and energy could be saved.

Awaluddin *et al.* (2016) managed to extract proteins from *Chlorella vulgaris* using subcritical water extraction and studying the effect of temperature (180-374ºC), extraction time (1-20 minutes), particle size (38-250 μm), and biomass loading (5-40 %ww). The highest protein concentration of 31.16 g/100 g (31% yield) was obtained when 5 wt.% microalgal biomass with an average 90 μm particulate size was treated at 277°C, for 5 minutes. However, by statistical analysis, the best results should be obtained at 281ºC for 17 minutes, with an average particle size of 75 μm and a biomass loading of 45%ww. They concluded that the most crucial factor for protein extraction was the initial biomass loading. For protein extraction, a smaller particle size seems to improve the extraction yield. At a size of 38 μm the yield was around 17%, while for 250 and 90 μm, with the other parameters constant, the protein extraction yield was 11 and 10%, respectively. Interestingly, for sugar extraction the particle size was not very important, as stated by Rogalinski *et al.* (2008). Temperatures too high have a negative effect on protein extraction due to protein denaturation. Denaturation occurs when the molecular kinetic energy of the proteins increases, leading to the protein vibration and consequently destroying the protein's tertiary structure. Therefore, after an optimum temperature point is found, the temperature should no longer be increased to avoid denaturation (Awaluddin *et al.* , 2016).

Sereewatthanawut *et al.* , (2008) investigated the recovery of proteins and amino acids from deoiled rice brans. Their study changed the parameters of temperature (100-220 ºC) and time (0-30 min). It concluded that SCW can be used to effectively hydrolyze proteins from deoiled rice brans. The yields were generally higher as time and temperature were. However, thermal degradation occurred at higher temperatures and residence times. The highest yield of protein was 219 mg protein/ g rice bran, obtained at 200 ºC and at a time of 30 min. The study also tested the performance of protein extraction with alkaline hydrolysis (with a solution of NaOH 0.2M), but only at the low temperature of 30ºC. The

result from the alkaline hydrolysis was not as satisfactory as the ones from SCW at higher temperatures, nevertheless, it was higher than the extraction using plain water at 25ºC.

Another study with *C. vulgaris* from Phusunti *et al.* , (2017) focused on the recovery of proteins and further pyrolysis of the spent algae to produce bio-oil. The effect of time (90-180 minutes), temperature (150-220ºC) at a pH of 7.47 was studied**.** The biomass to solvent ratio was 1:6. The greatest protein removal was obtained at a temperature of 200 °C and a time of 180 min: 52.68% of the initial protein content of the biomass was retrieved. Afterward, these conditions were selected to study the effect of pH (2-12). In this case, lower pH (2) indicated higher protein extraction: 92% of the proteins contained in the C. vulgaris were extracted.

2.5.3 Alkaline Hydrolysis for the Extraction of Amino Acids

Generally, alkaline protein extractions present better results than acidic ones. The use of alkalis breaks the disulfide cross-links in proteins. Also, neutral and acidic amino acids are ionized at higher pH (Contreras *et al.* , 2019). The reactions involving amino acids and bases, or acids, are displayed in Figure 2.23 (Ball, 2019):

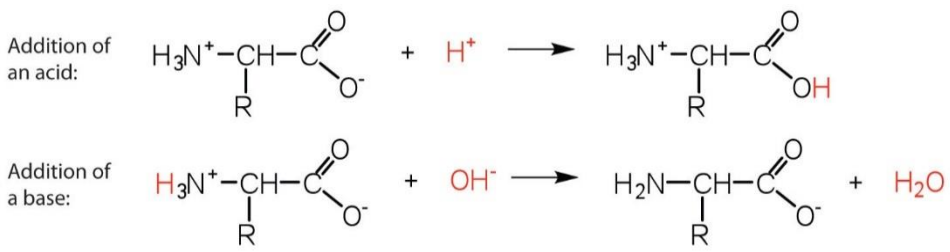

Figure 2. 23: Reaction of amino acid with base or acid. “R” indicates an organic chain deprived from a functional group (Ball, 2019).

At high pH values, the concentration of OH^- is higher, and hydroxide acts a proton acceptor, the positively charged amino side from the AA donates a proton, thus forming a salt and a water molecule.

Zhang *et al.* , (2014) studied the effect of pH, temperature and the total amount of alkali using green tea residues (GTR). They stated that applying higher temperatures on alkaline hydrolysis improves the protein yield. They also demonstrated that the absolute amount of alkali (in mmol) as a function of the mass residue is important for a successful

extraction. To obtain high yields (95% recovery of the initial protein content in the biomass) at 95ºC from green tea residue at least 3.2 mmol of NaOH was required to process 1g of proteins. To reach a yield of 80%, 4 mmol NaOH was needed at 60 ºC to process 1 g GTR, whereas at 80 ºC only 3 mmol of NaOH was required.

Sari (2015) studied the effect of pH on the extraction of proteins from soybeans, the results are displayed in Figure 2.24

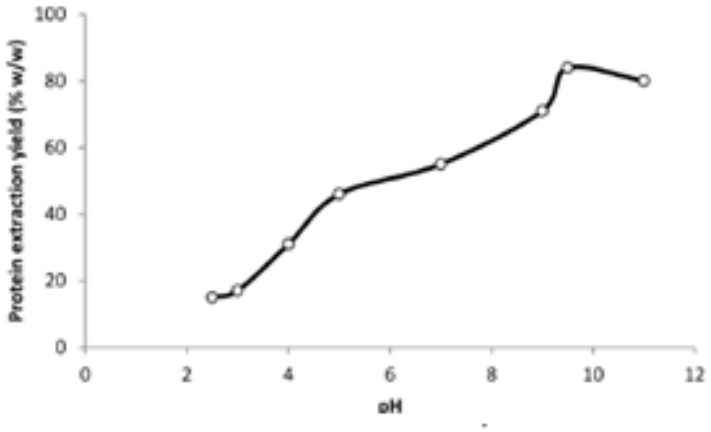

Figure 2. 24: Protein extraction yield from soybeans as a function of pH (Sari, 2015)

While the results obtained by Phusunti *et al.* (2017) indicated that low pH favor the extraction of proteins from algae, Sari (2015) attained higher extraction yields at high pH values as indicated by Figure 2.24. This might demonstrate that the origin and composition of the biomass is an important factor for extraction yield. Different biomasses have different protein profiles, therefore different solubilities. Biomass rich in acidic (negatively charged) amino acids is expected to present better results at high pH.

Fernández *et al.* , (1999) studied the effect of pH and biomass ratio on the extraction of proteins from *Atriplex lampa* leaves. Their results are present in extractable nitrogen. Higher concentrations of nitrogen correspond to greater concentrations of proteins and amino acids. Higher nitrogen values were obtained at the pH of 10 and at the minimum leaves-solvent ratio (1:5). It was suggested that chloroplasts are destroyed more easily at high pH, making amino acids more easily accessible to OH^-.

Another study in a fixed bed reactor concluded that the optimum conditions for protein extraction from wheat bran were 80ºC, for 30 minutes at a pH of 9.3. With these

conditions, 92% of the proteins present in the wheat bran where recovered (Alonso, 2018).

It can be concluded that a consensus regarding the perfect conditions for protein extraction does not exist regarding the effect of pH. However, higher temperatures generally promote the extraction of proteins if the denaturation temperature is not reached. The different characteristics of every sort of raw matter play an important role in the yield as a function of temperature, pH, biomass loading, particle size, the total amount of alkali (in the case of alkaline hydrolysis), and reaction time.

2.5.4 Recovery of Proteins from Coffee Silverskin using LWH, acid and alkaline hydrolysis

The extraction of proteins and sugars from coffee silverskin was carried out by Narita & Inouye (2012)using SCW, acid and alkaline hydrolysis at different temperatures. The results are displayed in Table 2.9**.**

Table 2. 8: Protein extraction yield from coffee silverskin at different conditions (Narita & Inouye, 2012).

Solvent	**Temperature (ºC)**	**Protein yield (%)**
Water	25	3.3
Water	80	4.5
Water	180	9.5
Water	210	15.7
Water	240	15.5
Water	270	12.5
Sol.[9] 0.1M HCl	25	4
Sol.[9] 0.1M HCl	80	5
Sol.[9] 0.1M NaOH	25	7.6
Sol.[9] 0.1M NaOH	80	9.7

The protein yield for coffee silverskin was maximum at 210 and 240ºC, 15.7 and 15.5%, respectively, while using subcritical water as the solvent. This represents a recovery of roughly 83.4% of the proteins present in the coffee silverskin used in their study. At higher temperatures it dropped to 12.5%, leading to believe that denaturation of coffee silverskin proteins started between 210 and 240ºC. Basic hydrolysis demonstrated better results than an acid one at both temperatures. The sugars yields were the lowest at 240 and 270ºC, 2.3 and 1.6% respectively. This indicated a higher selectivity of proteins at

[9] Solution of

higher temperatures. The high extraction degree obtained under the subcritical water condition could be caused by the enhanced hydrolysis of proteins, solubilization of insoluble proteins, and degradation of coffee silverskin cell wall.

LHW processes also were able to extract permit. The results by Narita & Inouye (2014) were analogous with the protein ones. A maximum yield was attained at 210ºC, and it started to decrease afterward. Their study also showed that sugars were also recovered from LHW treatment.

3. Methods and Materials

3.1. Coffee Silverskin

The coffee silverskin pellets were provided by Coffein Compagnie (Bremen, Germany). They presented a cylindric shape with an average length of 16.15 mm and a diameter of 5.99 mm. They were then submitted to drying pretreatments to decrease their humidity. All the experiments of this work were performed with dried coffee silverskin except when noted.

3.2. Drying and Determination of the Moisture Content

The drying rate at 45 ºC was calculated by performing mass balances. Each sample was weighed before being placed in the oven and after being taken out.

All the coffee silverskin pellets used throughout this project were oven-dried for 72 hours at 45ºC.

The initial moisture content of the pellets was calculated by two methods: oven-drying for 3 hours at 105ºC (performed by the author), and freeze-drying (performed by TUHH Central Lab). The samples were weighed before and after their respective drying method, and a mass balance was performed. The mass losses were assumed to be just from water.

The moisture removed from the drying was calculated according to equation 3.1:

$$Water\ removed\ (\%w/w)\ =\ \frac{M_{Input}\ -\ M_{final,drying}}{M_{input}} \times 100 \qquad (3.1)$$

Where M_{input} is the initial amount of coffee silverskin placed in the oven, and $M_{final,drying}$ is the mass of remaining coffee silverskin after 3 hours of drying at 105'C.

3.3. Milling

The coffee silverskin pellets were submitted to two sorts of particle size reduction methods. Coffee silverskin indicated as "Crushed Pellets" was crushed manually using a mortar and a pestle. Coffee silverskin designated as "Milled Pellets" was milled with a simple coffee grinder. A 3-tray sieving tower (630, 125, 32 µm wide) was used to separate the different particle sizes of the milled pellets. Of the particles that were retained in the top sieve (630 µm), it was considered that the largest particle was 1500 µm. For the

particles that were retained under the bottom sieve (32 µm), it was considered that smallest particle was 10 µm.

3.4. Supercritical Fluid Extraction Set-up

All supercritical fluid extraction experiments were performed in a 1.4 cm x 30 cm cylindric extractor manufactured by SPe-Ed Separations, Allenton (USA). Two pieces of glass wool were placed in both ends of the extractor to the passage of smaller particles to the capillary tubes. Figure 3.1 displays a simple sketch of the extractor used. The temperatures and pressures displayed in the sketch are merely for illustrative purposes:

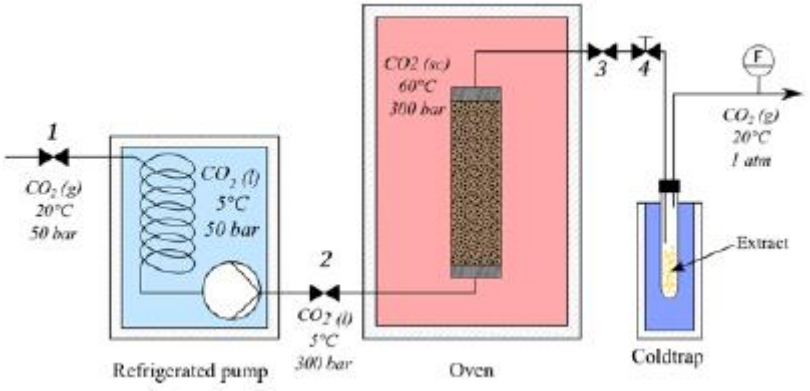

Figure 3. 1: Schematic diagram of the supercritical fluid extraction set-up.

Carbon dioxide entered the refrigerator pump at room temperature and 50 bar, and it was cooled down until -15ºC and pressurized up to the operational conditions (350, 400 or 450 bar, according to the experiment). Afterward, it was heated up to the operational temperature (40, 50 or 60ºC, according to the experiment). After the extraction, carbon dioxide is decompressed to atmospheric pressure whilst being heated (Valve 4), this avoids the formation of dry ice. At lower pressure, CO_2 loses its solvent power, and the extract is precipitated. Valve 4 is also responsible for the carbon dioxide flow control.

At first, the crushed coffee silverskin pellets were submitted to supercritical fluid extraction with carbon dioxide for 90 minutes at different pressures (350, 400, and 450 bar) and temperatures (40, 50 and 60ºC). Samples were taken after 5, 10, 15, 30, 45, 60, and 90 minutes. This way, it was possible to build an extraction yield curve as a function of time. The batch input for each experiment was of about 25 grams.

At 450 bar and 60ºC, four different particle size ranges were studied. For calculation purposes, the particles were considered spheres with the following diameter range: [630-

1500], [125-630], [32-125], and [10-32] µm. Samples of extract were taken after 5, 10, 15, 30, 45, 60, and 90 minutes to build an extraction curve for subsequent modeling. The batch load was of about 20 grams for each experiment.

In every experiment, the average solvent flow was approximately 1,96gCO_2/min. All biomass loads were measured using an analytical scale (±0.001g).

3.5. Extracted Lipids Characterization

The extract samples were analyzed by the "Zentrallabor Chemische Analytik/Central Lab". The lipidic composition of the extract was determined by gas-liquid chromatography with a flame ionization detector of the free acid methyl esters (FAME). The FAMEs are produced through a transesterification process between methanol and triglycerides in the presence of sodium hydroxide. The results were presented in the amount of FAME per amount of sample.

3.6. Liquid Hot Water Treatment

The liquid hot water treatment for the extraction of proteins was performed in the batch reactors displayed in Figure 3.2:

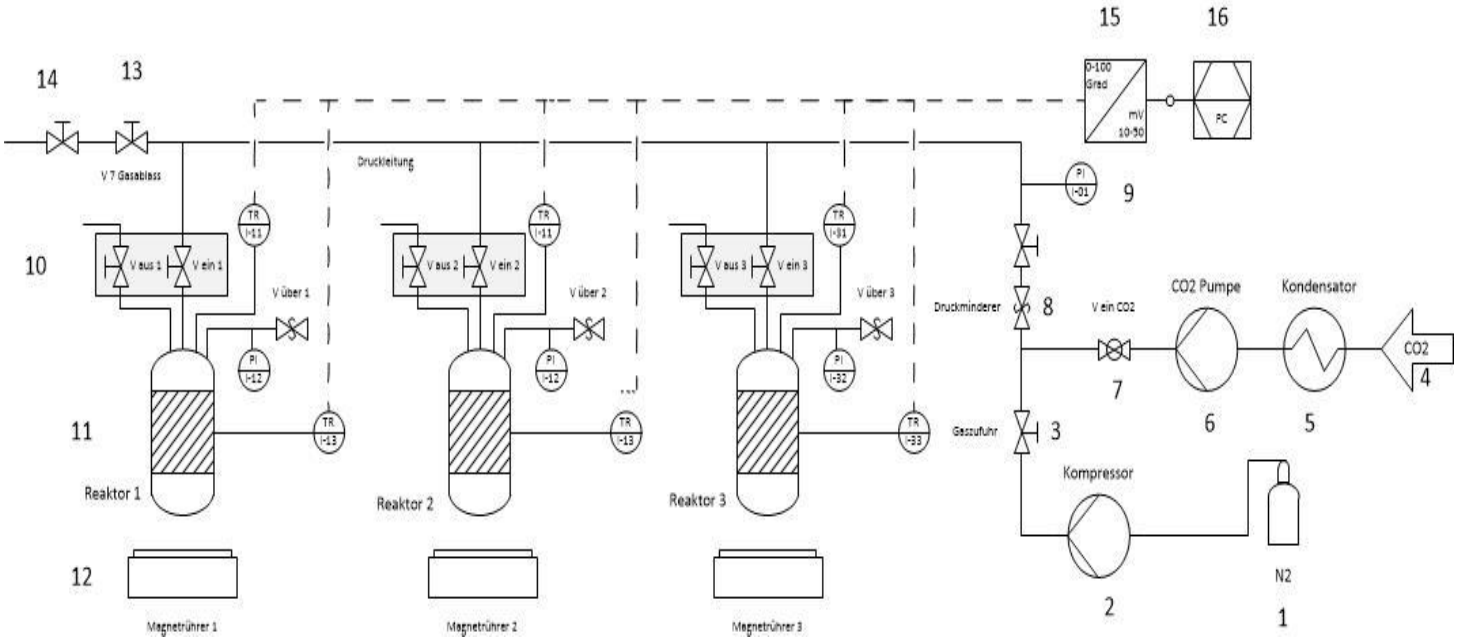

Figure 3. 2: Sketch of liquid hot water treatment equipment used.

Table 3.1 links the different parts of the whole apparatus to their respective indices:

Table 3. 1: Constituents of the LHW Equipment used

Index	Apparatus	Index	Apparatus
1	N_2 supply	**9**	Manometer
2	N_2 compressor	**10**	Valve panel for reactor
3	N_2 blocking valve	**11**	Batch reactor
4	CO_2 supply	**12**	Magnetic stirring plate
5	Condenser	**13**	Pressure unloading valve
6	CO_2 pump	**14**	Valve
7	Ball valve for CO_2 supply	**15**	Data collector
8	Pressure valve	**16**	PC with control software

For every experiment, an amount of about 0.6 g of coffee silverskin and 29.4 g of water were used. These masses were measured on an analytical scale (±0.001g).

The LHW treatment of coffee silverskin was divided into two parts:

-The effect of NaOH concentration in the protein extraction of full raw pellets, crushed pellets and extracted (by SFE) crushed pellets at 120ºC for 30 minutes. This allowed studying the impact of pH, granulometry and a previous supercritical fluid pretreatment.

-The effect of residence time (30 and 60 minutes) and temperature (90, 105 and 120ºC) on full extracted pellets at a constant NaOH concentration of 0.05 mol/L.

All experiments were conducted at 20 bar (using nitrogen gas), with a stirring of 250 rpm. The reactor temperature was increased using heating jackets controlled by a proportional–integral–derivative controller (PID). The sodium hydroxide had a purity of 99% and was provided by Sigma-Aldrich.

After the end of each experiment, the liquid (hydrolysate) was separated from the remaining coffee silverskin using a filter and a funnel. Afterward, to separate the hydrolysate from the finer particles that passed through the filter, centrifugation for 10 minutes at 4500 rpm (acceleration factor of 9, and deacceleration factor of 4) and 25ºC was performed. The hydrolysate was sent to the central lab for subsequent analysis.

The yield was calculated according to equation 3.2:

$$Y_{Proteins} = \frac{M_{Amino\ Acids}}{M_{input}} \times 100 \quad (3.2)$$

In which:

$Y_{Proteins}$: Protein extraction yield

$M_{Amino\ Acids}$: Total amino acids mass present in the sample

M_{input}: Input mass

3.7. Other Methods

The following methods were not performed by the author of this work:

Characterization of the Extracted Amino Acids

The samples were analyzed by the "Zentrallabor Chemische Analytik/Central Lab". The free amino acid content was determined by High-Performance Liquid Chromatography coupled with a Fluorescence Detector.

Apparent and Skeletal Density of the Milled CS Pellets

The apparent density of the milled coffee silverskin pellets was calculated by filling a 20±0.03 mL volumetric flask and measuring its mass in an analytic scale (±0.001 g).

The measurement of the skeletal density of the milled coffee silverskin particles was performed using a helium gas pycnometer. All the experiments were performed by lab technicians.

Cloud Point Solubility of the Lipids Extract by SFE

Cloud point solubility was performed by the lab technicians. It estimated the solubility of the obtained extracts in supercritical carbon dioxide at different temperatures and pressures.

The cloud point solubility is calculated by introducing a known amount of extract (complex mixture) in a high-pressure cell. Two sapphire windows are mounted on the cell and there is a light source on one side and a magnifying glass on the other. The unoccupied volume of the cell is filled with a given mass of supercritical CO_2. The cell is heated and pressurized to a point where only one phase can be found. Afterward, the pressure is gradually reduced until a two-phase system is observable. When this new phase appears, the liquid droplets or the solid particles absorb the light and the mixture

becomes cloudy, thus the name cloud point solubility. The solubility at that given temperature and pressure will be quotient between the input mass of extract and the mass of CO_2 inside the cell. If this process is repeated with different extract or CO_2 masses, a solubility plot as function of pressure and temperature can be rendered.

4. Results and Discussion

4.1. Drying and Supercritical Carbon Dioxide Extraction of Lipids

4.1.1 Dimensions of the Pellets Before and After Drying and Supercritical Fluid Extraction

The length and diameter of the original pellets were measured. Originally, the coffee silverskin pellets had a length of 16.15 ±2.22 mm, and a diameter of 5.99 ±0.09mm. As for the diameter after drying, a sample of 20 pellets was taken out of the oven after 1, 4, 24, 48 and 72 hours and then measured. The average results are shown in Table 4.1.

Table 4. 1: Diameter change of the pellets during the drying process at 45ºC as a function of time.

Time (hours)	Diameter (mm)
0	5.99 ± 0.09
2	5.93 ± 0.09
4	5.86 ± 0.07
24	5.81 ± 0.08
48	5.83 ± 0.05
72	5.88 ± 0.09

By analyzing Table 4.1, it is possible to verify a small reduction of the pellet's diameter. After 72 hours there was a decrease of diameter from 5.99 to 5.88 mm. Percentage-wise, this decrease corresponds to 1.89% of the original diameter. After 24 hours the smallest average diameter was found. It is likely that 24 hours inside the oven is enough to obtain the maximum decrease in diameter (5.81±0.08). The subsequent increases in diameter after 48 (5.83±0.05mm) and 72 hours (5.88±0.09mm) can be attributed to a lack of exactness since only 20 samples were measured in a population of thousands of pellets. Moreover, taking into account the standard deviations, all the measured diameters overlap each other after 4 hours of the drying process.

Two supercritical fluid extractions at 350 bar and 60ºC were performed with original and dried pellets to determine the change of the pellet's diameter after the extraction, the results of both experiments are shown in Table 4.2.

Table 4. 2: Diameter change of original and dried pellets after supercritical fluid extraction at 350 bar and 65ºC

		Diameter (mm)	Deviation(mm)	Swelling (%)
Original	Before	6	0.09	5.96
	After	6.35	0.23	
Dried	Before	5.91	0.09	4.29
	After	6.17	0.18	

In both cases, swelling of the pellets occurred, which indicates that supercritical carbon dioxide affected the cellular wall of the coffee silverskin.

Exposition at pressurized carbon dioxide before supercritical fluid extraction has been proven by Stamenic *et al.* (2010) to be an efficient way of improving the overall extraction yield for valerian root and ginger rhizome particles, and thyme, mint, sage and rosemary leaves. When exposed to pressurized CO_2 for 6 hours, the different biomasses obtained an increase of its thickness up to 45%. The effect of this pretreatment had a greater impact on the second stage of the extraction, which is controlled by the rate of diffusion through the particles of the plants. In every type of biomass studied, there were energy saving when using pretreated biomass. Stamenic *et al.* (2010) suggested two effects: first, the effect of a quick decompression and tensions inside the material leading to rapid expansion of the gas inside the solid matrix, second, the diffusion of supercritical CO_2 inside the pores of the material, partly dissolving in the tissues and taking more volume than the one that is available.

In conclusion, previous exposure of the biomass at pressurized CO_2 before the supercritical extraction itself can lead to better yields.

4.1.2 Absolute and Equilibrium Moisture Content

As mentioned in Chapter 3.2, the initial moisture content of the biomass was determined using two different methods: oven-drying at 105ºC for 3 hours and freeze-drying. The results of both methods are shown in Table 4.3.

Table 4. 3: Coffee silverskin pellet's initial moisture content on a wet basis.

	Water content (%w/w)
Oven-dried	18.70±0.11
Freeze-dried	17.8

Both methods showed similar values, but much higher than the ones found in the literature. For instance, Narita & Inouye (2014) reported a maximum 7.3% of water (in wet basis) in coffee silverskin, while Hijosa-Valsero *et al.* (2018) reported 4.97% (on dry basis). This can be explained by different pretreatments that the coffee silverskin pellets used during the study and the ones of the literature suffered.

For all further calculations, the moisture content that was considered was the one determined by the oven-drying method: 18,7%.

The evolution of the moisture content as a function of time was measured. It was assumed that initially, the pellets contained 18.7% of water on a wet basis. Figure 4.1 shows the moisture content as a function of the time of drying.

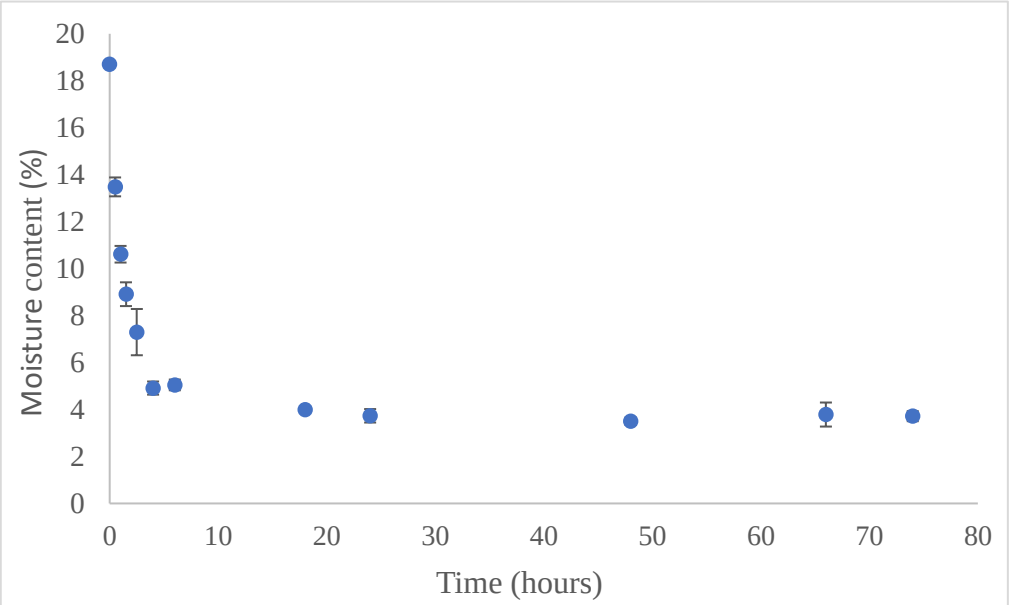

Figure 4. 1: Moisture content of the coffee silverskin pellets as a function of time of drying

The moisture content quickly decreases within the first 4 hours and completely stabilizes after 24 hours inside the oven. Therefore, 72 hours of drying are enough for the pellets to reach their equilibrium moisture content. After 72 hours, the pellets moisture content is 3.72 ±0.21 % on a wet basis. The biomass lost 14.98% of its original weight.

The effect of moisture content on supercritical fluid extraction was already studied. Mouahid *et al.* (2016), concluded that adding water to increase the moisture content of *Dunaliella salina* from 6% to 23%, increases the extraction yield by 1.8 times by means of sc-CO_2 extraction at 300 bar and 60ºC. However, moisture content did not play a significant role in the extraction of paprika oil using sc-CO_2 extraction (at 450 bar and 50ºC) when the initial moisture content of paprika ranged from 7 to 18%. For values above 20%, the extraction was undermined (Nagy & Simándi, 2008). Taher *et al.* (2014) concluded that freeze-dried algae (*Scenedesmus sp*.) obtain better extraction yield than untreated ones. After freeze-drying, the moisture content of the algae drops from 18.0 to 8.3% and a lipidic yield of 5.5 and 6.6% was obtained, respectively. These conclusions might indicate that different kinds of biomass are more easily extractable with higher moisture contents than others, as well as process conditions.

On an industrial scale, less drying time is a synonym of energy savings. Furthermore, if the drying step can be avoided, it is a tremendous advantage in terms of operating costs.

4.1.3 Effect of Temperature and Pressure on the Total Extraction Yield of Crushed Coffee Silverskin Pellets

The following figures (4.2-4.4), show the yield of extraction at different pressures and temperatures as a function of time of crushed silverskin pellets. The calculation of the lipid's extraction yield was done according to Equation 4.1:

$$Y_{lipids} = \frac{M_{fat,t}}{M_{input}} \times 100 \quad (4.1)$$

Where Y_{lipids} is the yield of the SFE, M_{input} is the input load of coffee silverskin, and $M_{fat,t}$ is the mass of extract collected at a given time.

By observing Figure 4.2 it is possible to verify that there is a small increase in the extraction yield at a higher temperatures. At 350 bar the obtained yields after 90 minutes were 2.33, 2.51, and 2.57% at 40, 50, and 60ºC, respectively. No major discrepancies are visible in the extraction rate during the first minutes of the extraction. In other words, at 350 bar, the temperature did not affect how fast the extraction happened. The effect of temperatures between 40 and 60ºC at this pressure can be assumed to be negligible. Differences in the extraction yields can be attributed to the lack of reproducibility since each experiment was only performed once, therefore no standard deviation can be calculated.

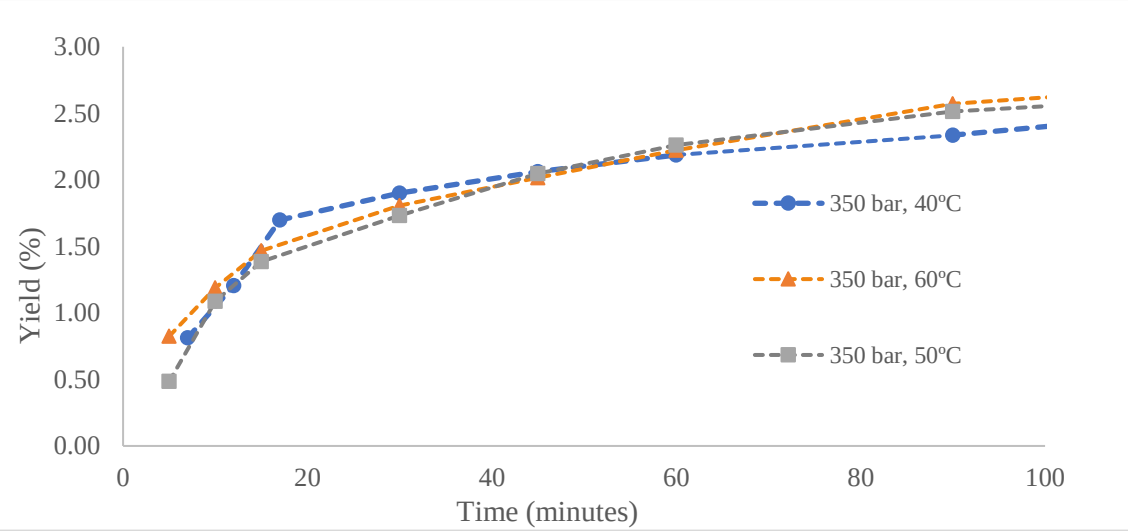

Figure 4. 2: Yield of recovery at 350 bar and different temperatures as a function of time.

At 400 bar, temperature as a greater impact on the initial extraction rates. This is observable in Figure 4.3. The yields obtained were 2.81, and 3.12% after 90 minutes at 40 and 50ºC, respectively, and 3.08% after 80 minutes at 60ºC. However, the extraction at 60ºC ended 10 minutes earlier, which can explain a slightly smaller yield when compared to the one at 50ºC. During the constant extraction rate phase, the extraction was faster at 60ºC, within the first 15 minutes, a yield of 2.18% had been attained, whereas at 40 and 50ºC, both yields were lower than 1.50%. Interestingly, the extraction was initially faster at 40ºC than at 50ºC, within the first 15 minutes a yield of 1.52, and 1.16% was obtained at 40, and 50ºC, respectively. But with the increase of time, the yields become very similar to each other. At 400 bar the difference between the maximum yields of the smallest and highest temperatures is similar to the one at 350 bar. For example, at 350 increasing the temperature from 40 to 60ºC led to a yield increase of 10.1%, while performing the same temperature changes at 400 bar, an increase of 9.61% was obtained.

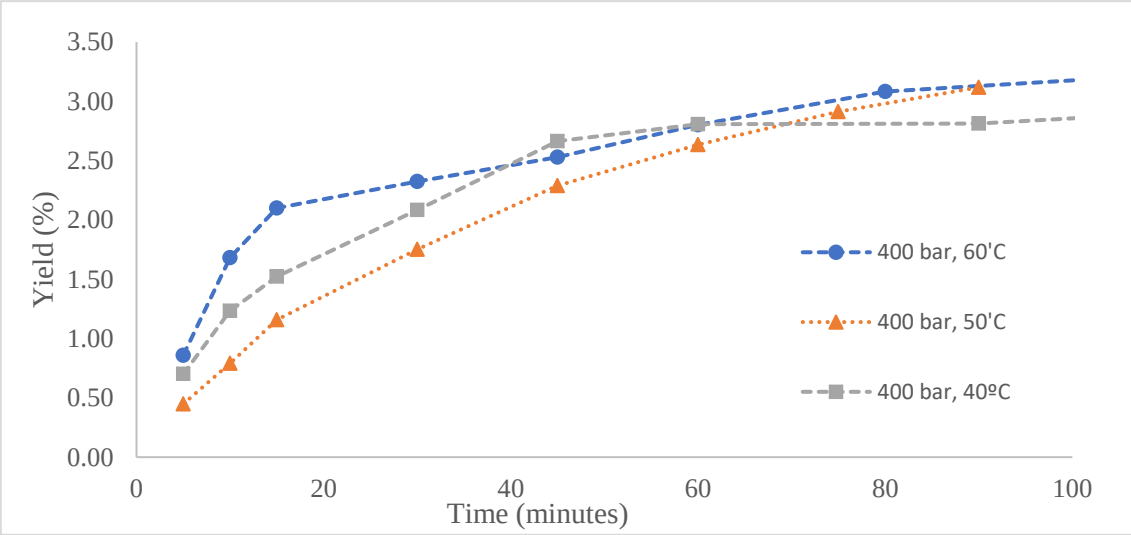

Figure 4. 3: Yield of recovery at 400 bar and different temperatures as a function of time.

Figure 4.4 displays the yield of recovery at 450 bar and different temperatures. Unlike at 400 bar, at different temperatures, the extraction rate did not suffer any significant changes, although that in the first 15 minutes the extraction at 60ºC is 29.2% greater than at 50ºC, while at 400 bar that difference was of 81.0%. The maximum extraction yields were 2.49, 2.54, and 3.34% at 40, 50, and 60ºC respectively. At this pressure., increasing the temperature sharply increased the yield. An increase of 34.1% was obtained from

changing the temperature from 40ºC to 60ºC. This large variation in the yield goes in conformity with literature data, as at higher pressures, temperature plays a more significant role in the solubility of oils in supercritical carbon dioxide (Baudron, 2014).

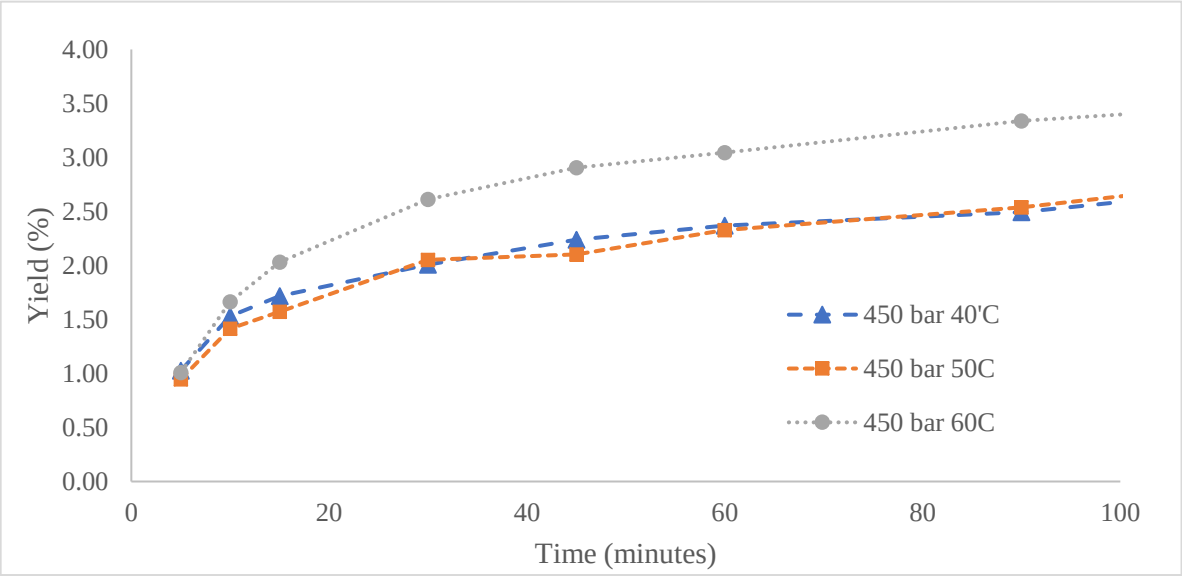

Figure 4. 4: Yield of recovery at 450 bar and different temperatures as a function of time

Figure 4.5 displays the maximum extraction yields for each set of experiments.

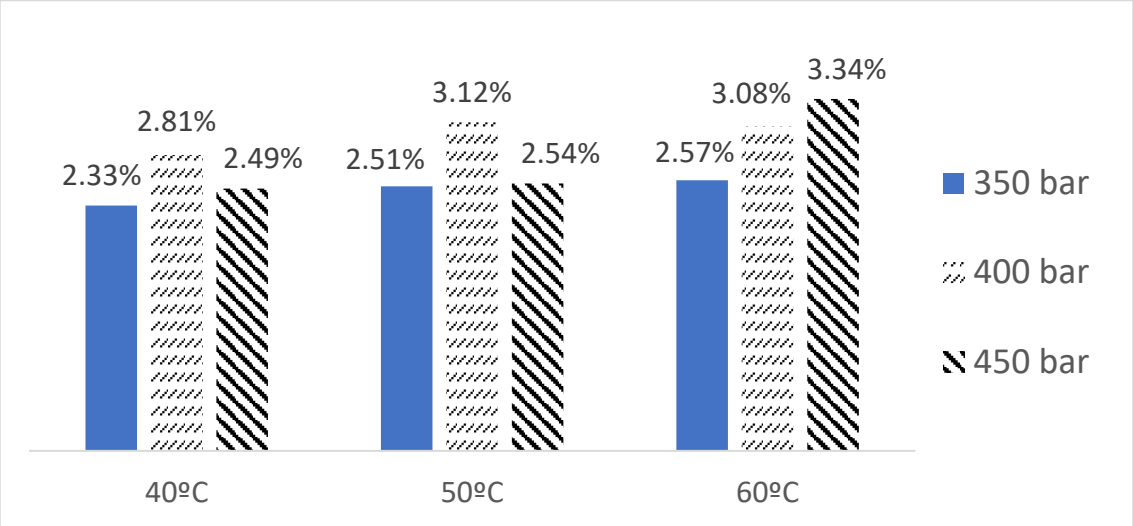

Figure 4. 5: Maximum yields obtained for each set of experiments.

The highest yield obtained after a period of 90 minutes was verified at 450 bar and 60ºC, which was the experiment performed at the highest pressure and temperature. At 60ºC higher pressures always enhanced the extraction yield, while at 40 and 50ºC, the yield

increased when the pressure was set up from 350 bar to 400 bar, but then decreased when the pressure changed to 450 bar.

The data from Figure 4.5 indicate that the extraction performed at 40 and 50ºC attained their highest yields at 400 bar rather than at 450 bar. These results subvert the theoretical expectations mentioned in Chapter 1. At constant temperature, the density of CO_2 increases with pressure, which means that the solvent power of CO_2 increases as well. If the solvent power increases, it would be expected that the yield increased as well, as long as the other process conditions were maintained constant. When the experiments were carried out at 60ºC, the extractions yields did in fact increased with increasing pressure.

A possible explanation for the lower yields at 450 bar and 40ºC and 50ºC could be the formation of dry ice during those experiments (due to a sudden expansion of CO_2 at a lower temperature), which led to the blockage if the extractor's capillary tubes, and the solute was "trapped" inside them. Other possibilities include loss of pressure during those experiments, unsteady flow rate, lack of duplicates/triplicates performance, which leads to dubious results.

Starting at 350 bar, the temperature already had a positive effect on the extraction. At 50 and 60ºC, the results were always better than at 40ºC, suggesting that the inflection point for the extraction of coffee silverskin oil was surpassed. If the inflection point had not been yet surpassed at 350 bar, the results at 40ºC should be better than at 50 and 60ºC, because the density of CO_2 is lower at higher temperatures. Nevertheless, it was not the case. So, at 350 bar, the vapor-pressure probably already plays a more significant role than density in the solubility of CSS

At every pressure, the temperature had a benefic effect on the extraction, with the exception of the extraction at 400 bar between 50 and 60ºC. The most expressive one was found at 450 bar, where the yield increased from 2.49% at 40ºC to 3.34 at 60ºC. At the lowest pressure, 350 bar, the effect of temperature was not very noticeable, with the yield only increasing from 2.33% at 40ºC to 2.57% at 60ºC, fitting theoretical expectations, as at lower pressures after the inflection point is overtaken, the effect of temperature is not so big as at higher pressures. At 400 bar the yield decreased from 3.12% at 50ºC to 3.08% at 60ºC. This is mostly due to experimental errors, however, without performing more experiments, this cannot be confirmed, since no standard deviation can be calculated. But

from a theoretical point of view, at 60ºC the yield should have maintained the same value or have a slight increase

Although some inconsistencies with literature are found, the obtained yields at the pressures and temperatures tested ranged from 2.33 to 3.34%. This value is within the range of fats contained in coffee silverskin found in the literature (Ballesteros *et al.* , 2014; Hijosa-Valsero *et al.* , 2018; Narita & Inouye, 2014). Assuming that all the extract was made up of fat, it is possible to assume that supercritical fluid extraction is an efficient method to remove the totality of the lipids present in CSS. A gas-chromatography analysis of the Fatty Acid Methyl Ester (FAME) was performed using the extract obtained at 450 bar and 60ºC. The goal was to determine the composition of the extract and its purity regarding the amount of lipids. As it has happened with the moisture content of the used biomass (18.3%, while literature mentioned 7.3%), differences between lipids of literature's CSS and the one used in this work could exist. Moreover, it is highly unlikely that all the extract is made up of lipids, as SFE is proven to remove from coffee beans phenolic compounds, caffeine, and water (de Azevedo *et al.* , 2008b).

4.1.4 Quantitative Analysis of the Extracts at 450 bar and 60ºC.

A quantitative analysis of the extract was performed in order to obtain its lipidic composition. The analysis was performed according to the method described in Chapter 3.6, and it was carried out two times with two different samples. Table 4.4 shows the weight percentage (w%) on a wet basis of each component and its standard deviation (w%).

Table 4. 4: Lipidic composition of the extract at 450 bar and 60ºC. Percentage of FAME per amount of initial sample and relative amount of saturated and unsaturated fatty acids.

Component (CX:Y)	**Weight (w%)**	**Component**	**Weight (w%)**
Lauric acid C12:0	ND[10]	**11-Eicosenoic acid C20:1**	0.17±0.01
Myristic acid C14:0	0.41±0.03	**11,14-Eicosenoic acid C20:2**	0.04±0.01
Myristoleic acid C14:1	0.02±0.00	**11,14,17-Eicosenoic acid C20:3**	0.02±0.00
Pentadecanoic acid C15:0	ND[1]	**Arachidonic acid C20:4**	0.05±0.00
Palmitic acid C16:0	19.50±0.50	**Eicosapentaenoic acid C20:5**	0.20±0.00
Palmitoleic acid C16:1	0.10±0.00	**Heneicosylic acid C21:0**	ND[1]
Heptadecanoic acid C17:0	ND[1]	**Behenic acid C22:0**	3.77±0.18
Stearic acid C18:0	4.90±0.30	**Erucic acidC22:1**	0.05±0.00
Oleic acid C18:1	4.45±0.35	**Docosahexaenoic acid C22:6**	0.20±0.00
Vaccenic acid C18:1	0.41±0.00	**Tricosylic acid C23:0**	ND[1]
Linoleic acid C18:2	19.00±1.00	**Lignoceric acid C24:0**	0.90±0.05
Linolenic acid C18:3	0.91±0.08	**Nervonic acid C24:1**	0.04±0.01
Arachidic acid C20:0	4.28±0.24		
TOTAL			
59.40±2.75%			
Saturated (relative amount): 56.82%			
Unsaturated (relative amount): 43.18%			

The gas-chromatography revealed that 59.4% of the extract was made up from lipids, however, this percentage can be even higher as C12:0, C15:0, C17:0, C21:0, and C23:0 were not detected using this method. However, Toschi *et al.* (2014) reported that the

[10] ND: Non detected

presence of C15:0 can go as high as 1.98% of the total lipid fraction. The extract is rich in palmitic acid (C16:0) and linoleic acid (C18:2), which correspond to 19.5, and 19.0% of the mass of the extract. Representative amounts of stearic acid (C18:0), oleic acid (C18:1), arachidic acid (C20:0), and behenic acid (C22:0) are present in the sample. The other missing 39.6% can be attributed to other compounds such as water.

Table 4.5 displays a comparison between the composition of coffee silverskin oil obtained during this work, by Toschi *et al.* (2014) using Soxhlet method with n-hexane as the solvent, and of green coffee bean oil extracted with supercritical carbon dioxide at 300 bar and 60ºC by Cornelio-Santiago *et al.* (2017). Only the significant FAME/acids detected are displayed.

Table 4. 5: Coffee silverskin oil extracts composition in the percentage of the most prominent FAME per total amount of oil retrieved and literature values

Compound (CX:Y)	**This work (%w)**	**Toschi et al (CS oil) (2014) (%w)**	**Cornelio-Santiago *et al.* (2017) (%w)**
C14:0	0.69±0.05	0.76±0.13	0.21±0.01
C16:0	32.82±0.84	27.5±0.13	31.2±0.05
C18:0	8.25±0.13	6.7±0.29	11.77±0.03
C18:1 (Oleic)	7.49±0.59	6.9±0.65	12.58±0.03
C18:2	31.98±1.68	29.2±2.14	33.4±0.16
C18:3	1.53±0.13	1.27±0.13	6.25±0.02
C20:0	7.2±0.4	10.8±1.54	2.49±0.02
C22:0	6.34±0.30	11.5±1.86	2.1±0.01

In every case, the richest fractions corresponded to palmitic and linoleic acid. Oil from green coffee beans appears to be poorer in C20:0 and C22:0 acids, and richer in C18:1 and C18:0 in comparison with coffee silverskin oil. These differences could be explained by that fact that Cornelio-Santiago *et al.* (2017) experiments were carried at 300 bar, while in this work the extract was retrieved at 450 bar. However, Cornelio-Santiago noted that the lipid profile of the extract retrieved from green coffee beans did not change significantly at different temperatures of SFE (Cornelio-Santiago *et al.* , 2017). Couto *et al.* (2009) studied the effect of temperature and pressure from the spent coffee ground at

200, 250 and 300 bar at 50ºC. In every case, the richest compounds were C16:0 and C18:2, with representative amounts of C18:0 and C20:0, the same as in this work. The composition of saturated fatty acids retrieved increased from 46 to 56% when pressure increased from 200 to 250 bar, however it decreased to 50% when pressure was increased further to 300 bar (Couto *et al.* , 2009). Sanchéz-Camargo *et al.* (2010), studied the lipid profile of red spotted shrimp waste by means of SFE at different temperatures and pressures. They concluded that increasing the pressure hinders the extraction of saturated fatty acids while enhancing the extraction of polyunsaturated fatty acids (Sánchez-Camargo *et al.* , 2011).

Time is also an aspect that influences the lipid profile of supercritical fluid extracts. Roy *et al.* (2006) reported that in the sc-CO_2 extraction of sunflower oil, low carbon fatty acids were extracted in their totality at the beginning of the experiment. The extraction of oleic acid (C18:1, the major fatty acid found) remains constant throughout the experiment, while the extraction of palmitic (C16:0) and stearic acid (C18:0) increases. The extraction of linoleic acid (C18:2) decreases because high unsaturated lipids are more soluble, therefore are extracted first. The lipid composition as a function of time was not carried out during this work.

Considering that the composition of green coffee oil and coffee silverskin oil is very similar, the solubility equation for green coffee oil obtained by de Azevedo *et al.* (2008a) can be adapted to coffee silverskin for the modeling of the mass transfer parameters.

During this work, the extract was collected at the end of the experiment at 450 bar and 60ºC. The effect of time, temperature and pressure on the extract composition was not carried out. However, by being aware that according to some authors the lipid composition depends on some operating parameters, the study of their effect on the composition of coffee silverskin extracts could be rendered in future research. For instance, if the most valuable lipids can be extracted more efficiently at low times, temperatures, and pressures, this would mean less operational costs while increasing the monetary value of the extract.

4.1.5 Effect of Moisture in the Total Extraction Yield of Crushed Coffee Silverskin Pellets

To study the effect of the presence of moisture (the dried pellets contained and average of 3.72% of water in a wet basis), an extraction was performed using freeze-dried crushed pellets (without humidity, theoretically) for 90 minutes at 450 bar and 60ºC. The results were compared with the ones from "standard" (dried in an oven at 45ºC for 72 hours) pellets extracted under the same conditions. Figure 4.6 displays the results obtained.

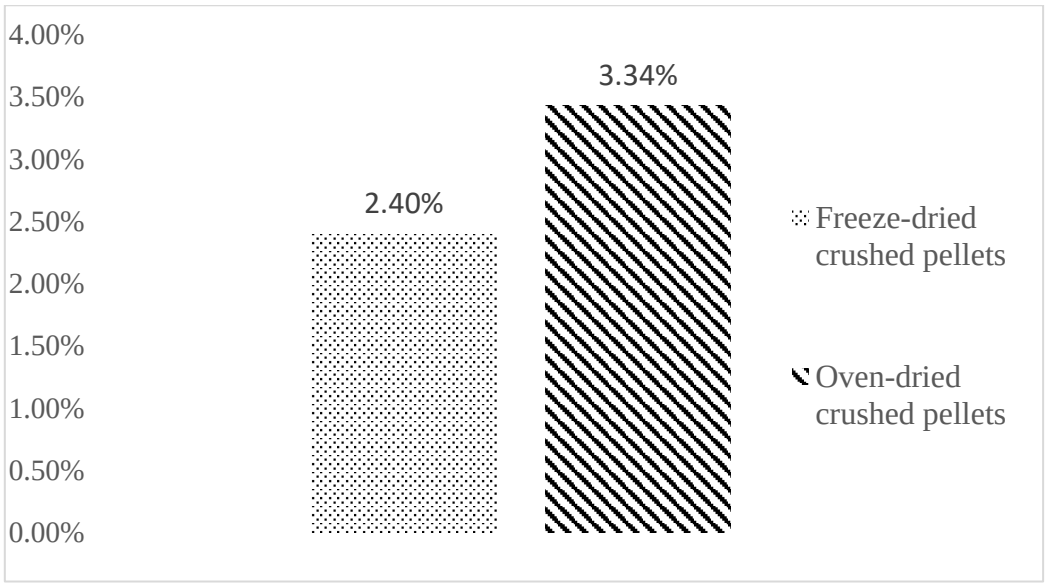

Figure 4. 6: Total extraction yield obtained using freeze-dried and oven-dried (45ºC for 72 hours) crushed coffee silverskin pellets at 450 bar and 60ºC.

The total extraction yield dropped from 3.34 to 2.40% after a freeze-drying was performed on the oven-dried pellets.

One of the possible explanations, is that when extracted, the oven-dried pellets that contain around of 3.72% of water, and that water is extracted alongside with lipids, thus increasing the total extraction yield. The FAME analysis was not performed for the freeze-dried pellets extract, so this premise cannot be confirmed. However, if true, the extract obtained from freeze-dried pellets should have a higher lipidic purity than the one from standard-dried pellets, which contained 59.4% of lipids.

On the other hand, some authors reported that the presence of the water on the biomass matrix can enhance the yield of a supercritical fluid extraction by helping to break the interaction that the solute has with the biomass matrix (Ponte, 2017).

4.1.6 Effect of Granulometry on the Total Extraction Yield

A 3-tray sieving tower was used, allowing to obtain four different particle range sizes. It was estimated that the average particle size for each range was the average between the width of the respective lower and upper tray. The particles above the top tray were assumed to be in the range of [0.63-1.5 mm], whereas the particles bellow the bottom tray were assumed to be in the range of [0.011-0.032 mm]. Table 4.6 displays the different ranges of the sieving tower and the estimated average particle diameter for each one of them:

Table 4.6: Size range of the four different trays used and average estimated particle diameter.

Range (mm)	**Average diameter (µm)**
[0.011-0.032]	22
[0.032-0-125]	79
[0.125-0.613]	379
[0.613-1.5]	1057

Total extraction Yield Curves as a function of the Diameter of the Particle

Figure 4.7 displays the total extraction yields curves at 450 bar and 60ºC for the different particle diameters obtained and full pellets as well as a function of time:

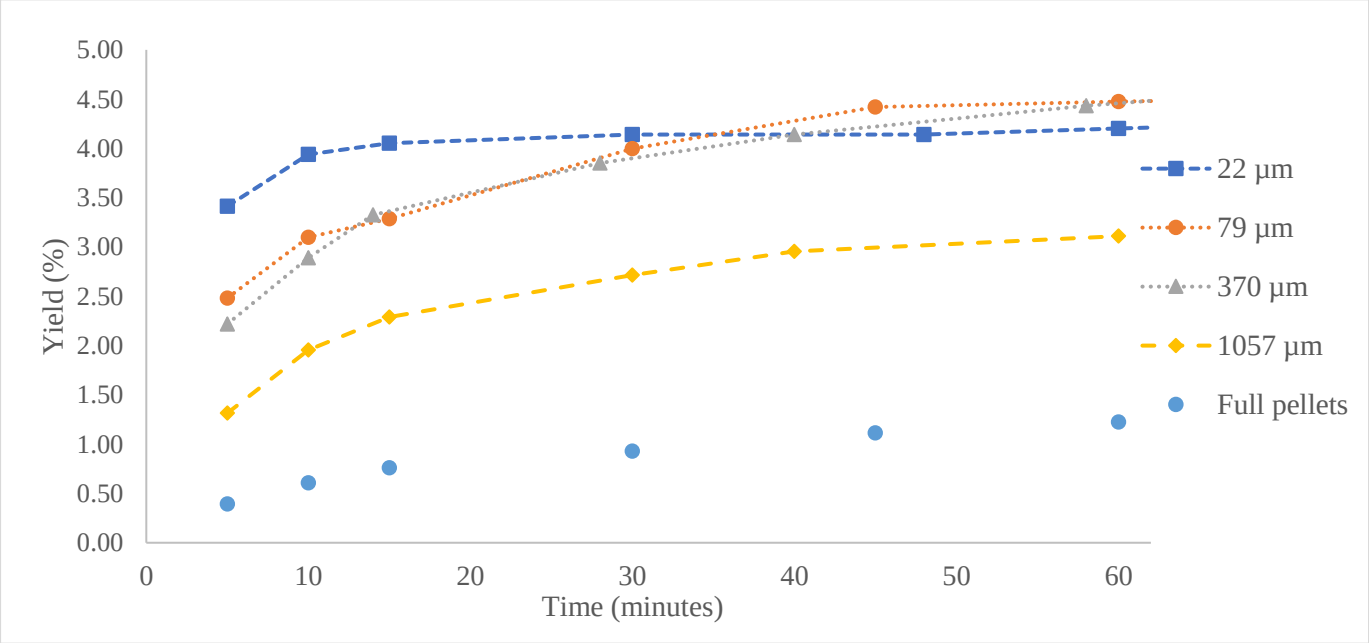

Figure 4. 7: Total extraction yield curves for different diameter sizes and full pellets at 450 bar and 60ºC as a function of time.

By analyzing Figure 4.7 it is clear that full pellets obtain a poorer extraction yield when compared with the ones obtained using milled pellets. Only 1.22% of the batch input mass was extracted after 60 minutes when using full pellets. The smaller fraction of the milled pellets, with an average of 1057 μm, obtained a maximum total extraction yield of 3.11% after 60 minutes. The sizes of 22, 70 and 379 μm attained maximum extraction yields of 4.20, 4.58, and 4.43%, respectively.

For the three smaller particle sizes, the maximum extractions yields obtained were alike. It can be argued, that the maximum extraction yield from these specific coffee silverskin was attained, and that even for particles sizes smaller than 22 μm, the yield would remain the same or similar. However, the extraction rate was visibly faster for 22 μm diameter particles. After 10 minutes of extraction the Falling Extraction Rate was reached and a yield of 3.94% was obtained. Such a (close) value to that yield was only attained by the 79 and 370 μm diameter particles around 30 minutes of extraction, implying that the smaller the particle, the higher the extraction rate. Indeed, literature indicates that smaller average particle size enhances the extract rate during the CER stage. This is because for smaller particles, due to disruption of the cell wall, the total surface area of the biomass input is greater and the amount of solute on the surface of each particle is greater. On this stage, the extraction is controlled by external convection. According to Equation 2.15, the driving force of the extraction is the difference of concentrations between the surface of the particle and the concentration of the solute on the bulk of the fluid. The bigger the difference in those concentrations the higher the extraction rate will be (Silva & Martínez, 2014). On the internal level, smaller particle size shortens the diffusion pathway that the solute has to go through. Therefore, smaller particle sizes promote both internal diffusion and external convection, according to literature and these expectations were met during this work.

Furthermore, the maximum extraction yields for the largest particle size (1057 μm and full (cylindrical) pellets) were significantly smaller than the ones from the remaining particle sizes, indicating that not only the extraction rate is affected by particle size, but the maximum obtainable yield is it as well. If a longer experiment had been performed in those two cases, it would be expected that the extraction yield would only suffer a slight increase. As mentioned before, grinding the biomass promotes the exposure of the solute to the surface of the particles, but before the grinding that same amount of solute is bond to the matrix of the biomass, as mentioned in Chapter 2.4.5. Meaning that before the

particle size is reduced, the quantity of "*solute-bonded-to-the-matrix*" is higher. This kind of solute is difficult to be extracted or even unextractable, therefore affecting the maximum extraction yield. By reducing the particle size, the cell wall is destroyed, liberating more solute from the matrix, consequently more solute can be extracted and the maximum obtainable extraction yield increases (Huang (2015), Silva & Martínez, (2014)).

Modeling and Optimization of the Mass Transfer Parameters

To model the extraction curves and determine the different mass transfer parameters some variables needed to be measured or calculated (such solvent volume flow, porosity of the bed, volume of the extractor, etc.), some were estimated by means of extrapolation (solubility of the extract on sc-CO_2), whereas some values were bluntly assumed (tortuosity and porosity of the particle).

According to equation 2.2, the solubility of green coffee beans oil at 450 bar and 60ºC is 13.51 g_{oil}/L_{CO2}. At these conditions the density of CO_2 is 913.7 g/L (calculated by the BatchSFE software), meaning that the solubility of coffee oil is 0.0148g_{oil}/g_{CO2}. According to Table 4.5, the composition of coffee silverskin oil is similar to the one from green coffee beans oil, therefore, they should have similar solubilities. However, according to Table 4.4, only 59.4% of the obtained extract at 450 bar and 60ºC is composed by lipids. In other words, as the extract was not pure, its solubility cannot be compared to the one obtained by de Azevedo et al (2008a). Therefore, a cloud point solubility was performed by the University's laboratory technicians to estimate the solubility (or concentration of saturation) of the extract at 60ºC and different pressures (230, 285 and 355 bar). The results are displayed in Figure 4.8.

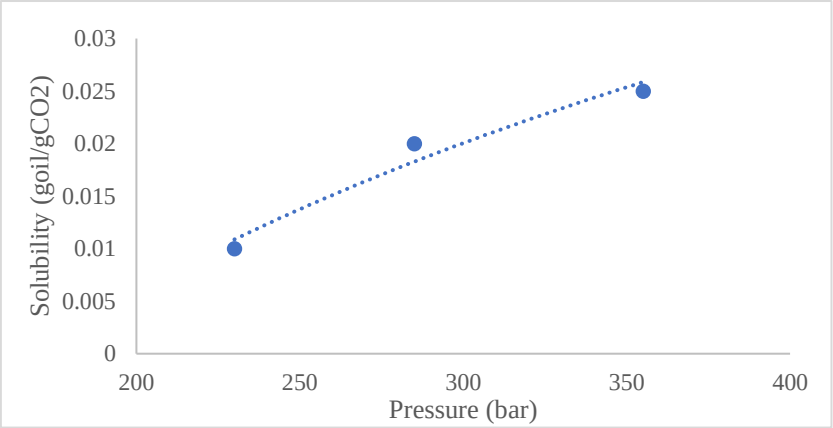

Figure 4. 8:Solubility curve of the extract obtained at 450 bar and 60ºC by means of cloud point solubility at three different pressures and 60ºC.

A mathematical expression as a function of the logarithm of the pressure was chosen because it obtained the highest coefficient of correlation (r^2= 0.9617) of all the mathematical expressions available in Microsoft Excel.

$$C_{sat} = 0.345 \ln P - 0.1768 \quad (4.2)$$

By extrapolation, at 450 bar and 60ºC the solubility of the extract should be 0.340 g_{oil}/g_{CO2}, which is more than twice as high as the one predicted by Equation 2.2. Nevertheless, this value should be taken with skepticism, since it was extrapolated and not interpolated using the experimental data.

To calculate the porosity of the bed (ε_{bed}) the apparent (ρ_{app}) and skeletal (ρ_{skel}) densities of each milled pellets particle size fraction was calculated as described in Chapter 3.9. With these values, it was possible to determine the porosity of the reactor using equation 4.3:

$$\varepsilon_{bed} = \frac{\rho_{skel} - \rho_{app}}{\rho_{skell}} \quad (4.3)$$

Where ρ_{skel} stands for the skeletal density of the biomass input, and ρ_{app} is the apparent density of the biomass input.

These results are displayed in Table 4.7:

Table 4. 7: Apparent and skeletal density and porosity of the bed for each particle diameter.

d_p (μm)	ρ_{app} (g/L)	ρ_{skel} (g/L)	ε_{bed}
22	0.400±0.010	1.516±0.008	0.74
79	0.415±0.014	1.515±0.013	0.73
379	0.542±0.010	1.483±0.004	0.63
1057	0.574±0.009	1.4±0.008	0.63

The porosity of the bed increased with smaller particle size. According to Equation 2.4 and 2.7, the Reynold (Re) number increases with fluid velocity, that in turn increases with lower porosities.

Table 4.8 displays the constants that were inserted in the software and remained the same for each experiment:

Table 4. 8: Operation constants inserted in the "*BatchSFE*" software.

Constant	**Value**	**Units**
Temperature	60	ºC
Pressure	450	bar
CO_2 mass flow	1.96	g/min
CO_2 density	913.7	g/L
CO_2 volume flow	3.58×10^{-8}	m^3/s
Diameter of the extractor	0.014	m
Length of the extractor	0.3	m
μ_{CO2}	7.5×10^{-5}	Pa.s
C_{sat}	0.0340	g_{fat}/g_{CO2}

Table 4.9 displays the results provided by the "*BatchSFE*" software for each particle diameter and their respective units:

Table 4. 9: Parameters calculated using "*BatchSFE"* software.

Parameter	22 µm	80 µm	379 µm	1057 µm	Units
Re	0.161	0.572	2.03	5.82	//
v	0.032	0.032	0.036	0.036	m/s
a_v	2.73×10^{5}	7.50×10^{4}	1.58×10^{4}	5.71×10^{3}	m^{-1}
β_F	2.16×10^{9}	6.43×10^{-8}	4.46×10^{-7}	1.46×10^{-6}	m/s
β	3.08×10^{-10}	2.1×10^{-9}	2.7×10^{-9}	2.02×10^{-9}	m/s
Biot	3.8	44	139	434	//
$\delta_{eff, solid}$ (CER)[11]	5.93×10^{-14}	2.27×10^{-13}	4.28×10^{-12}	1.85×10^{-11}	m^2/s
K	9.5	4	7	10	//
$a_v \times \beta_F$	5.89×10^{-4}	4.82×10^{-3}	7.04×10^{-3}	8.34×10^{-3}	s^{-1}

The increase of particle size revealed an increase on the $a_v\beta_F$ factor, which goes against the data in the literature. It decreased from 8.34×10^{-3} to 5.94×10^{-4} s^{-1} when the particle diameter changed from 1057 to 22 µm. Silva & Martínez (2014), modeled the supercritical fluid extraction of oleoresin from red pepper, and determined that their $a_v\beta_F$ factor decreased as particle diameter increases due to the fact that bigger particles have less surface of contact with the solvent (Silva & Martínez, 2014). The same results are mentioned by Huang (2015) for the extraction of apricot oil.

The Biot number also increased with particle increase. Once again, this contradicts the findings of Silva & Martinez (2014). In fact, higher Bi indicates that the external mass transfer coefficient is larger than the internal one. For extractions where Biot numbers is above 10 the extraction will be controlled by internal diffusion, whereas for Bi under 10, the convection on the bulk of the fluid is probably the controlling factor (Huang, 2015). Therefore, according to the results of this work, for the larger particle diameters, internal diffusion will play a more influent role in the extraction of coffee silverskin oil.

The fact that the obtained $a_v\beta_F$ factors contradicted the theoretical expectations might be explained by an underestimation of the external mass transfer for smaller particle sizes, or and overestimation of it for larger particle sizes coefficient, by the software. The latter could be justified by the fact that the used saturation concentration was extrapolated from

[11] Calculated from a mass balanced performed to the Constant Extraction Rate phase. I t must be taken as a first guess of the effective diffusion coefficient.

Chrastil's equation, which is more suitable for interpolations. If the calculated concentration of saturation by means of cloud point solubility is lower than the real one, then to maintain the same experimental extraction rate, β_F must go up. This relationship between external mass transfer coefficient, external mass transfer rate and concentration of saturation is explicit in Equation 2.15.

An imprecise measurement of the average particle diameter by the sieving process can also be a possible justification for the disparities, as the a_v value is directly dependent of the particle diameter. For instance, if the particles that were considered to be 1057 μm are, in fact, smaller, then the value of $a_v\beta_F$ would be smaller, and, possibly, the theoretical expectations could be met. A laser diffraction analysis, as performed by Baudron (2014), would provide much more precise results regarding the particles average diameter.

Table 4.10 displays more parameters calculated analytically by using the data provided by Table 4.9. By knowing the value of β and recurring to equation 2.25 and 4.4 the software iterates the value of the effective diffusion coefficient, $\delta_{eff,}$ thus calculating the value of the Schmidt number using equation 2.5. The value of β_S is calculated by using Equation 2.18.

Unlike referenced in Equation 2.6, the software calculates the Sherwood number from the overall mass transfer coefficient, instead of using the external mass transfer coefficient. Therefore, Equation 4.4, goes against the definition that some authors use to calculate the Sherwood number (Oliveira *et al.* (2011); Sinaei Nobandegani *et al.* (2016)).

$$Sh = \frac{\beta\, d_p}{\delta_{eff}} \tag{4.4}$$

Table 4. 10: Parameters calculated analytically by using the data from Table 4.9

Parameter	22 μm	79 μm	379 μm	1057 μm	Units
Sh	505	268	455	688	//
δ_{eff}	1.34×10^{-17}	6.27×10^{-16}	2.25×10^{-15}	3.08×10^{-15}	m^2/s
Sc	5.83×10^{9}	1.25×10^{8}	3.47×10^{7}	2.54×10^{7}	//
$Sh/Sc^{1/3}$	2.81×10^{-1}	5.36×10^{-1}	1.40	2.34	//
βs	3.59E-10	2.17×10^{-9}	2.72×10^{-9}	2.02×10^{-9}	m/s
$\beta s \times A_v$	9.80E-05	1.63×10^{-4}	4.29×10^{-5}	1.15×10^{-5}	s^{-1}

Using Microsoft Excel, it was possible to obtain an equation (Equation 4.4) that displays the value of the obtained Sherwood numbers as a function of Reynolds and Schmidt number. The obtained correlation coefficient was of 0.993 and the equation is:

$$Sh = 0.83Re^{0.61}Sc^{1/3} \quad (4.4)$$

Equation 4.4 displays parameters very similar to the Catchpole (1993) correlation mentioned in Table 2.5. Therefore, the *BatchSFE* software calculated the Sherwood number and the effective diffusion coefficient based on it.

Figure 4.9 shows the experimental points obtained and the curves modelled by the software for particle diameters of 22, 479 and 1057 μm. By observing it, it is possible to conclude that there is a lot of disparity between the models and the actual results. In all three cases, the modelled curves present lower yields during the Constant Extraction Rate when compared with the experimental points. For example, using 22 μm particles, after 10 minutes of extraction, a yield of 3.94% was obtained, however, for the same time, the model predicted a yield of about 2.45%. However, for this particle diameter, the software was capable of fitting the experimental data correctly for the last two stages of the extraction. Visually speaking, the most imprecise modelling was performed for the 379 μm particles. Both the first and second part of the curve present significant differences with the experimental results. In the CER stage, the experimental values were above the modelling curve, indicating an underestimated external mass transfer coefficient. During the FER phase, the experimental points are below the curve, which can mean that the diffusion coefficient or the internal mass transfer coefficient is overestimated. According to the *BatchSFE* user manual, discrepancies between the simulation and the experimental data are mostly caused by imprecise estimations of the initial concentration of the solute in the solid and the saturation concentration of the solute in the solvent. Such imprecisions could be solved by performing a Soxhlet extraction to determine the initial amount of lipids in the coffee silverskin, whereas to obtain a more reliable concentration of saturation, more cloud point solubilities should be performed at different pressures, and temperatures and recurring to Equation 2.1, a more precise results could be obtained.

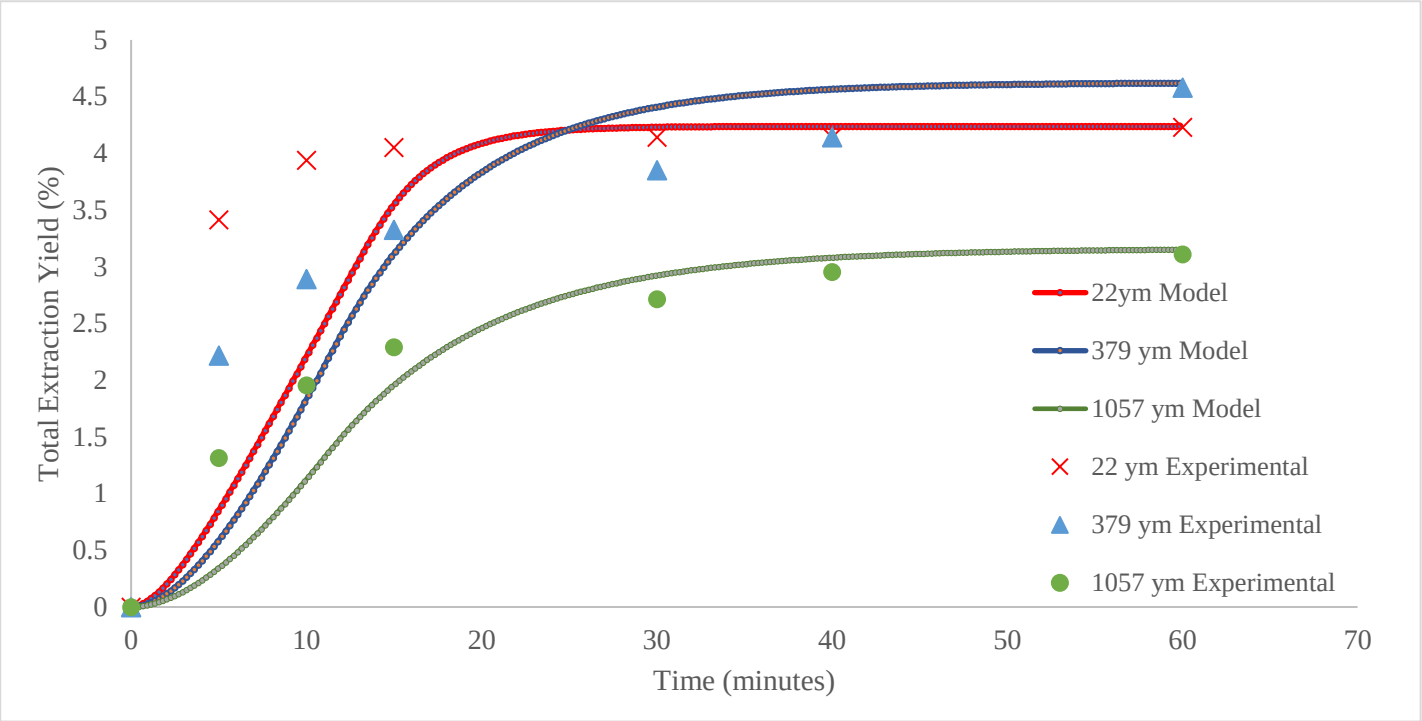

Figure 4. 9: Experimental and model results for the total extraction yield curve as a function of time for different particle diameters.

The absolute relative deviation (AAR) between the experimental values and the modeling values was calculated according to Equation 4.5 and are displayed in Table 4.11:

$$AAR\ (\%) = \frac{|Experimental\ yield - Modeled\ yield|}{Modeled\ yield} \times 100 \qquad (4.5)$$

Table 4. 11: Absolute relative deviation for 22, 379 and 1057 μm particles as a function of time.

Time (minutes)	AAR_{22ym} (%)	AAR_{379ym} (%)	AAR_{1057ym} (%)
5	75.3	73.9	74.2
10	44.6	37.6	43.3
15	35.1	32.1	38.7
30	2.2	14.6	7.9
40	2.3	10.9	5.4
60	0.2	0.9	1.4

The data from Table 4.11 indicates that the software was unable to calculate precise modeling curves. The disparities between the experimental and modeled values is more noticeable within the first 15 minutes of the extraction, ranging from a deviation of 32.1% up to 75.3% and it decreases with time of extraction. This data leads to the conclusion

that the obtained models are inaccurate, and therefore, the obtained mass transfer parameters by the software may not represent the real ones.

4.2. Liquid Hot Water for the Recovery of Proteins/Amino Acids

4.2.1 Effect of Alkalinity and Pretreatment on the Protein/Amino Acid Extraction Yield

The effect of alkalinity and pretreatment (crushing and sc-CO_2 extraction) was studied at constant temperature (120ºC), pressure (20 bar) and residence time (30 minutes). The concentration of the NaOH solutions ranged from 0 mol/L to 0.05 mol/L. The overall protein yield was calculated by performing mass balances that considered the concentration of the analyzed extracts and the input load of solvent and coffee silverskin according to Equation 3.2.

Figure 4.10 displays the protein extraction yield of raw pellets, crushed raw pellets, and crushed extracted pellets as a function of the concentration of NaOH in the solution.

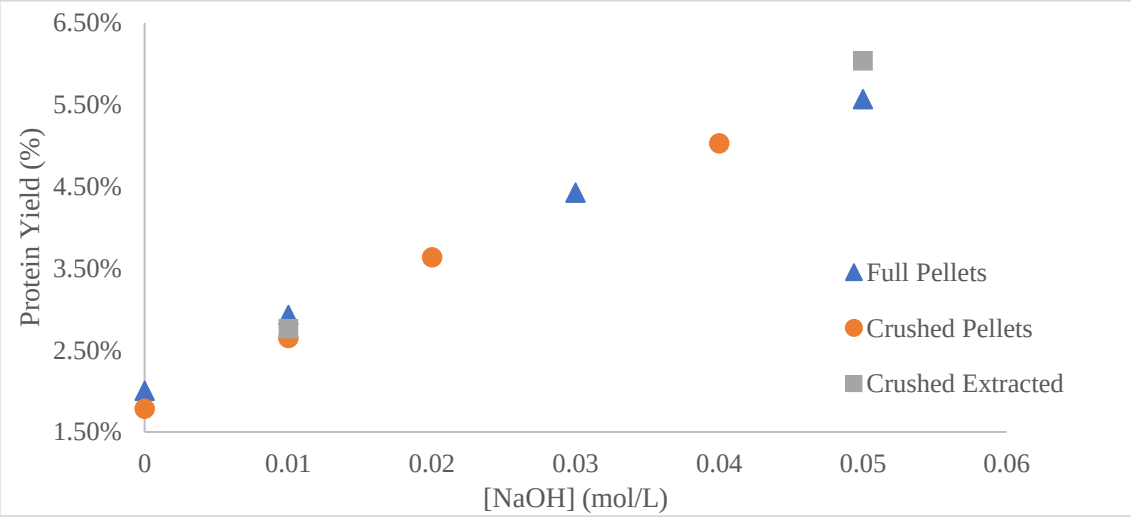

Figure 4. 10: Evolution of the protein extraction yield as a function of the concentration of the NaOH.

By observing Figure 4.10, the addition of sodium hydroxide has, undeniably, a positive effect in the overall extraction of proteins. The yield increase was proportional to the concentration of the NaOH solution. A limiting yield was not found, leading to believe that if more NaOH had been added, the yield would have been even greater.

Using pure distilled water as a solvent, the yield was 2.00 and 1.78% for raw and crushed raw pellets, respectively. This indicates that pure hot water is enough to extract some of the existing proteins in coffee silverskin and, at these conditions, grinding the biomass, can lead to lower yields. The maximum yield, 6.03%, was obtained using crushed and extracted pellets and a 0.05 mol/L NaOH solution, followed by raw pellets at the same NaOH concentration (5.56%). The fact that the yield was higher using pretreated biomass indicates that performing a supercritical extraction for the recovery of lipids does not have a negative impact on the protein hydrolysis, on the contrary, the yield increased 0.47%. However, it could also mean that the grinding of the biomass has a positive effect on protein extraction at higher pH.

Due to the lack of resources, it was only possible to analyze the three types of biomass that were hydrolyzed under the exact same conditions, once. This occurred at a concentration of NaOH equal to 0.01 mol/L. In this case, the extraction yields were 2.93, 2.76 and 2.65% for raw pellets, crushed raw pellets, and SFE crushed pellets, respectively. The differences in the yields could be disregarded, however as no duplicates were performed, no standard deviation can be calculated to verify this hypothesis. The conclusion that can be drawn from these 3 points is that the effect of grinding and pretreatment for protein extraction is not significant. From an industrial point of view, these are excellent conclusions, as the utilities required for crushing the biomass could be spared, and the lipids can be extracted by means of supercritical fluid extraction without hindering the following steps for protein recovery.

4.2.2 Effect of Alkalinity and Pretreatment on the Profile of the Extracted Amino Acids

The different amino acids retrieved from the hydrolysis were quantified by the TUHH's Central Lab. As mentioned in the literature review, different amino acids have different solubilities according to their isometric point. Figure 4.11 displays the amount of the different amino acids extracted from raw full pellets (in milligrams per liter of extract) when the NaOH concentrations were 0 and 0.05 mol/L.

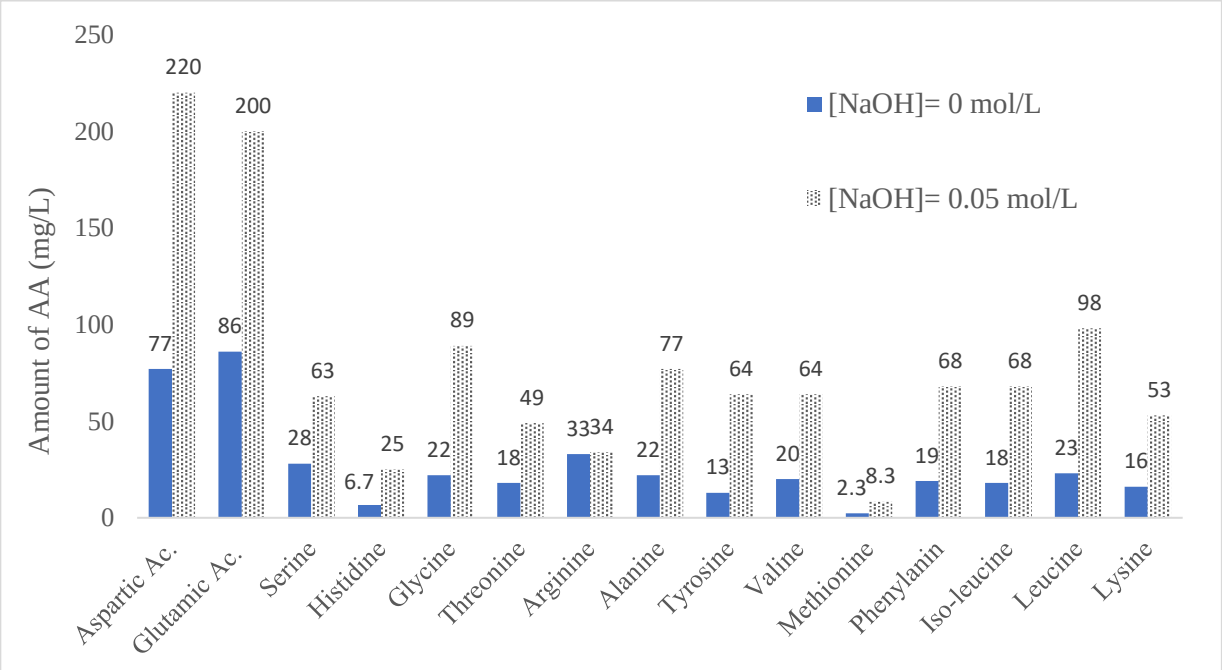

Figure 4. 11: Amount of a certain amino acid (mg/L of extract) extracted from full raw pellets at two different concentrations of NaOH.

The amino acids retrieved were the negatively charged aspartic acid and glutamic acid, the positively charged like arginine, histidine and lysine, hydrophobic amino acids such as alanine, valine, isoleucine, leucine, methionine, tyrosine and phenylalanine, and the polar uncharged amino acids like serine and threonine, and finally glycine (a special case).

In both scenarios, the most representative AA extracted were aspartic acid (77 mg/L at [NaOH]= 0, and 220 mg/L at [NaOH]=0.05 mg/L) and glutamic acid 86 mg/L at [NaOH]= 0, and 200 mg/L at [NaOH]=0.05 mg/L, while histidine and methionine were extracted in lower quantities (6.7 and 2.3 mg/L at [NaOH]= 0, respectively, and 25 and 8.3 mg/L at [NaOH]=0.05 mg/L, respectively). All the other amino acids were retrieved

at a concentration between 13 and 28 mg/L at null concentration of sodium hydroxide, and 49 and 98 mg/L at [NaOH] equal to 0.05 mol/L.

It is noticeable that the addition of sodium hydroxide promoted the extraction of every amino acid, nevertheless, some have increased more than others. Figure 4.12 shows the increase of each sort of amino acid in percentage, according to the data of Figure 4.11.

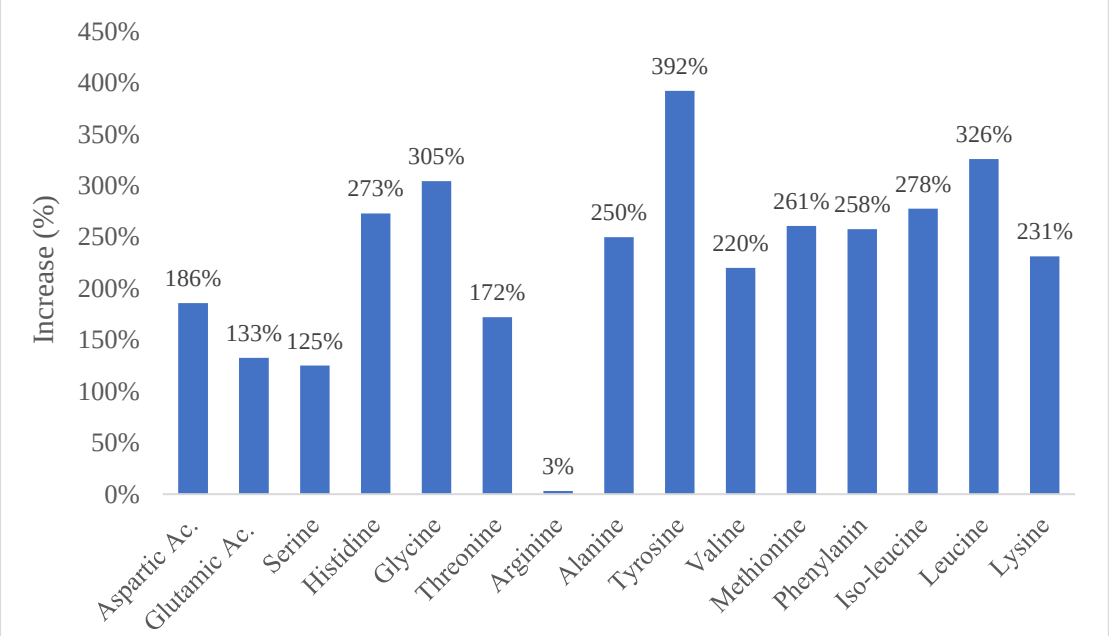

Figure 4. 12: Amino acid increase percentage from [NaOH]= 0 to [NaOH]= 0.05 mol/L.

Tyrosine had the most expressive increase, 392%, followed by leucine (326%), glycine (305%) and isoleucine (278%). Tyrosine, leucine, and isoleucine are hydrophobic amino acids, meaning that they have a non-polar side chain, which is not as affinitive towards water as other amino acids. Arginine had the lowest increase, only of 3%, but of all amino acids, it presents the highest isoelectric point, therefore, it has less affinity towards alkali solutions (Sigma Aldrich, 2019). Notwithstanding, the positively charged amino acids histidine and lysine obtained increases much higher (273% and 231%, respectively) than their counterpart, arginine (only 3%). Amend & Helgeson (1997), concluded that the solubility of arginine decreases at higher pH. This is because its isoelectric point is of 10.8 (Amend & Helgeson, 1997).

Figure 4.13 and 4.14 display the amount of a group of amino acids (positively and negatively charged, polar uncharged, hydrophobic and glycine) per total amount of amino acids extracted at [NaOH] = 0 and [NaOH]= 0.05 mol/L. This is considered to be a protein

profile of the extracted amino acids. These pie charts take into account the data from Figures 4.11 and 4.12.

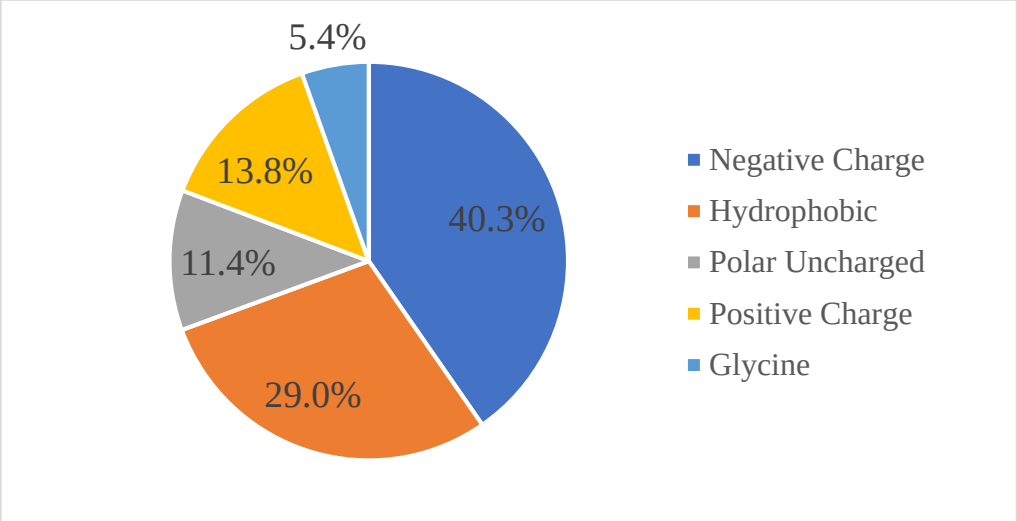

Figure 4.13: Amino acid profile for raw full pellets treated at [NaOH] = 0 mol/L.

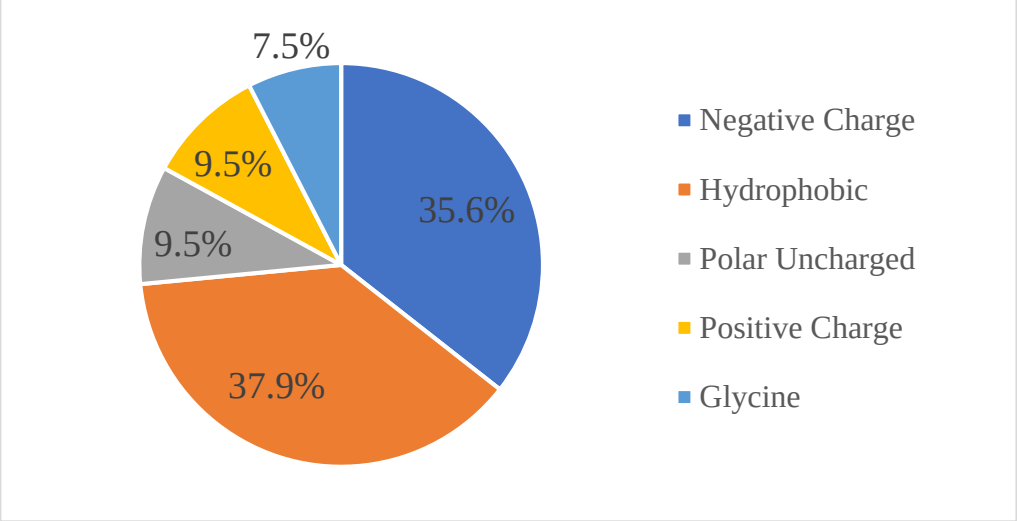

Figure 4.14: Amino acid profile for raw full pellets treated at [NaOH] = 0.05 mol/L.

The relative amount of hydrophobic amino acids grew the most (from 29.0 to 37.9%), followed by glycine (from 5.4 to 7.5%), while negatively charged amino acids suffered the highest cut (from 40.3 to 35.6%). Therefore, the addition of NaOH to the solution improves the extraction of hydrophobic amino acids and glycine, while undermines the extraction of amino acids with a negative charge.

In conclusion of these chapters: the addition of sodium hydroxide favored the protein extraction from coffee silverskin by means of liquid hot water treatment. The increase of

hydrophobic amino acids and glycine at higher concentrations of NaOH was more significant than the one of the remaining amino acids.

4.2.3 Effect of Temperature and Residence Time on Full SFE Pellets

SFE full pellets were treated at different temperatures and residence times whilst maintaining a pressure of 20 bar inside the reactor's inlet and a concentration of NaOH of 0.05 mol/L. Figure 4.15 displays the overall protein yield at the tested conditions using sc-CO_2 extracted full pellets.

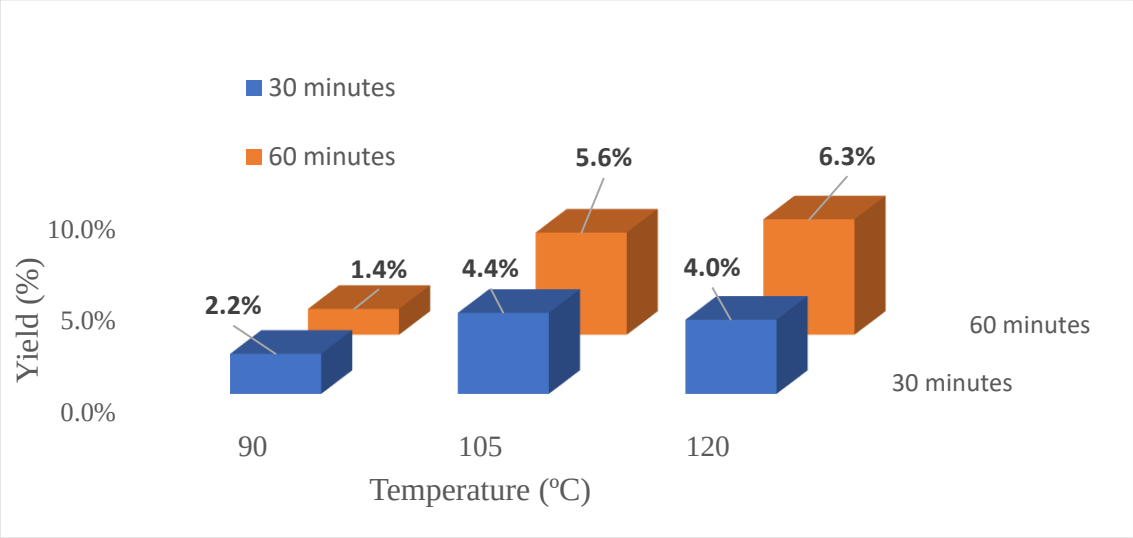

Figure 4. 15 : Protein extraction yield using sc-CO2 extracted full pellets as function of temperature and residence time.

The highest protein yield was obtained at the most severe conditions. At 120ºC and 60 minutes, 6.3% of the extracted mass was composed of amino acids. This was the highest protein yield obtained throughout this work. On the other hand, the lowest yield (1.4%) was obtained at 90ºC and 60 minutes. At 90ºC the yield was higher for shorter residence time, a yield of 2.2% was obtained. At higher temperatures, higher residence times always managed to obtain higher yields, inferring that time could play a more crucial role in the extraction at higher temperatures. Surprisingly, for a 30 minutes extraction, the yield was higher at 105ºC (4.4%) than at 120ºC (4.0%), either meaning that a 15ºC difference is negligible when low residences times are considered or that experimental errors occurred. At 60 minutes of residence time, the yield grew with temperature every time. From 90 to 105ºC the protein yield increased more than 3 times, from 1.4 to 5.6%, after the temperature was raised to 120ºC, the yield only increased by 0.7%. As no duplicates were performed, no standard deviation can be calculated to confirm these hypotheses.

The changes in the amino acid profile in this case were also carried out. This time the influence of time and temperature were the studied parameters. Figure 4.16 and 4.17 display the amino acid profile of the extracted AA from full extracted pellets at 90 and 120ºC, respectively.

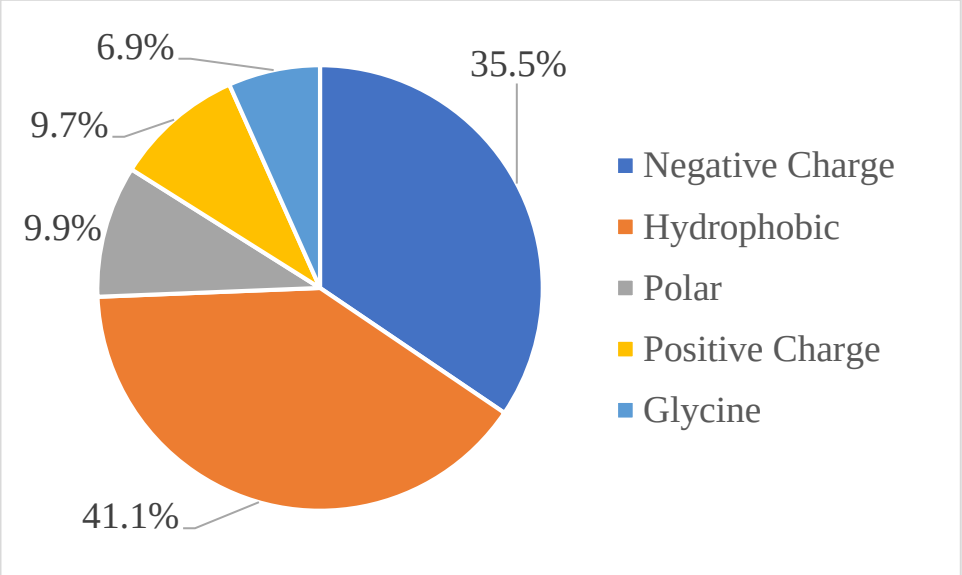

Figure 4. 16: Amino acid profile of recovered amino acids at 90ºC for 30 minutes from SFE extracted pellets

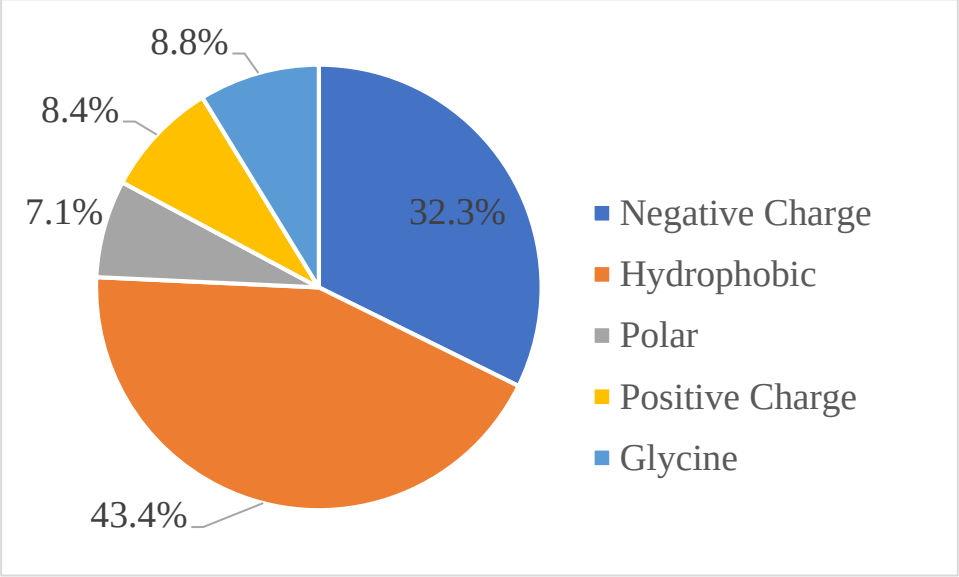

Figure 4. 17:Amino acid profile of recovered amino acids at 120ºC for 30 minutes from SFE extracted pellets.

There was a small change in the protein profile when the hydrolysis temperature increased. Higher temperatures seem to improve the extraction of hydrophobic amino acid and glycine in comparison with the remaining amino acids. As mentioned in the bibliographic review, the amount of hydronium and hydroxide is bigger in water at elevated temperatures, since the K_W increases, which facilitates the dissolution of amino acids which are more insoluble at lower temperatures.

Figure 4.18 shows the profile for amino acids retrieved at 120'C for 60 minutes.

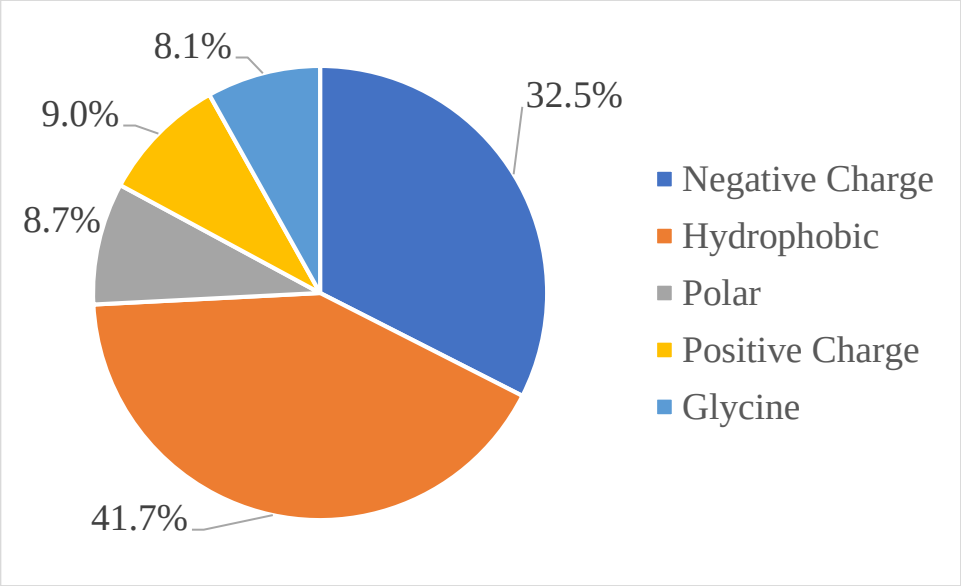

Figure 4. 18: Amino acid profile of recovered amino acids at 120ºC for 60 minutes from SFE extracted pellets.

In comparison with Figure 4.17, Figure 4.18 is more similar than Figure 4.16 in terms of negatively charged AA. The relative amount of negatively charged amino acids only changed from 32.3 to 32.5%. In this case, the only decrease found was with hydrophobic amino acids which dropped from 43.4% to 41.7%, leading to believe that in alkaline hydrolysis the reaction rate for hydrophobic amino acids is greater at the beginning of the process. Although, as the changes were very little, it could be due to experimental errors and lack of precision.

An amino acid profile for coffee silverskin extracts was successfully made. For the first time in literature, it is now known which amino acids can be retrieved from CSS by means of liquid hot water hydrolysis.

4.2.4 Comparison with Narita & Inouye (2012)

The highest yield from this study was 6.3% obtained using approximately 0.6 grams of sc-CO_2 extracted full pellets in 30 mL of solvent at 120ºC at a concentration of NaOH of 0.05 mol/L, for 60 minutes. Narita & Inouye (2012) obtained a protein yield of 15.7% using subcritical water at 210ºC, using 1 gram of raw coffee silverskin in 50 mL of solvent, for 10 minutes. In both cases, the biomass-solvent ratio was the same (1:50), but the other parameters were different. However, they obtained a maximum protein yield 2.5 times higher than the highest one in this work.

The most comparable data from both works are the ones from raw pellets at 120ºC and without the addition of NaOH, for 30 minutes, in which the protein yield obtained was 2.00%. Narita & Inouye were able to obtain a 4.5% yield at a lower temperature of 80ºC, without the addition of an acid or base. In fact, at 25ºC they were already able to obtain a yield higher than 2.00%, at those conditions they got a yield of 3.3%.

Using a concentration of NaOH of 0.1 mol/L at 25 and 80ºC, Narita & Inouye obtained yields of 7.6 and 9.7%, respectively. In this study, the highest concentration of sodium hydroxide was 0.05 mol/L, which is half of the one used by Narita & Inouye. From raw pellets at 120ºC for 30 minutes and at a concentration of NaOH of 0.05 mol/L, a yield of 5.56% was obtained, implying that the concentration of NaOH as a greater impact on the amino acid extraction than temperature.

Nevertheless, an analysis of the protein content of the coffee silverskin used in this work was not performed. As far as it is known, the total amount of the coffee silverskin used in this work can be lower than the amount of proteins in the coffee silverskin used by Narita & Inouye (2012).

5. Conclusions and Suggestions for Future Works

The extraction of lipids and amino acids from coffee silverskin by means of supercritical extraction and liquid hot water, respectively, was carried out.

The received pellets had a cylindrical shape and contained 18.7% of water. After 72 hours of drying, the moisture content decreased to 3.72%. However, the moisture content stabilized after 24 hours in the oven. Therefore, periods no longer than 24 hours are necessary to obtain the final moisture content at a drying temperature of 45ºC.

With crushed pellets, the supercritical extraction with CO_2 of coffee silverskin was more efficient at 450 bar and 60ºC (extraction yield of 3.34%). For that reason, when studying the effect of granulometry, that were the chosen operating conditions. The extract, at this conditions, was composed by 59.4% of lipids. The yield values for the supercritical extraction are within the range of lipid content of coffee silverskin that is found in the literature (2.2% on a total basis, 4.78-4.97% on a dry basis). Crushing and milling the pellets had a positive effect on the extraction. When the pellets were extracted, as received, the yield was no greater than 1.22%. By milling the already crushed pellets, the yield increased from 3.34% up to 4.58% when the average particle size was 70 μm. The positive effect of the milling seems to be negligible for particle sizes under 370 μm. For smaller particle sizes, the final yield is within the range of 4.20-4.58 % after 60 minutes of extraction.

The modeling of the extraction when using different particle size was carried out. However, the results obtained go against those taken from literature. The factor $a_v\beta_F$ increased with particle diameter. This was not expected, since larger particles require a longer diffusion path, which hinders the mass transfer. Moreover, the model curves do not fit the experimental values, especially during the CER stage of the extraction. Within the first 5 minutes of the extraction, relative difference between the experimental data and the model results is always above 70% for 22, 379 and 1057 μm coffee silverskin particles. This indicates that the rendered modeling is inaccurate. However, the absolute relative deviation decreases with time of extraction for all the tested particle sizes.

The moisture content also plays a significant role on the extraction. At 450 bar and 60ºC, the extraction yield dropped from 3.34% to 2.40% when freeze-dried crushed pellets (no moisture) were used, instead of oven-dried pellets (3.72% of moisture).

Regarding the liquid hot water pretreatment, the results show that the addition of solutions of NaOH improves the recovery of amino acids from coffee silverskin, especially the ones that exhibit hydrophobic or negative charged side chains.

The effect of granulometry appears to be of low impact on the protein extraction yield. Full pellets and crushed pellets when treated at 120ºC for 30 minutes at a concentration of NaOH of 0 mol/L obtained a yield of 2.00 and 1.78% respectively, and when treated at a concentration of NaOH 0.01 mol/L, the yields obtained were 2.93 and 2.65%, respectively.

The effect of supercritical fluid extraction with CO_2 was studied, but not extensively. When raw crushed pellets and extracted crushed pellets were treated at 120ºC for 30 minutes at a concentration of NaOH of 0.01 mol/L, the obtained yields were 2.65 and 2.76%, respectively. This indicates that a prior SFE does not undermine the protein extraction. However, when raw full pellets and extracted full pellets were treated at 120ºC for 30 minutes at a concentration of NaOH of 0.05 mol/L the yields were 5.56 and 4.00%. In this case, the effect of SFE is visible.

The effect of temperature and residence time was carried using sc-CO_2 extracted pellets using a concentration of NaOH of 0.05 mol/L. Three different temperatures (90, 105 and 120 ºC) and two different times (30 and 60 minute) were used and combined in a total of six experiments. Overall, the increase of time and temperature has, as expected, a positive effect on the protein extraction. In fact, 120 ºC is a low temperature for LHW treatment, and that this point the degradation of proteins does not occur. Therefore, in future experiments the temperature could be increased even higher. The highest yield obtained was 6.3% at 120ºC for 60 minutes and it was the highest yield obtain from all LHW experiments.

Despite the fact that proteins were retrieved, the yield is far from the range of 18.1% (total basis) of protein content of coffee silverskin, according to the literature. The maximum yield obtained in this study was 6.3%. Narita & Inouye (2012) where able to obtain a yield of 15.7% using pure water at 210ºC.

The following amino acids were detected on coffee silverskin: alanine, arginine, aspartic acid, glutamic acid, glycine, histidine, iso-leucine, leucine, lysine, methionine, phenylamine, serine, threonine, tyrosine and valine. This work displays, so far, the first amino acid profile of coffeesilverskin.

For future works it would be suggested to perform more experiments and quantitative analysis (both for supercritical extraction and liquid hot water) to improve the reliability and predictability of the results. One of the main blights of this work was the lack of resources to analyze several times the extracts obtained, and consequently obtain more reliable results.

The precision of the modeling would improve if the particle diameter would be measured by laser diffraction. This method is more precise than the sieving method used in this work to calculate the average diameter of the particles used.

The coffee silverskin pellets received were not analyzed to determine the initial amount of lipids and proteins. Therefore, there is no certainty if the full amount of fats and amino acids were retrieved with the used methods or how much was still there to be extracted. For instance, to determine the initial amount of lipids in CS, one could use a Soxhlet extraction.

The following steps of the work would be the scale-up to medium sized extractors for SFE and a reactor for LHW (for instance, 1 L). Eventually, an industrial scale-up would be the ultimate goal.

Finally, a market evaluation for the cost of the lipids and amino acids extracted would be of paramount importance. This would a allow an economic evaluation of the investment required for the scale-up, utility costs and possible profits.

References

Alonso, E. (2018). The role of supercritical fluids in the fractionation pretreatments of a wheat bran-based biorefinery. *Journal of Supercritical Fluids*, *133*(May 2017), 603–614.

Amend, J. P., & Helgeson, H. C. (1997). Solubilities of the common L-α-amino acids as a function of temperature and solution pH. *Pure and Applied Chemistry*, *69*(5), 935–942.

Awaluddin, S. A., Thiruvenkadam, S., Izhar, S., Hiroyuki, Y., Danquah, M. K., & Harun, R. (2016). Subcritical Water Technology for Enhanced Extraction of Biochemical Compounds from Chlorella vulgaris. *BioMed Research International*, *2016*, 1–10.

Ball, D. (2019). Reactions of Amino Acids. Retrieved June 5, 2019, from LibreTexts: Chemistry: https://chem.libretexts.org/Bookshelves/Introductory_Chemistry/Book%3A_The_Basics_of_GOB_Chemistry_(Ball_et_al.)/18%3A_Amino_Acids%2C_Proteins%2C_and_Enzymes/18.02_Reactions_of_Amino_Acids

Ballesteros, L. F., Teixeira, J. A., & Mussatto, S. I. (2014). Chemical, Functional, and Structural Properties of Spent Coffee Grounds and Coffee Silverskin. *Food and Bioprocess Technology*, *7*(12), 3493–3503.

Basu, P. (2013). *Biomass Gasification, Pyrolisis and Torrefaction 2nd Editon*. San Diego: Elsevier.

Baudron, V. (2014). *Added Value on Lignocellulose by menas of high pressure and enzyme technology: Master Thesis*. Hamburg University of Technology.

Bitencourt, R. G., Ferreira, N. J., Oliveira, A. L., Cabral, F. A., & Meirelles, A. J. A. (2018). High pressure phase equilibrium of the crude green coffee oil – CO2 – ethanol system and the oil bioactive compounds. *Journal of Supercritical Fluids*, *133*(July 2017), 49–57.

Bresciani, L., Calani, L., Bruni, R., Brighenti, F., & Del Rio, D. (2014). Phenolic composition, caffeine content and antioxidant capacity of coffee silverskin. *Food Research International*, *61*, 196–201.

Brunner, G. (1994). *Gas Extraction: An Introduction to Fundamentals of Supercritical*

Fluids and the Application to Separation Processe. Springer New York.

Coats, H., & Wingard, M. (1950). The effect of Particle Size on Extraction Rate. *The Journal of the American Oil Chemists Society*, 93–96.

Cocero, M. J., Cabeza, Á., Abad, N., Adamovic, T., Vaquerizo, L., Martínez, C. M., & Pazo-Cepeda, M. V. (2018). Understanding biomass fractionation in subcritical & supercritical water. *Journal of Supercritical Fluids*, *133*, 550–565.

Contreras, M. del M., Lama-Muñoz, A., Manuel Gutiérrez-Pérez, J., Espínola, F., Moya, M., & Castro, E. (2019). Protein extraction from agri-food residues for integration in biorefinery: Potential techniques and current status. *Bioresource Technology*, *280* (February), 459–477.

Cornelio-Santiago, H. P., Gonçalves, C. B., de Oliveira, N. A., & de Oliveira, A. L. (2017). Supercritical CO 2 extraction of oil from green coffee beans: Solubility, triacylglycerol composition, thermophysical properties and thermodynamic modelling. *Journal of Supercritical Fluids*, *128* (May), 386–394.

Couto, R. M., Fernandes, J., da Silva, M. D. R. G., & Simões, P. C. (2009). Supercritical fluid extraction of lipids from spent coffee grounds. *Journal of Supercritical Fluids*.

Cristina, A. (2014). *The agroindustrial residue valorisation with high pressure CO 2 within biorefinery concept: Dissertação para obtenção do Grau de Mestre em Engenharia Química e Bioquímica*. Universidade Nova de Lisboa.

de Azevedo, A. B. A., Kieckbush, T. G., Tashima, A. K., Mohamed, R. S., Mazzafera, P., & Melo, S. A. B. V. de. (2008a). Extraction of green coffee oil using supercritical carbon dioxide. *Journal of Supercritical Fluids*, *44*(2), 186–192.

de Azevedo, A. B. A., Mazzafera, P., Mohamed, R. S., Vieira De Melo, S. A. B., & Kieckbusch, T. G. (2008b). Extraction of caffeine, chlorogenic acids and lipids from green coffee beans using supercritical carbon dioxide and co-solvents. *Brazilian Journal of Chemical Engineering*, *25*(3), 543–552.

Fernández, S. S., Padilla, A. P., & Mucciarelli, S. (1999). Protein extraction from Atriplex lampa leaves: Potential use as forage for animals used for human diets. *Plant Foods for Human Nutrition*, *54*(3), 251–259.

Fuchs, D., Fischer, J., Tumakaka, F., & Sadowski, G. (2006). Solubility of amino acids:

Influence of the pH value and the addition of alcoholic cosolvents on aqueous solubility. *Industrial and Engineering Chemistry Research*, *45*(19), 6578–6584.

Gunawardena, G. (2019). Peptide Bond. Retrieved June 5, 2019, from LibreTexts: Chemistry website: https://chem.libretexts.org/Ancillary_Materials/Reference/Organic_Chemistry_Glossary/Peptide_Bond

Hijosa-Valsero, M., Garita-Cambronero, J., Paniagua-García, A. I., & Díez-Antolínez, R. (2018). Biobutanol production from coffee silverskin. *Microbial Cell Factories*, *17*(1), 1–9.

Huang, Z. (2015). Mass Transfer Models for Supercritical Fluid Extraction. In *High Pressure Fluid Technology for Green Food Processing*. Springer.

Isikgor, F. H., & Becer, C. R. (2015). Lignocellulosic biomass: a sustainable platform for the production of bio-based chemicals and polymers. *Polymer Chemistry*, *6*(25), 4497–4559.

Jahongir, H., Miansong, Z., Amankeldi, I., Yu, Z., & Changheng, L. (2019). Journal of King Saud University – Engineering Sciences The influence of particle size on supercritical extraction of dog rose (Rosa canina) seed oil. *Journal of King Saud University - Engineering Sciences*, *31*(2), 140–143.

Jahurul, M., Akanda, H., Zaidul, M., Sarker, I., Ferdosh, S., Yazid, M., … Kadir, A. (2012). Applications of Supercritical Fluid Extraction (SFE) of Palm Oil and Oil from Natural Sources. *Molecules*, *17*(January 2014), 1764–1794.

Kehili, M., Kammlott, M., Choura, S., Zammel, A., Zetzl, C., Smirnova, I., … Sayadi, S. (2017). Supercritical CO2 extraction and antioxidant activity of lycopene and β-carotene-enriched oleoresin from tomato (Lycopersicum esculentum L.) peels by-product of a Tunisian industry. *Food and Bioproducts Processing*, *102*(October), 340–349.

Kehili, M., Schmidt, L. M., Reynolds, W., Zammel, A., Zetzl, C., & Smirnova, I. (2016). Biotechnology for Biofuels Biorefinery cascade processing for creating added value on tomato industrial by - products from Tunisia. *Biotechnology for Biofuels*, 1–12.

Kovach, T. (2013). Classification of amino acids. Retrieved June 5, 2019, from Khan

Academy: https://www.khanacademy.org/test-prep/mcat/biomolecules/amino-acids-and-proteins1/v/classification-amino-acids

Kumar, S. (2015). *Herbal Bioactives and Food Fortification: Extraction and Formulation*. CRC Press.

Li, M., Cao, S., Meng, X., Studer, M., Wyman, C. E., & Ragauskas, A. J. (2017). The effect of liquid hot water pretreatment on the chemical – structural alteration and the reduced recalcitrance in poplar. *Biotechnology for Biofuels, 10:237*, 1–13.

Lin, T. M., Ping, T. S., Saptoro, A., & Freddie, P. (2013). Mass transfer coefficients and correlation of supercritical carbon dioxide extraction of Sarawak black pepper. In *International Journal of Food Engineering* (Vol. 10, pp. 1–15).

Mood, S., Hossein Golfeshan, A., Tabatabaei, M., Salehi Jouzani, G., Najafi, G. H., Gholami, M., & Ardjmand, M. (2013). Lignocellulosic biomass to bioethanol, a comprehensive review with a focus on pretreatment. *Renewable and Sustainable Energy Reviews, 27*, 77–93.

Mouahid, A., Crampon, C., Toudji, S. A. A., & Badens, E. (2016). Effects of high water content and drying pre-treatment on supercritical CO2 extraction from Dunaliella salina microalgae: Experiments and modelling. *Journal of Supercritical Fluids*, *116*(October), 271–280.

Nagy, B., & Simándi, B. (2008). Effects of particle size distribution, moisture content, and initial oil content on the supercritical fluid extraction of paprika. *Journal of Supercritical Fluids*.

Nahar, M. K., Zakaria, Z., Hashim, U., & Bari, M. F. (2017). Effect of pH and salt concentration on protein solubility of slaughtered and non-slaughtered broiler chicken meat. *Sains Malaysiana, 46*(5), 719–724.

Narita, Y., & Inouye, K. (2012). High antioxidant activity of coffee silverskin extracts obtained by the treatment of coffee silverskin with subcritical water. *Food Chemistry, 135*(3), 943–949.

Narita, Y., & Inouye, K. (2014). Review on utilization and composition of coffee silverskin. *Food Research International, 61*, 16–22.

Needham, T. (1970). *The Solubility of Amino Acids in Different Solvent Systems: A Thesis*

Submitted as Partial Fullfillment of the Requirments for the Degree of Doctor of Philosophy in Pharmaceutical Sciences. University of Rhode Island.

NPTEL. (2019). National Programme on Technology Enhanced Learning: MODULE 3: MASS TRANSFER COEFFICIENTS. Retrieved July 11, 2019, from Mass Transfer Operation 1 website: https://nptel.ac.in/courses/103103035/module3/lec3.pdf

Oliveira, E. L. G., Silvestre, A. J. D., & Silva, C. M. (2011). Review of kinetic models for supercritical fluid extraction. *Chemical Engineering Research and Design*, *89*(7), 1104–1117.

Ortega, J. H. (2015). *Process design of lignocellulosic biomass fractionation into cellulose, hemicellulose and lignin by prehydrolysis and organosolv process*. Wageningen University, Wageningen.

Phusunti, N., Phetwarotai, W., Tirapanampai, C., & Tekasakul, S. (2017). Subcritical Water Hydrolysis of Microalgal Biomass for Protein and Pyrolytic Bio-oil Recovery. *Bioenergy Research*, *10*(4), 1005–1017.

Ponte, M. (2017). Supercritical Fluids in Natural Product and Biomass Processing - An Introduction. In R. M. Łukasik (Ed.), *Supercritical Fluids in Natural Product and Biomass Processing - An Introduction* (pp. 1–8).

Powell, T., Bowra, S., & Cooper, H. J. (2016). Subcritical Water Processing of Proteins: An Alternative to Enzymatic Digestion? *Analytical Chemistry*, *88*(12), 6425–6432.

Reynolds, W., Baudron, V., Kirsch, C., Schmidt, L. M., Singer, H., Zenker, L., … Smirnova, I. (2016). Odor-Free Lignin from Lignocellulose by Means of High Pressure Unit Operations : Process Design , Assessment and Validation. *Chemie Ingenieur Technik*, *88*(10), 1–6.

Rogalinski, T., Ingram, T., & Brunner, G. (2008). Hydrolysis of lignocellulosic biomass in water under elevated temperatures and pressures. *Journal of Supercritical Fluids*, *47*(1), 54–63.

Roy, B. C., Sasaki, M., & Goto, M. (2006). Effect of temperature and pressure on the extraction yield of oil from sunflower seed with supercritical carbon dioxide. *Journal of Applied Sciences*, Vol. 6, pp. 71–75.

Sánchez-Camargo, A. P., Martinez-Correa, H. A., Paviani, L. C., & Cabral, F. A. (2011).

Supercritical CO2 extraction of lipids and astaxanthin from Brazilian redspotted shrimp waste (Farfantepenaeus paulensis). *Journal of Supercritical Fluids*.

Sapkale, G. N., Patil, S. M., Surwase, U. S., & Bhatbhage, P. K. (2010). - A REVIEW SUPERCRITICAL FLUID EXTRACTION. *International Journal of Chemical Science*, *8*(2), 729–743.

Sari, Y. (2015). *Biomass and its potential for protein and amino acids; valorizing agricultural by-products: PhD thesis*. Wageningen University.

Schlunder, E., & Tsotsas, E. (1988). *Warmeubertragung in Festbetten, durchmischten Schuttguttern und Wirbelschichten*. Georg Thieme Verlag Stuttgart.

Seader, J., Henley, E., & Roper, K. (2011). *Separation Process Principles: Chemical and Biochemical Operations, 3rd Edition*. John Wiley & Sons, Inc.

Sereewatthanawut, I., Prapintip, S., Watchiraruji, K., Goto, M., Sasaki, M., & Shotipruk, A. (2008). Extraction of protein and amino acids from deoiled rice bran by subcritical water hydrolysis. *Bioresource Technology*, *99*(3), 555–561.

Sigma Aldrich. (2019). Amino Acids Reference Chart. Retrieved July 3, 2019, from SIGMA ALDRICH website: https://www.sigmaaldrich.com/life-science/metabolomics/learning-center/amino-acid-reference-chart.html

Silva, L. P. S., & Martínez, J. (2014). Mathematical modeling of mass transfer in supercritical fluid extraction of oleoresin from red pepper. *Journal of Food Engineering*, *133*, 30–39.

Sinaei Nobandegani, M., Darbandi, T., Honarvar, B., & Sarafraz, M. M. (2016). Mathematical modeling and simulation of supercritical CO2 extraction of Ziziphora Tenuior essential oil. *Anadolu University Journal of Science and Technology-A Applied Sciences and Engineering*, *17*(1), 1–11.

Smirnova, I., Zetzl, C., Gairola, K., Kirsch, C., & Perez-cantu, L. (2011). High Pressure Processes in Biorefineries. *Chemie Ingenieur Technik*, *83*(7), 1016–1025.

Ståhl, M., Granström, K., Berghel, J., & Renström, R. (2004). Industrial processes for biomass drying and their effects on the quality properties of wood pellets. *Biomass and Bioenergy*, *27*(6), 621–628.

Stamenic, M., Zizovic, I., Eggers, R., Jaeger, P., Heinrich, H., Rój, E., … Skala, D. (2010). Swelling of plant material in supercritical carbon dioxide. *Journal of Supercritical Fluids*.

Taher, H., Al-Zuhair, S., Al-Marzouqi, A. H., Haik, Y., Farid, M., & Tariq, S. (2014). Supercritical carbon dioxide extraction of microalgae lipid: Process optimization and laboratory scale-up. *Journal of Supercritical Fluids*.

Toschi, T. G., Cardenia, V., Bonaga, G., Mandrioli, M., & Rodriguez-Estrada, M. T. (2014). Coffee silverskin: Characterization, possible uses, and safety aspects. *Journal of Agricultural and Food Chemistry*, *62*(44), 10836–10844.

Wu, H., Fu, Q., Giles, R., & Bartle, J. (2008). Production of mallee biomass in Western Australia: Energy balance analysis. *Energy and Fuels*, *22*(1), 190–198.

Zetzl, C. (2019). *"Stoffübergang bei der Feststoffextraktion und beim Färben", slides provided by the supervisor of this work to its author*. Hamburg.

Zhang, C., Sanders, J. P. M., & Bruins, M. E. (2014). Critical parameters in cost-effective alkaline extraction for high protein yield from leaves. *Biomass and Bioenergy*, *67*(0), 466–472.

Appendix

A. Drying of the Pellets

A.1. Initial Moisture of the Pellets

Table A.1 displays the values obtained that were used to calculate the initial moisture content of the coffee silverskin pellets. The results were calculated according to Equation 3.1.

Table A.1: Data used to calculate the initial moisture content of coffee silverskin.

Samples	Aluminum's tray mass (g)	Total initial mass (g)	Total final mass (g)	Initial CS mass (g)	Mass lost (g)	Moisture Content (%)	Average (%)
1	1.776	10.930	9.230	9.154	1.700	18.57	18.70±0.11
2	1.769	11.011	9.279	9.242	1.732	18.74	
3	1.779	10.944	9.222	9.165	1.722	18.79	

The calculation bellow is an example, using Sample 1 from Table A1, for the calculation of the initial moisture content of the coffee silverskin (as received):

$$Initial\ moisture\ content\ = \frac{(10.930 - 9.230)}{(10.930 - 1.766)} \times 100\ =\ 18.57\%\ (web\ basis)$$

A.2. Moisture Evolution at 45ºC as a function of drying time

Table A.2: Data used to calculate the evolution of coffee silverskin moisture content after a certain amount of time of drying.

Time (h)	Initial CS mass (g)	Mass lost (g)	Drying yield (%)	Average drying yield (%)	Moisture content (%)	Average moisture content (%)
0				0	18.7	18.7
0.5	9.367	0.509	5.43	6.03	14.03	13.48
	9.737	0.63	6.47		13.08	
	9.679	0.599	6.19		13.34	
1	9.945	0.929	9.34	9.05	10.32	10.61
	9.92	0.847	8.54		11.11	
	9.742	0.902	9.26		10.40	
1.5	9.606	1.066	11.10	10.74	8.55	8.91
	9.608	1.066	11.09		8.55	
	10.04	1.008	10.04		9.63	
2.5	9.939	1.165	11.72	12.29	7.91	7.30
	10.135	1.378	13.60		5.91	
	9.501	1.098	11.56		8.08	
4	9.911	1.463	14.76	14.50	4.62	4.91
	9.976	1.454	14.57		4.83	
	9.98	1.413	14.16		5.29	
6	10.049	1.466	14.59	14.38	4.81	5.05
	9.59	1.352	14.10		5.36	
	9.726	1.405	14.45		4.97	
18	9.947	1.518	15.26	15.31	4.06	4.00
	9.617	1.468	15.26		4.05	
	9.33	1.438	15.41		3.89	
24	9.918	1.509	15.21	15.55	4.11	3.73
	9.985	1.58	15.82		3.42	
	9.717	1.516	15.60		3.67	
48	9.848	1.558	15.82	15.75	3.42	3.50
	9.86	1.534	15.56		3.72	
	9.763	1.549	15.87		3.37	
74	9.772	1.546	15.82	15.56	3.42	3.72
	9.516	1.464	15.38		3.92	
	9.516	1.473	15.48		3.81	

The initial moisture content was assumed to the one present in Table A.1. To calculate the moisture content at a given time, the initial moisture content was subtracted by the percentage of mass loss at that given time. The calculation bellow is an example, using the 0.5 hours sample from Table A2, for the calculation of the moisture content of the coffee silverskin after 0.5 hours of drying at 45ºC.:

$$Moisture\ content\ (0.5\ h)\ =\ 18.7 - \left(\frac{9.367 - 0.509}{9.367}\right) \times 100\ = 13.48\%$$

B. Supercritical Carbon Dioxide Extraction of Lipids

B.1. Effect of Temperature and Pressure on the total extraction yield from Crushed Pellets

The results displayed in Table B.1 were calculated according to Equation 4.1.

Table B. 1: Data used to calculate the total extraction yields of SFE at different temperature and pressures.

Pressure (bar)	Temperature (ºC)	Batch Input (g)	Mass Extracted (g)	Total Yield (%)
350	40	25.745	0.601	2.33
350	50	26.222	0.659	2.51
350	60	26.453	0.68	2.57
400	40	23.258	0.654	2.81
400	50	24.754	0.772	3.12
400	60	24.903	0.768	3.08
450	40	24.068	0.6	2.49
450	50	26.271	0.678	2.54
450	60	27.777	0.927	3.34

The calculation bellow is an example, using the sample at 350 bar and 40ºC from Table B1, for the calculation of the total extraction yield of the SFE according to Equation 4.1:

$$Total\ extraction\ yiel\ (350\ bar, 40ºC) = \frac{0.601}{25.745} \times 100\ =\ 2.33\%$$

B.2. Effect of average particle diameter on the total extraction yield from Crushed Pellets

The examples of calculation present in Chapter B.2. are relative to the modelling of the extraction that used particles with an average diameter of 22 μm.

$$\beta = \frac{2.16 \times 10^{-9}}{(1 + 3.8 \times \frac{6}{9.5})} = 3.08 \times 10^{-10}\, m/s$$

$$Sh = \frac{3.08 \times 10^{-10} \times 22 \times 10^{-6}}{1.34 \times 10^{-17}} = 505$$

$$\beta_S = \left(\frac{1}{3.08 \times 10^{-10}} - \frac{1}{2.16 \times 10^{-9}}\right)^{-1} = 3.59 \times 10^{-10}\ \mathrm{m/s}$$

C. Liquid Hot Water Treatment for Protein Extraction

C.1. Effect of the concentration of NaOH on the protein extraction yield from raw pellets, crushed raw pellets and crushed SFE pellets

Table C.1, C.2, C.3 display the data and results from the liquid hot water treatment for protein recovery for raw pellets, crushed raw pellets and crushed SFE pellets, respectively.

Table C.1: Data used to calculate the protein extraction yield of raw pellets by mean of liquid hot water treatment as a function of the concentration of NaOH:

[NaOH] (mol/L)	**Input Mass (g)**	**Solution (mL)**	**Protein Concentration (mg/L)**	**Yield (%)**
0	0.605	29.950	404	2.00%
0.01	0.591	28.586	605.3	2.93%
0.03	0.61	29.115	926.7	4.42%
0.05	0.617	29.090	1180.3	5.56%

Table C.2: Data used to calculate the protein extraction yield of crushed raw pellets by mean of Liquid Hot Water treatment as a function of the [NaOH]:

[NaOH] (mol/L)	**Input Mass (g)**	**Solution (mL)**	**Protein Concentration (mg/L)**	**Yield (%)**
0	0.671	30.288	394.6	1.78%
0.01	0.599	29.072	545.1	2.65%
0.02	0.612	29.638	750	3.63%
0.04	0.627	28.773	1095	5.02%

Table C.3: Data used to calculate the protein extraction yield of crushed SFE pellets by mean of Liquid Hot Water treatment as a function of the [NaOH]:

[NaOH]	**Input Mass (g)**	**Solution (mL)**	**Protein Concentration (mg/L)**	**Yield (%)**
0.01	0.591	31.027	526	2.76%
0.05	0.621	29.671	1263	6.03%

The calculation bellow is an example, using raw pellets treated with in a solution of [NaOH]= 0 from Table C1, for the calculation of the protein extraction yield of the LHW hydrolysis. All the remaining protein extraction yields were calculated according to the same line of thought:

$$Protein\ extraction\ yield\ = \frac{29.950\ \times\ 404\ \times \frac{1}{1000}}{0.605 \times\ 1000} \times\ 100\ =\ 2.00\%$$

C.2. Protein Profile of the extract from Raw Pellets at [NaOH] = 0 AND [NaOH]= 0.05 mol/L

Table C.4 displays the amino acid profile of the extract when no NaOH was added and when the liquid hot water treatment was performed using a solution of NaOH with a concentration of 0.05 mol/L.

Table C. 4: Protein Profile of the extract from Raw Pellets at a concentration of NaOH of 0 and 0.05 mol/L.

Amino Acid	Amount of AA at 0 mol/L (mg/L)	Amount of AA at 0.05 mol/L (mg/L)	Relative amount of AA at 0 mol/L (%)	Relative amount of AA at 5 mol/L (%)
Alanine	22	77	5.45%	6.53%
Arginine	33	34	8.17%	2.88%
Aspartic Acid	77	220	19.06%	18.64%
Glutamic Acid	86	200	21.29%	16.95%
Glycine	22	89	5.45%	7.54%
Histidine	6.7	25	1.66%	2.12%
Iso-leucine	18	68	4.46%	5.76%
Leucine	23	98	5.69%	8.31%
Lysine	16	53	3.96%	4.49%
Methionine	2.3	8	0.57%	0.68%
Phenylamine	19	68	4.70%	5.76%
Serine	28	63	6.93%	5.34%
Threonine	18	49	4.46%	4.15%
Tyrosine	13	64	3.22%	5.42%
Valine	20	64	4.95%	5.42%
Total	404	1180	100.00%	100.00%

C.3. Effect of residence time and temperature on the protein extraction yield from SFE full pellets

Table C. 5 : Data used to calculate the protein extraction yield of full SFE pellets by mean of liquid hot water treatment as a function of the temperature and residence time.

Sample	Temperature	[NaOH]	time (min.)	AA (mg/L)	Mass Input (g)	Solution (mL)	Total AA(g)	Yield
1	120	0.05	30	755	0.538	28.818	0.022	4.04%
2	120	0.05	60	1455	0.69	29.85	0.043	6.29%
3	90	0.05	30	538	0.7	28.321	0.015	2.18%
4	90	0.05	60	326.7	0.744	32.214	0.011	1.41%
5	105	0.05	30	967	0.632	28.801	0.028	4.41%
6	105	0.05	60	1144	0.631	30.724	0.035	5.57%

C.4. Effect of residence time and temperature on the protein profile of the extract from SFE Full Pellets

Table C.6: Protein Profile of the extracts from full SFE pellets at different temperatures and residence times:

Sample	120ºC, 30 minutes	120ºC, 60 minutes	90 ºC, 30 minutes	90ºC, 60 minutes	105ºC, 60 minutes	105ºC, 60 minutes
Alanine (mg/L)	46	89	28	18	56	68
Arginine (mg/L)	28	60	26	16	43	46
Aspartic Acid (mg/L)	120	220	97	65	160	180
Glutamic Acid (mg/L)	130	250	94	61	170	190
Glycine (mg/L)	65	120	37	25	78	98
Histidine (mg/L)	15	26	10	6.4	18	19
Iso-leucine (mg/L)	62	94	43	24	63	80
Leucine (mg/L)	76	150	47	23	91	120
Lysine (mg/L)	22	48	16	8.3	27	34
Methionine (mg/L)	0	0	0	0	0	0
Phenylamine (mg/L)	51	100	34	16	63	80
Serine (mg/L)	31	68	31	21	52	56
Threonine (mg/L)	22	58	22	13	38	36
Tyrosine (mg/L)	33	62	19	11	40	50
Valine (mg/L)	54	110	34	19	68	87
Total (mg/L)	755	1455	538	326.7	967	1144